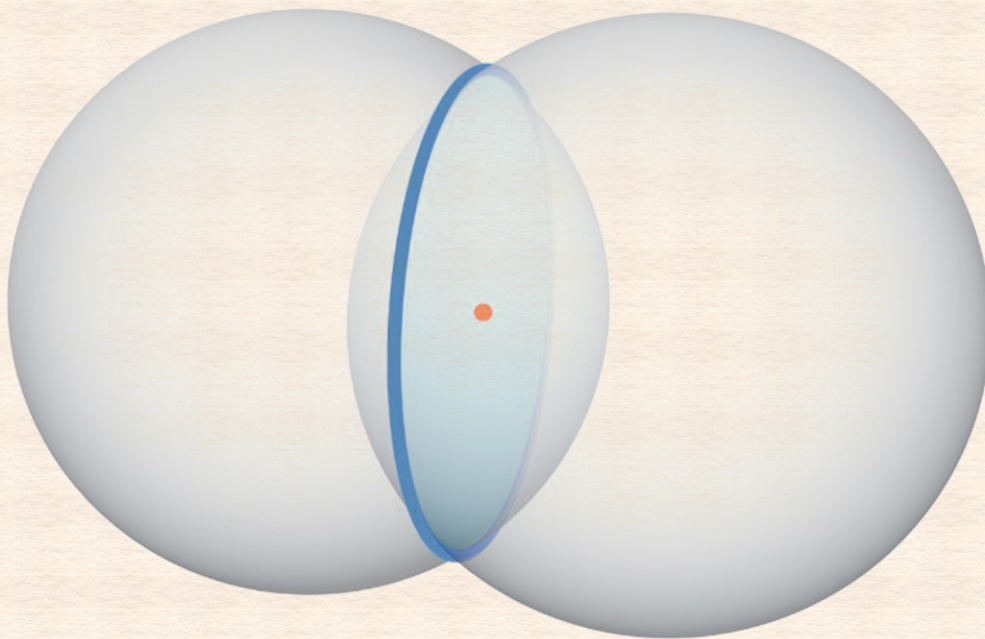


Journal of Modern Physics

Special Issue on Gravitation, Astrophysics and Cosmology



ISSN: 2153-1196



<https://www.scirp.org/journal/jmp>

Journal Editorial Board

ISSN: 2153-1196 (Print) ISSN: 2153-120X (Online)

<https://www.scirp.org/journal/jmp>

Editor-in-Chief

Prof. Yang-Hui He

City University, UK

Editorial Board

Prof. Nikolai A. Sobolev

Universidade de Aveiro, Portugal

Prof. Mohamed Abu-Shady

Menoufia University, Egypt

Dr. Hamid Alemohammad

Advanced Test and Automation Inc., Canada

Prof. Emad K. Al-Shakarchi

Al-Nahrain University, Iraq

Prof. Antony J. Bourdillon

UHRL, USA

Prof. Tsao Chang

Fudan University, China

Prof. Wan Ki Chow

The Hong Kong Polytechnic University, China

Prof. Jean Cleymans

University of Cape Town, South Africa

Prof. Stephen Robert Cotanch

NC State University, USA

Prof. Claude Daviau

Ministry of National Education, France

Prof. Peter Chin Wan Fung

University of Hong Kong, China

Prof. Ju Gao

The University of Hong Kong, China

Dr. Sachin Goyal

University of California, USA

Dr. Wei Guo

Florida State University, USA

Prof. Karl Hess

University of Illinois, USA

Prof. Peter Otto Hess

Universidad Nacional Autónoma de México, Mexico

Prof. Ahmad A. Hujeirat

University of Heidelberg, Germany

Prof. Haikel Jelassi

National Center for Nuclear Science and Technology, Tunisia

Dr. Magd Elias Kahil

October University for Modern Sciences and Arts (MSA), Egypt

Prof. Santosh Kumar Karn

Dr. APJ Abdul Kalam Technical University, India

Prof. Yu-Xian Li

Hebei Normal University, China

Dr. Ludi Miao

Cornell University, USA

Dr. Grégory Moreau

Paris-Saclay University, France

Prof. Christophe J. Muller

University of Provence, France

Dr. Rada Novakovic

National Research Council, Italy

Dr. Vasilis Oikonomou

Aristotle University of Thessaloniki, Greece

Prof. Tongfei Qi

University of Kentucky, USA

Prof. Mohammad Mehdi Rashidi

University of Birmingham, UK

Prof. Haiduke Sarafian

The Pennsylvania State University, USA

Prof. Kunnat J. Sebastian

University of Massachusetts, USA

Dr. Ramesh C. Sharma

Ministry of Defense, India

Dr. Reinoud Jan Slagter

Astronomisch Fysisch Onderzoek Nederland, Netherlands

Dr. Giorgio SONNINO

Université Libre de Bruxelles, Belgium

Prof. Yogi Srivastava

Northeastern University, USA

Dr. Mitko Stoev

South-West University “Neofit Rilski”, Bulgaria

Dr. A. L. Roy Vellaisamy

City University of Hong Kong, China

Prof. Anzhong Wang

Baylor University, USA

Prof. Yuan Wang

University of California, Berkeley, USA

Prof. Peter H. Yoon

University of Maryland, USA

Prof. Meishan Zhao

University of Chicago, USA

Prof. Pavel Zhuravlev

University of Maryland at College Park, USA

Table of Contents

Volume 12 Number 6

May 2021

Relativity Isoframes—A Useful and Potentially Unifying Conceptual Framework

E. T. Tatum.....731

A Potentially Unifying Constant of Nature (Brief Note)

E. T. Tatum, U. V. S. Seshavatharam, S. Lakshminarayana.....739

Black Holes in Role, Essence and Function

W. S. Daher.....744

Detection and Determination of the Variation of the Speed of Time

R. M. L. Baker, B. S. Baker, F. Y. Li.....761

Reconstruction Method in $\mathcal{F}(G)$ Gravity: Stability Study and Inflationary Survey

C. Aïnamon, M. J. S. Houndjo, A. A. L. Ayivi, M. G. Ganiou, A. Kanfon.....781

Tensor and Effective Vector Approach to Gravitational Radiation in the Weak Field Limit

P. Christillin.....798

Inflation, Dark Energy, Acceleration, Missing Mass?

P. Christillin.....806

Homological Solution of the Lanczos Problems in Arbitrary Dimension

J.-F. Pommaret.....829

Journal of Modern Physics (JMP)

Journal Information

SUBSCRIPTIONS

The *Journal of Modern Physics* (Online at Scientific Research Publishing, <https://www.scirp.org/>) is published monthly by Scientific Research Publishing, Inc., USA.

Subscription rates:

Print: \$89 per issue.

To subscribe, please contact Journals Subscriptions Department, E-mail: sub@scirp.org

SERVICES

Advertisements

Advertisement Sales Department, E-mail: service@scirp.org

Reprints (minimum quantity 100 copies)

Reprints Co-ordinator, Scientific Research Publishing, Inc., USA.

E-mail: sub@scirp.org

COPYRIGHT

Copyright and reuse rights for the front matter of the journal:

Copyright © 2021 by Scientific Research Publishing Inc.

This work is licensed under the Creative Commons Attribution International License (CC BY).

<http://creativecommons.org/licenses/by/4.0/>

Copyright for individual papers of the journal:

Copyright © 2021 by author(s) and Scientific Research Publishing Inc.

Reuse rights for individual papers:

Note: At SCIRP authors can choose between CC BY and CC BY-NC. Please consult each paper for its reuse rights.

Disclaimer of liability

Statements and opinions expressed in the articles and communications are those of the individual contributors and not the statements and opinion of Scientific Research Publishing, Inc. We assume no responsibility or liability for any damage or injury to persons or property arising out of the use of any materials, instructions, methods or ideas contained herein. We expressly disclaim any implied warranties of merchantability or fitness for a particular purpose. If expert assistance is required, the services of a competent professional person should be sought.

PRODUCTION INFORMATION

For manuscripts that have been accepted for publication, please contact:

E-mail: jmp@scirp.org

Relativity Isoframes—A Useful and Potentially Unifying Conceptual Framework

Eugene Terry Tatum

Independent Researcher, Bowling Green, KY, USA

Email: ett@twc.com

How to cite this paper: Tatum, E.T. (2021) Relativity Isoframes—A Useful and Potentially Unifying Conceptual Framework. *Journal of Modern Physics*, 12, 731-738. <https://doi.org/10.4236/jmp.2021.126046>

Received: March 8, 2021

Accepted: May 5, 2021

Published: May 8, 2021

Copyright © 2021 by author(s) and Scientific Research Publishing Inc.

This work is licensed under the Creative Commons Attribution International License (CC BY 4.0).

<http://creativecommons.org/licenses/by/4.0/>



Open Access

Abstract

This brief note introduces the conceptual framework of special and general relativity isoclocks and isoframes. Isoclocks and isoframes, as defined herein, can be used to create geometrical maps of space and time (“space-time”) with and without matter embedded. They are useful for having a mental picture of space-time relationships without having to picture 4-dimensional manifolds, which very few students and scientists are able to do. With the aid of the optical lensing definition of curvature as inverse radius, a new gravitational force equation is derived, which also incorporates Einstein’s mass/energy relation in the m_x term. Thus, one may see how it is that gravitational force correlates with its time-embedded curvature-squared (C_x^2) space in a more accurate formulation than could be envisioned by Newton. This becomes more apparent in high gamma fields, such as found near a black hole horizon. It is hoped that probability theories, such as quantum field theories in curved space-time, might be adaptable to the general relativity isoframe concept introduced herein.

Keywords

Isoframe, Isoclock, General Relativity, Special Relativity, Space-Time, Black Holes, Krogdahl, Unification

1. Introduction and Background

Kip Thorne, who shared the 2017 Nobel Prize in physics for his theoretical work on black holes, began his *Black Holes & Time Warps* book [1] with thought experiments for three black holes of radically-different sizes. As Thorne pointed out on page 33 of his book, bizarre things should happen to radio signals received by observers as the transmitter approaches very close to the horizon of a black hole of any size. The signal frequency plummets rapidly towards zero, and

the signal disappears entirely at the horizon (as the wavelength becomes infinite and the wave energy becomes zero). For the outside observer at a fixed *radius* from the horizon, it is as if a clock (or radio transmitter of a given frequency) becomes *frozen in time relative to that observer*. For observers falling into a black hole, it is an entirely different perspective (*i.e.*, reference frame), but that is not the focus of this paper.

Albert Einstein's genius had much to do with his ability to find the right thought experiment and reference frame in which to simplify and understand a complex problem at a fundamental level [2]. With special relativity, his concept of the *proper time* clock of an observer in a *chosen* reference frame in comparison to the time clock of an observer in a *different* reference frame was of paramount importance. It was this clock comparison that mattered most to him, if one were to accept the embedded assumption of invariance of speed of light measurements.

In relativity theory, the proper time clock of a given reference frame (we'll call it T_o) can be compared to those of different reference frames. In fact, an ordering of all other reference frame clocks can be mapped with respect to the chosen clock of reference. One can utilize a subscript numbering system of the various clocks, such that clocks within the same reference frame can be numbered the same, and faster-ticking and slower-ticking clocks within different reference frames can be numbered higher or lower, respectively. Clocks keeping the same proper time are defined herein as "isoclocks," and their collective reference frame is defined herein as their "isoframe."

2. Results: Isoframe Mapping in Special and General Relativity

Since a relativity isoframe is defined as one in which variously-positioned observers all keep the same proper time, their clocks can be considered to be perfectly synchronized at all times within their isoframe map.

2.1. Special Relativity

One can map out a special relativity Minkowskiian space-time isoframe in the following way (see **Figure 1**).

This is a 2-dimensional slice of rectilinear space-time (*i.e.*, no curves in the latticework). For the purpose of this thought experiment, one can think of every point of line intersection as a *fixed* point with respect to an observer at the centrally-located T_o point. Therefore, all such points of intersection can be considered to be in the same reference frame (isoframe) with respect to this T_o clock, and to have identical T_o clocks (isoclocks), one of which is shown. Anyone moving inertially in this Minkowskiian plane relative to any T_o clock moves the same with respect to all T_o clocks, and *must* have a non- T_o clock of their own. One can readily envision the Minkowskiian space to be filled with many *different* non- T_o clocks, depending upon their particular reference frame velocity with

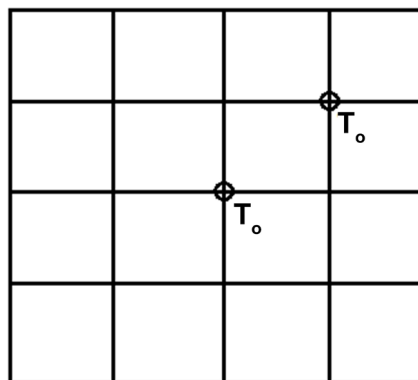


Figure 1. Special relativity isoframe (Minkowskiian space-time).

respect to the T_o isoframe. So, the T_o special relativity isoframe map of **Figure 1** is one of *stationary* (in a relative sense) imaginary clocks in a field devoid of matter and its ever-present gravity.

2.2. General Relativity

Einstein's gravity theory, incorporating thought experiments with light beams and *accelerating* reference frames, necessitates that gravitationally-attractive matter positively curves space-time in a very specific way, according to a metric tensor (the "metric"). Without immersing oneself for years in this arcane branch of mathematics, one can nevertheless have a very good idea of how general relativity improves somewhat on the Newtonian concept of gravity in flat space and absolute time.

The key to this understanding is, once again, an isoframe mapping of identical time clocks, but within the gravity space surrounding a concentration of matter and/or energy. One must remember that matter and energy are two sides of the same coin, by $E = mc^2$. In contrast to the special relativity isoframe map of T_o clocks fixed in position relative to a specified T_o observer clock, *the general relativity isoframe map is a curved manifold of different clocks at different distances (i.e., radii) within the gravity well surrounding a centralized focus of matter/energy.* See **Figure 2**.

As well-proven by clocks in satellite orbits around Earth, clocks farther from a center of gravity tick faster (hence the higher subscript numbers) than clocks deeper in a gravity well. Four such orbital clocks are shown in **Figure 2** for comparison. Each orbital sphere *surface* (represented by a circle in the two-dimensional figure) can, therefore, be considered to be a gravity isoframe, as defined by its isoclock. The slowest clocks, in comparison to any of these orbital clocks, are those on Earth's surface, which, assuming continuance of the numbering sequence, would be labelled as T_o in **Figure 2**.

For the purposes of a general relativity thought experiment, let us consider a perfectly homogeneous and spherical extended body of matter which we will call a "planet." This planet has no angular momentum (*i.e.*, it does not rotate) and all of its mass can be effectively treated as if it were concentrated at a point at the

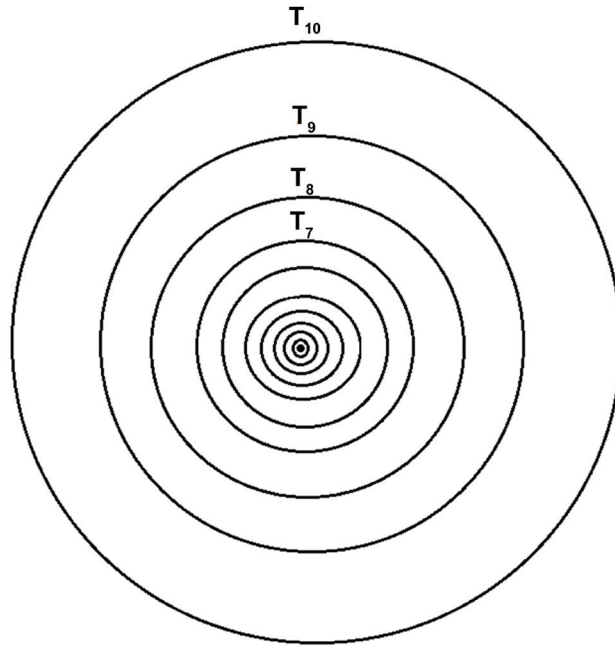


Figure 2. General relativity isoframes (T_x curved space-time).

geometric center of the sphere. Furthermore, this planet has no atmosphere and rests in a vacuum of infinite space with no other matter or energy.

We know from Newtonian mechanics that perfectly circular orbits centered on the planetary center can be achieved at any distance from the planetary center which is also beyond the planetary surface. We also know that a centripetal gravitating force of attraction on a body (x) in a given circular orbit closely approximates

$$F_{Gx} = GMm_x r_x^{-2} \quad (1)$$

wherein the usual Newtonian symbolic representation applies. Furthermore, each circular orbit (x) can be defined by its *curvature* C_x according to r_x^{-1} . This curvature definition is as useful for gravity in this simplified isoframe approach as it has been for the field of lens optics. **Figure 3** replicates **Figure 2**, except that each orbital in the gravity well is now designated by its curvature C_x . The only important difference to keep in mind here is that a *smaller* curvature subscript (x) in **Figure 3** corresponds to a *greater* degree of curvature.

3. Discussion

One of the interesting features about this correlation between an x -orbital's curvature C_x in space and its own proper time T_x is that the square of its curvature (C_x^2) correlates with gravitational force in proportion to r_x^{-2} . Thus,

$$F_{Gx} = GMm_x C_x^2 \quad (2)$$

Furthermore, while the GMm_x term is a constant in the Newtonian theory, it can now actually be considered a *variable* according to $E = mc^2$. The rest mass-energy of body m_x on the planetary surface is fractionally *less* than the mass-

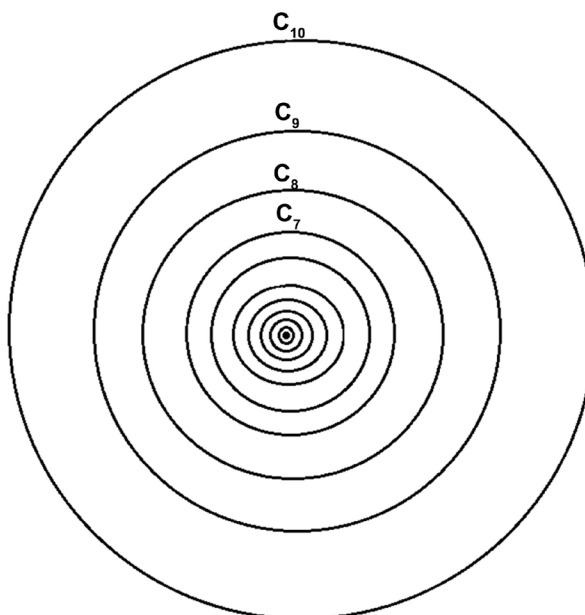


Figure 3. General relativity isoframes (C_x curved space-time).

energy of orbiting body m_x at a certain height h above the surface, according to $m\gamma h$ (gravitational potential energy) added to the rest mass-energy. Herein, we are using gravity field symbol γ (acceleration due to gravity) in a generic sense, corresponding to a given height above a planet of mass M . The importance of now *requiring* the incorporation of $E = mc^2$ into the m_x term of $GMm_x C_x^2$ is to show how it is that the centripetal gravitational force calculated by Newton always *very slightly* underestimates the general relativity force on orbiting bodies in relatively weak gravity fields. However, more importantly, it would be expected to *greatly underestimate* the general relativity force (including tidal forces) on orbiting bodies in strong (*i.e.*, high energy density) gravity fields, such as those bordering black hole event horizons. Thus, Newton's theory can only be considered to be a very good approximation where gravitational energy density (and its associated space-time curvature) is relatively weak.

One of the reasons why $F_{Gx} = GMm_x C_x^2$, when it incorporates $E = mc^2$ into the equation, appears to be a significantly better approximation of the true gravitational force than Newton's approximation is that *Kroghdahl's incorporation of $E = mc^2$ into his own flat space-time cosmology formulation has already been shown to be remarkably accurate* with respect to the canonical tests of any gravity theory competing with general relativity [3] [4].

Just as one can transform a square into a cube by multiplying by a measure of the 2-dimensional object (namely, its length), a squaring of the 2-dimensional circle curvature according to $C_x^2 = r_x^{-2}$ can be considered to be a 3-dimensional representation of a T_x orbital. In this way, a 2-dimensional spatial object with an embedded time clock corresponding to its curvature radius becomes a 3-dimensional spatial object with an embedded time clock corresponding to its curvature radius. Thus, *the manifold of concentric spheres with different embedded isoc-*

locks becomes a conceptually useful model of 4-D space-time.

With respect to black holes, curved general relativity isoframes, with the third spatial dimension withheld for clarity, can be mapped around a perfectly spherical Schwarzschild black hole (see **Figure 4**).

In this figure, T_o represents the frozen time clock of the black hole horizon, as perceived by a stationary or orbiting outside observer at any fixed radius outside the black hole horizon. It is often said that if one could instantaneously convert the sun into a Schwarzschild black hole of identical mass, the curved space-time of known planetary orbitals would look identical. The known planets would all be at such sufficient distances from the three-kilometer radius solar mass black hole horizon that we would not observe any appreciable difference in their orbital paths or periods.

The key difference in the adaptation of general relativity isoframes to black holes is what happens in *close proximity* (*i.e.*, within several Schwarzschild radii) to the horizon. Here the gravitational field strength and tidal forces deviate significantly from Newtonian theory, and the *myh* mass-energy contribution to m_x becomes of paramount importance. At this point, by *not* incorporating $E = mc^2$ into m_s , Newtonian theory fails to be a close approximation of the extreme tidal forces and other phenomena occurring at orbital radii near a black hole horizon. Obviously, the frozen horizon clock T_o in **Figure 4** marks the boundary of the black hole isoframe map. Nothing certain or useful can be said about the interior of a black hole. And no one wants to be the free-falling observer to pass this horizon and explore the interior!

One wonders if the above general relativity isoframe conceptualization could be of use in terms of unification with quantum physics. Quantum field theories

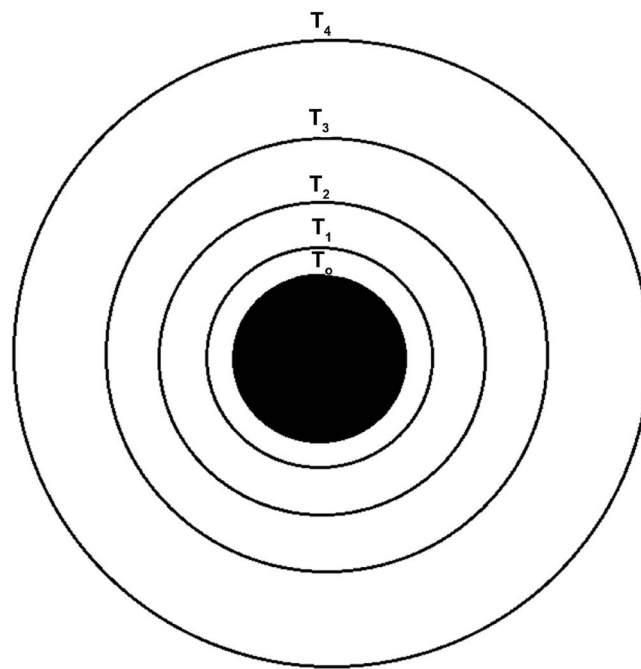


Figure 4. General relativity isoframes around a black hole.

in curved space-time do, in fact, exist. These generally follow the local structure (*i.e.*, the geometry) of space-time. Therefore, it is hoped that the conceptual framework presented herein may be useful in some way to quantum physicists working towards unification.

4. Summary and Conclusions

This paper has introduced readers to the definition and mapping of isoclocks and isoframes in special and general relativity. Particular attention has been paid to general relativity isoframe mapping around an ideal spherical body of matter/energy, according to the mapping of isoclocks and their isoframe orbitals. Application of the $C_x = r_x^{-1}$ curvature definition, borrowed from optical lensing, allows one to define and represent time-embedded orbital curvature in 2-dimensional space. Furthermore, squaring of curvature ($C_x^2 = r_x^{-2}$) allows one to define and represent time-embedded curvature in 3-dimensional space. And because of its time-embedded nature, this becomes a useful analogue of 4-dimensional space-time. The mapping of concentric time-embedded spheres of this type is conceptually useful for the majority of us who cannot otherwise picture 4-dimensional manifolds. Furthermore, the introduction of isoframe formula $F_{Gx} = GMm_x C_x^2$, may allow one to see how it is that gravitational force not only correlates with r_x^{-2} , but also time-embedded curvature space (space-time). Finally, the author speculates that probability theories, such as quantum field theories in curved space-time, might be adaptable to the general relativity isoframe concept introduced herein.

Data Availability

Due to the purely theoretical nature of this undertaking, no new data were generated or analyzed in support of this research.

Dedications and Acknowledgements

This paper is dedicated to Dr. Wasley S. Krogdahl for his work on cosmology in flat space-time, and to Drs. Stephen Hawking and Roger Penrose for their groundbreaking work on black holes and cosmology. Dr. Tatum also thanks Dr. Rudolph Schild of the Harvard-Smithsonian Center for Astrophysics for his past support and encouragement.

Conflicts of Interest

The author declares no conflicts of interest regarding the publication of this paper.

References

- [1] Thorne, K.S. (1994) Black Holes & Time Warps. W.W. Norton & Company, New York.
- [2] Pais, A. (1982) Subtle is the Lord: The Science and the Life of Albert Einstein. Ox-

ford University Press, Oxford.

- [3] Krogdahl, W.S. (2006) Cosmology in Flat Space-Time. arXiv:gr-qc/0402016.
- [4] Tatum, E.T. (2017) *Journal of Modern Physics*, **8**, 2087-2095.
<https://doi.org/10.4236/jmp.2017.813127>

A Potentially Unifying Constant of Nature (Brief Note)

Eugene Terry Tatum^{1*}, U. V. S. Seshavatharam², S. Lakshminarayana³

¹Independent Researcher, Bowling Green, KY, USA

²Honorary Faculty, I-SERVE, Survey No-42, Hitech City, Hyderabad, Telangana, India

³Department of Nuclear Physics, Andhra University, Visakhapatnam, AP, India

Email: *ett@twc.com

How to cite this paper: Tatum, E.T., Seshavatharam, U.V.S. and Lakshminarayana, S. (2021) A Potentially Unifying Constant of Nature (Brief Note). *Journal of Modern Physics*, 12, 739-743.

<https://doi.org/10.4236/jmp.2021.126047>

Received: March 21, 2021

Accepted: May 5, 2021

Published: May 8, 2021

Copyright © 2021 by author(s) and Scientific Research Publishing Inc. This work is licensed under the Creative Commons Attribution International License (CC BY 4.0).

<http://creativecommons.org/licenses/by/4.0/>



Open Access

Abstract

This brief note describes a method by which numerous empirically-determined quantum constants of nature can be substituted into Einstein's field equation (EFE) for general relativity. This method involves treating the ratio G/\hbar as an empirical constant of nature in its own right. This ratio is represented by a new symbol, N_T . It turns out that the value of N_T (which is $6.32891937 \times 10^{23} \text{ m}\cdot\text{kg}^{-2}\cdot\text{s}^{-1}$) is within 5% of Avogadro's number N_A , although the units are clearly different. Nevertheless, substitutions of N_T or N_A into the EFE, as shown, should yield an absolute value similar in magnitude to that calculated by the conventional EFE. The method described allows for quantum term EFE substitutions into Einstein's gravitational constant κ . These terms include \hbar , α , m_e , m_p , R , k_B , F , e , M_U , and m_U . More importantly, perhaps, one or more of the many new expressions given for κ may provide a more accurate result than κ incorporating G . If so, this may have important implications for additional forward progress towards unification. Whether any of these new expressions for Einstein's field equation can move us closer to quantizing gravity remains to be determined.

Keywords

Unification, General Relativity, Quantum Theory, Einstein's Gravitational Constant, Tatum's Number, Avogadro's Number

1. Introduction and Background

There are a myriad of difficulties in attempting to unite gravity with the other fundamental forces of nature. Not the least of these is that our best gravity theory, general relativity, has classical deterministic features, whereas quantum theory is anti-deterministic, probabilistic, and built upon the foundation of Hei-

senberg's uncertainty principle. To unite gravity with the other forces using these two theories, without some modifications to one or both theories, is a bit like mixing oil and water. It simply won't work. *An "emulsifier" approach, successfully combining certain features of both theories, is needed.*

One possible approach towards unification is to work towards quantizing gravity (*i.e.*, "quantum gravity"), as we see with the work of string theorists. The other possible approach is to work towards gravitizing quantum theory [1], although there seems to be less progress from this direction.

This brief note points to a potentially useful way of bringing elements of both theories together by harmonizing two of their most fundamental constants (G and \hbar) in the form of a ratio (G/\hbar). One can then insert this ratio into Einstein's most fundamental gravity and quantum equations as shown herein.

2. Results

The analytic process in this brief note primarily involves substituting various constants of nature into previously-established relativity and quantum equations, in order to better see their relationships. Only simple algebra is required. No figures or tables are necessary to elucidate these relationships.

The latest available values of G and \hbar are [2]:

$$G = 6.67430 \times 10^{-11} \text{ m}^3 \cdot \text{kg}^{-1} \cdot \text{s}^{-2} \quad (1)$$

$$\hbar = 1.054571817 \times 10^{-34} \text{ m}^2 \cdot \text{kg} \cdot \text{s}^{-1} \quad (2)$$

Their ratio, which we represent as N_T is:

$$G/\hbar = N_T = 6.32891937 \times 10^{23} \text{ m} \cdot \text{kg}^{-2} \cdot \text{s}^{-1} \quad (3)$$

Interestingly, this ratio *approximates* (within 5%) Avogadro's number N_A :

$$N_A = 6.02214076 \times 10^{23} \text{ mol}^{-1} \quad (4)$$

We will take advantage of this similarity ("near-equivalence") below.

Einstein's field equation (EFE) of general relativity can be expressed as follows:

$$G_{\mu\nu} + g_{\mu\nu}\Lambda = \left[\frac{8\pi G}{c^4} \right] T_{\mu\nu} \quad (5)$$

wherein $G_{\mu\nu}$ is the Einstein tensor, $g_{\mu\nu}$ is the metric tensor, Λ is the cosmological constant, G is Newton's gravitational constant, c is speed of light, and $T_{\mu\nu}$ is the stress-energy tensor.

Notice that the *bracketed coefficient* of the stress-energy tensor, sometimes referred to as κ or Einstein's gravitational constant, contains G . Thus, a rearrangement of relation (3) can be given as follows:

$$G = 6.32891937 \times 10^{23} \hbar \quad (6)$$

And substituted in relation (5) as follows:

$$G_{\mu\nu} + g_{\mu\nu}\Lambda = \left[\frac{8\pi N_T \hbar}{c^4} \right] T_{\mu\nu} \quad (7)$$

wherein N_T stands for $6.32891937 \times 10^{23} \text{ m}\cdot\text{kg}^{-2}\cdot\text{s}^{-1}$ [see relation (3)].

Thus, Newton's gravitational constant G has been removed from the κ term of the EFE and substituted by the $N_T\hbar$ factor. This allows Planck's reduced constant to become a part of the EFE, without sacrificing any accuracy of the mathematical expression. Furthermore, it has been shown by Seshavatharam & Lakshminarayana [3] that the *magnitude* of G can be expressed as:

$$G = \frac{16\pi^4 m_e^{14} \hbar c}{\alpha^2 m_p^{16}} \quad (8)$$

wherein m_e is mass of the electron, α is the fine structure constant, and m_p is mass of the proton. Therefore, one can rearrange this relation as follows:

$$\frac{G}{\hbar} = N_T = \frac{16\pi^4 m_e^{14} c}{\alpha^2 m_p^{16}} \quad (9)$$

And substitute for N_T in relation (7) as follows:

$$G_{\mu\nu} + g_{\mu\nu}\Lambda = \left[\frac{128\pi^5 m_e^{14} \hbar}{\alpha^2 c^3 m_p^{16}} \right] T_{\mu\nu} \quad (10)$$

This should also be an accurate expression of the EFE, but now with additional quantum terms integrated to express the magnitude of κ .

Furthermore, the near-equivalence of the *magnitude* of N_T and N_A allows for the magnitude of Einstein's gravitational constant to be expressed (approximately) as:

$$\kappa = \left[\frac{8\pi N_A \hbar}{c^4} \right] \quad (11)$$

Additionally, we know of several equivalent expressions for N_A as follows:

$$N_A = \frac{R}{k_B} \quad (12)$$

wherein R is the molar gas constant and k_B is Boltzmann's constant.

$$N_A = \frac{F}{e} \quad (13)$$

wherein F is the Faraday constant and e is the elementary charge.

$$N_A = \frac{M_U}{m_U} \quad (14)$$

wherein M_U is the molar mass constant and m_U is the atomic mass constant.

Relations (12) thru (14) are well-known [4]. These relations are mentioned here in order to provide for additional relations (15) thru (17). Thus, Einstein's gravitational constant term κ can also be expressed as follows:

$$\kappa = \left[\frac{8\pi R \hbar}{k_B c^4} \right] \quad (15)$$

wherein the EFE can now incorporate the molar gas constant, Boltzmann's constant, and Planck's reduced constant.

$$\kappa = \left[\frac{8\pi F \hbar}{ec^4} \right] \quad (16)$$

wherein the EFE can now incorporate the Faraday constant, elementary charge e , and Planck's reduced constant.

$$\kappa = \left[\frac{8\pi M_U \hbar}{m_U c^4} \right] \quad (17)$$

wherein the EFE can now incorporate the molar mass constant, the atomic mass constant, and Planck's reduced constant.

Furthermore, if one chooses to insert Newton's gravitational constant G into Einstein's quantum equation for photon energy, $E = h\nu$, one can re-express this relation with Planck's reduced constant, by $E = 2\pi\hbar\nu$, and then substitute G/N_T for \hbar as follows:

$$E = \frac{2\pi G\nu}{N_T} \quad (18)$$

Thus, Newton's gravitational constant can be worked into Einstein's most famous quantum equation. Of course, it is trivial to continue further substitutions for N_T along similar lines as given above. Unfortunately, nothing would be gained by this approach, as this would introduce into Einstein's (and Planck's) original *precise* quantum formula the roughly 5% absolute magnitude error of using N_A as a substitute for N_T . This would be an unacceptably large error in many quantum applications.

3. Discussion

The approach taken above with respect to substituting various empirically-determined quantum terms into the EFE may have some value, given the relative imprecision in measuring G to more than 3 or 4 decimal places. It is conceivable that one or more of the κ substitutions introduced herein [*i.e.*, in relations (10), (11), (15), (16) and (17)], when integrated into the EFE κ term of relation (5), could potentially *improve* upon the accuracy of the EFE employing G alone. Of course, this remains to be determined.

4. Summary and Conclusion

This brief note has described a method by which numerous empirically-determined quantum constants of nature can be substituted into Einstein's field equation for general relativity. This method involves treating the ratio G/\hbar as an empirical constant of nature in its own right. This ratio is represented by a new symbol, N_T . It turns out that the value of N_T ($6.32891937 \times 10^{23} \text{ m}\cdot\text{kg}^{-2}\cdot\text{s}^{-1}$) is within 5% of Avogadro's number N_A , although the units are clearly different. Nevertheless, substitutions of N_A into the EFE, as shown, should yield an absolute value of a similar magnitude to that calculated by the conventional EFE [*i.e.*, relation (5)]. More importantly, perhaps, one or more of these new expressions given for Einstein's gravitational constant term κ may provide a more accurate

result than κ incorporating G . If so, this may have important implications for additional forward progress towards unification. Whether any of these new expressions for Einstein's field equations can move us closer to quantizing gravity remains to be determined.

Data Availability

Due to the purely theoretical nature of this undertaking, no new data were generated or analyzed in support of this research.

Acknowledgements and Dedications

This paper is dedicated to Drs. Stephen Hawking and Roger Penrose for their groundbreaking work on black holes and cosmology. Dr. Tatum also thanks Dr. Rudolph Schild of the Harvard-Smithsonian Center for Astrophysics for his past support and encouragement. Author Seshavatharam is indebted to professors Shri M. Nagaphani Sarma, Chairman, Shri K.V. Krishna Murthy, founder Chairman, Institute of Scientific Research in Vedas (I-SERVE), Hyderabad, India and Shri K.V.R.S. Murthy, former scientist IICT (CSIR), Govt. of India, Director, Research and Development, I-SERVE, for their valuable guidance and great support in developing this subject.

Conflicts of Interest

The authors declare no conflicts of interest regarding the publication of this paper.

References

- [1] Howl, R., Penrose, R. and Fuentes, I. (2019). *New Journal of Physics*, **21**, Article ID: 043047. <https://doi.org/10.1088/1367-2630/ab104a>
- [2] Mohr, P.J., Newell, D.B. and Taylor, B.N. (2020) *Metrologia*, **55**, 125-146.
- [3] Seshavatharam, U.V.S. and Lakshminarayana, S. (2021) *International Journal of Physical Research*, **9**, 42-48.
- [4] Wikipedia Contributors (2021) Avogadro Constant. *Wikipedia, The Free Encyclopedia*. Web. 29 Mar. 2021.

Black Holes in Role, Essence and Function

Wassim S. Daher

Beirut, Lebanon

Email: daherw@terra.net.lb

How to cite this paper: Daher, W.S. (2021) Black Holes in Role, Essence and Function. *Journal of Modern Physics*, 12, 744-760. <https://doi.org/10.4236/jmp.2021.126048>

Received: March 18, 2021

Accepted: May 7, 2021

Published: May 10, 2021

Copyright © 2021 by author(s) and Scientific Research Publishing Inc. This work is licensed under the Creative Commons Attribution International License (CC BY 4.0). <http://creativecommons.org/licenses/by/4.0/>



Open Access

Abstract

This study endeavors to explain black holes through their role, essence and function. It utilizes a customized hypothetico-deductive methodology as a cognitive approach to construct and explain the model. The paper presents schematics as illustrations. Black holes are formed through a clash of Universal energy ripples, or through stellar collapse. Its micro level roles are to: re-cycle cosmological debris, stabilize the formation of galaxies, define the shape of galaxies, and stratify space around them. Their macro role is a subsystem in the preservation of the Universal balance, construct and shape. Black holes are made of two semi-cores of opposite spins. The cores are heterogeneous and made up of structures of dark matter particles. Surrounding the black hole are the process horizon, event horizon, and trap horizon. Primitive cores cannot survive; black holes which collapse to primitive cores decay and vanish. Black holes attract objects via energy fields, where energy tends to accumulate mass for more complex structure development in which more energy colonizes. Photons can either fall on the event horizon or directly cross to the process horizon depending on the black hole structure. This paper has transformed black holes from a set of scattered and vague ideas into structured objects of defined and necessary universal roles. The paper calls for empirical validation or falsification of its model, theoretical model, and hypothesis.

Keywords

Dark Energy, Dark Matter, Energy Ripples, Galaxies, Processing Core

1. Introduction

This paper belongs to a series that endeavors to perceive and comprehend the Universe from a novel perspective. It adopts a customized form of hypothetico-deductive approach [1] [2]. There were different perspectives towards the adopted methodology [3] [4]; however, this paper will not venture further into

the debate [5] [6]. This study assumes a number of theories that make up a hypothetical model of one part of the Universe, the black hole in this case. After the introduction of the model, the theories that build up the model are introduced. Then the hypothesis presents the main ideas on which the whole model relies.

This cognitive paradigm was introduced and discussed in two previous papers [7] [8]. Each paper addresses one aspect of the Universe, as a prerequisite for the following paper. Some of the previously proposed theories may be modified or developed in the process of cognitive presentation as a means of refining the model and not refuting it. The hypothesis is a group of more profound propositions that may call for a revisit of the model should they be falsified.

Objects are primarily identified through their role in the Universe. Their essence remains a secondary aspect necessary for the role. The reason for the existence of any object is its role and contribution to the Universal system. Its existence in its own right is a function of multiple variables that may be related to the local or macro Universal conditions.

Nature is necessarily, according to the cognitive paradigm, an optimizing entity that utilizes its resources of mass and energy efficiently [8]; one can assume multiple objects with multiple roles necessary to preserve this assumption. If, at one location of space, the necessary and essential conditions for the startup of a multiple structures entity, such as a galaxy, exist, then one can assume that debris and failing objects are part of the building process. An optimizing nature necessitates a recycling mechanism as essential for the scheme. Its role is to 'recycle' debris and store or release the constituents, at certain intervals, into space as raw materials for the building process itself. These intervals may depend on thresholds of fluctuations of energy [7] in the vicinity of the black hole. They may also be a function of straying volume of debris, the rate of formation of complex matter, and the strength of the initiating ripple [7] among others. As such, the recycling plant should have adequate ability to attract debris, break it down into primary building materials and release them, ability to release the energy that has been stored in the decomposed structures, and relevant interactive controls.

Another role that is required in the building process is an anchoring structure that acts as a reference for the new forming objects. Due to the huge turbulences created by the Universal dynamics, star dust and formed objects may stray in different directions which may squander the energy and mass involved in the galaxy formation. It is anticipated that planets and stars do change their locations to achieve equilibrium between their buoyancy and other Universal parameters. As such, an anchoring object which regulates the spatial formation of the galaxy is essential in the building process. Any object that, on the macro level, does not have a specific duty, or, on the galactic level, does not fall within the interacting subsystems, may eventually be sucked into a black hole and recycled into raw material.

The formation zones are formed when the ripples initiated by the Universal expansion clash together in a certain locality [7]. This is also coupled by the

energy tendency to attract masses to increase colonization capacity. This is further discussed below.

The ripples are energy waves transmitted through matter structures that fill the space. When the ripples collide, the released energy integrates dark matter and its structures, in the collision vicinity, into more complex forms of matter [7] [8] until they are perceived as star dust. The energy released by the collision of the ripples dictates the stage of integration of matter. Matter may be integrated into just star dust, or straying objects, or stars and planets in subsystems, or galaxies, or objects and subsystems still undefined to humans. The quantity or degree of integration of the produced objects depends on the quantity of energy dissipated by the collision of the ripples.

Energy colonizes matter. Energy tends to accumulate matter in order to form more complex structures through different energy forms and thus more capacity for energy colonization. For example, matter integration starts with one form of energy till nuclear structures are formed, then with sufficient matter available, nuclear energy forms atoms, then with sufficient matter, more energy forms molecules. So, as energy accumulates matter, energy builds itself complex forms and more complex forms for more energy colonization. This energy can be perceived, for instance, as electrical, nuclear, magnetic, chemical or gravitational. In space, the more the mass, the more the colonizing energy, the greater the attraction of other masses in order to build more complex structures.

In the space vicinity of Earth, the attraction among masses is proportional to certain constants and parameters. In other vicinities of space where different conditions may exist, energy may form different matter structures that can colonize more or less “quantities” of energy. In these parts of space, the attraction forces among masses may be proportional to different constants and parameters.

As the object formation stage ends, and the pull towards the formation vicinity weakens or the matter gets exhausted, the formed objects may stray in space. If there exists no pull towards a center, the formed objects eventually scatter in space. The different density zones decompose and the formed objects may even crash with each other.

As the formation energy depletes, nature ends up with objects floating at different density zones, debris, and different matter formations that failed to float away from the formation area. A certain “Object” has to form, organize, and preserve the different density zones, recycle debris, and maintain equilibrium in the newly formed environment, the galaxy. If this Object does not exist, the galaxy disintegrates. This “Object” is referred to as a ‘black hole’.

2. Literature Review

A classic definition of a black hole would be: a body with a high gravitational force such that the escape velocity exceeds the speed of light. Black hole can be defined as a “region where space is falling faster than light” [9].

Black holes have been mainly depicted in mathematical models rather than real

empirical work [10]. Researchers proposed numerous models of black holes. Many of these models were based on the general relativity theory. Penrose calculated, according to relative relativity, a singularity within a black hole [11]. Schwarzschild [12] among others conjectures that non-rotating black holes are perfectly spherical [13] [14] and their size depends on their mass only [15]. Others showed that the shape and size of rotating black holes at a constant velocity, depends on their mass and rate of rotation [16]. Some scientists argue that a black hole has no hair and can be classified via mass, electric charge, and angular momentum [17] others assume an additional scalar field [18] or soft quantum hair [19].

Some scientists believe that the event horizon has a non-decreasing property [10]. Zeldovich and Starobinsky believe that rotating black holes emit particles [10]. Hawking believed that emitting radiation, hawking radiation, is a property of non-rotating black holes as well, from the area outside the event horizon [10]. J. H. Taylor and R. A. Hulse confirmed that moving heavy objects in space, as predicted by the general relativity theory, emit gravitational waves, at the speed of light, which carry energy away from the emitting object. This will cause stars orbiting each other to spiral in towards each other. [20]

Some researchers presume that black holes form by the collapse of stars due to the gravity of their mass [10] [21] where they collapse into a spherical ball of uniform density [22]. Mathur proposed a fuzz ball model of the black hole which eliminates the singularity model [23]. In a string theory interpretation, black holes behave like “ordinary quantum mechanical objects” [24]. Black holes are interpreted as D-Brains in the string theory [24] [25].

3. The Model

This section presents black holes in role, function, and essence. It starts with a discussion of the roles and then continues with an assumption of the essence in light of the function.

3.1. The Role of Black Holes

Considering the local or micro role of the object, there are three possibilities for the intervals of formation of the black hole. Following the assumption of resource optimization, the formation time should be dictated by the necessity of foundation of the object's role/s. The first possibility is that the black hole is created as the first galactic object. This implies that it is the first object in any galaxy; and, it is necessarily the prerequisite for the formation of the galaxy; or it can form after the formation of other galactic objects; or, it can never form if the energy dissipated in the clash is below a certain threshold.

In the case the black hole is the first object to be formed, and there are still abundant energy and matter, a galaxy follows. The black hole is a concentrated center of mass colonized by enormous amounts of energy. Energy tends to attract energy in order to accumulate mass for further energy colonization. This makes it the destination of any and all energy colonized structures in its vicinity.

The structures attracted by the energy pull tendency have various densities. More compacted structures are heavier in density and thus form the first “sea” of matter, “sea 1” around the black hole. Less compacted structures, attracted by the black hole energy, but have less density than the more compacted structures form another sea of matter, sea 2, around sea 1. This continues until the black hole stratifies the space around it (**Figure 1**). The newly formed stars and planets float on/in these seas according to their densities. The stars and planets are attracted to the black hole as energy tends to accumulate mass. However, their density forbids them from sinking into the sea they are floating on.

If energy is abundant and matter is not abundant for the formation of other stars or planets, then matter can be compensated from two sources. The first source is the energy that will integrate simpler mass structures into star dust. The second source is the black hole itself through trapping and disintegrating passing by matter into simpler matter to be utilized by the abundant energy to form stars and planets. Until adequate matter accumulates to form cosmological objects, the black hole remains on its own as a trap for straying objects.

If matter is abundant and energy is not abundant, then the black hole disintegrates some of the matter into simpler forms and releases their stored energy. In this case, there should be more and greater seas of matter around the black hole. The released energy may or may not be enough to form planets or stars. Some smaller and lighter structures may be formed, such as rocks or comets, that float to the furthest sea due to their light density. At that far distances, their energy might not be enough to keep them attracted to the black hole; and thus they may stray in space. A time may come when the black hole consumes all matter in its vicinity without the formation of any galaxies. In this case, where matter and energy are scarce, the black hole remains on its own and may eventually collapse into a primitive core as will be discussed hereafter.

If the black hole is not the first structure to form in a high energy location, then the formed planets or stars will scatter around the region of formation and move around the turbulences of matter distribution around that area. If no black hole forms, the planets may move in irregular orbits forming a temporary galaxy and may end up clashing with each other, or straying in space. If a black hole is formed in the process, and the only way being due to the collapse of a star, then,

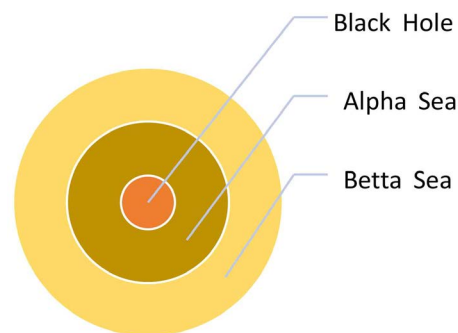


Figure 1. The stratified space around the black hole.

a galaxy may form and survive. The collapse of a star should be due to a strong concentration of energy within its center. This may be due to an energy ripple, or an energy lump in space that the star passed through, or maybe due to a structure deformation at the time of star formation. The structure of the matter comprising the star may have enormous variation in energy content between the surface and the center of the star which renders it unstable and collapsible at the adequate conditions.

These formed planets and stars in the temporary galaxy are relatively dispersed and gets aligned only after the black hole is created. The black hole stratifies the surrounding space, forming seas of matter, that move the formed objects into their balanced positions in the new forming galaxy. In the process, some objects that are dense enough and fail to float on any of the seas will be sucked in and recycled by the black hole. If the black hole is strong enough, and matter is abundant, then it will create seas that cover wider space. Dense objects, denser than sea 1, may all be sucked in and recycled. Nearby galaxies, falling within the seas of the new black hole, may also be sucked in and repositioned or even recycled. In the case a high energy black hole remains on its own, it will stabilize and reorganize the spatial location it exists in, playing a macro role that will be discussed hereafter.

So black holes have numerous essential and necessary roles in the Universe. Their first role is to recycle spatial debris and reproduce them as valid universal building material. As the black hole sucks and decomposes debris, it then releases the material and excess energy into space. The released material may well be the initial universal building particle, the dark matter. It may also release larger formation of particles. Particles released from black holes are much smaller than atoms. As matter gets decomposed into its simplest forms, energy is released. The released energy can be dark energy or other more complex forms. Tremendous quantities of simple released matter form the densest area, alpha, around the black hole. The more complex particles released from the black hole area floats on the alpha area to form the betta area, and so on. Each formed structure of particles floats on the denser structure of particles. This process goes on till the galactic boundary is defined. Planets and planetary systems formed float among the different particle levels (alpha, betta...) according to their relative densities.

A role other than the creation of galaxies is the definition of galactic shapes. The formation of the density zones defines the shape of the galaxy and the scatter of the planets. Galaxies are defined by the intersection of numerous black hole seas. A black hole distributes matter among seas that build above each other due to various densities of particles. The combination of the black holes dictates the shape of the galaxy through the intersection and interaction of different seas of matter. Planetary systems and their orbits are also defined by this interaction. This logic explains the planar planetary systems such as the solar system, which floats on one of the seas. The sun is a simple form of a black hole that creates seas of particles around it as well for planets to float on.

Figure 2 depicts the intersection of the spaces formed by two black holes. The resultant can vary from a disc shaped galaxy, to an ovoid, to other shapes depending on the penetration of the relative seas. If the intersection is among the seas of three main black holes then the galactic shapes become more complex. A galaxy, may in time, include several smaller internal black holes formed by collapsing stars. These black holes change the internal shape and the distribution of planets within the galaxy. The solar system itself, with its flat shape, is either floating on one of the seas of a black hole or is formed by the intersection of the seas of two internal black holes inside the Milky Way.

The black hole can exist for its own right if considered from a macro perspective. There can also be a universal essence for the black hole irrespective of the formation of a galaxy. This role is related to the dynamics of the Universe and the control of its turbulences. Controlling the universal turbulences and absorbing the energy and matter fluctuations are necessary to preserve the shape of the Universe and its balances. The conservation of universal shape [7], the egg shape, has to be supported. The universal expansion process has to be controlled in a manner that impedes a permanent mutation of the shape. For its own preservation and persisting expansion, the shape of the Universe has to maintain its elliptic curvature. This subject is beyond the scope of this paper and will be discussed in future research.

3.2. Energy Fields

Mass, in its own right, is a “dumb” vehicle colonized by energy. Energy has the affinity to lump mass together, else any formation of the simplest structure would be impossible. Energy can only manifest itself through matter. The attraction among matter is therefore the property of the stored energy. Its strength and reach are proportional to the volume of the colonizing energy.

This is referred to as “gravity” and “gravitational field” as exerted by the mass itself according to both theories of Newton and relativity. The proportionality to mass, according to this paper, is not an accurate approach. The proportionality, instead, is to the energy stored within the mass. The difference between the two

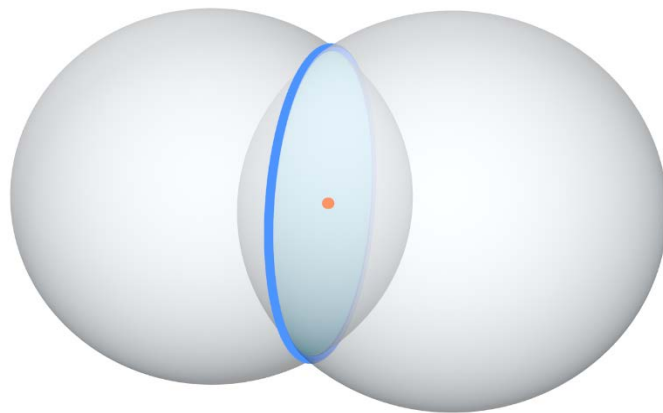


Figure 2. Disc shaped galaxy as an interaction between the seas of two black holes.

paradigms might not stand out in the present “lump sum” approach of modern science or in the macro scale individualistic perspective of our solar system or even of our galaxy. This, however, may drastically change on micro levels, or in systems, galaxies, or even universes other than ours.

Energy colonizes mass. Energy has the affinity to accumulate. In the process, energy pulls mass together. Energy accumulates mass, to build more complex structures also. More complex structures imply more energy stored. More stored energy implies stronger attraction for more mass; and the cycle goes on.

Energy manifests itself in different forms. Such manifestations are on the nuclear level; others are on the atomic or chemical levels. There are other manifestations of energy on the “pre-nuclear” level, such as what has been referred to in a previous paper [8]. These include the forms of energy on the “dark” level which bridge the states of dark matter and nuclear matter. The forms of energy manifestation will be dealt with in future publications.

3.3. Primitive Cores

A primitive core consists solely of dark matter particles. They resemble the state of matter at the end of the compression era [8]. However, a primitive core may not survive if it does not find the means to re-energize itself. Dark matter, in their simplest form and in their own right, cannot store energy. Dark energy builds preliminary structures that encompasses the simplest dark matter particles. These preliminary structures still belong to the dark matter class. As the primitive core consumes its energy, it breaks down these encompassing structures. Its ability to pull the surrounding horizons depletes. The surrounding horizons disintegrate into space. As the encompassing structures are consumed, the core dies and scatters into space.

3.4. The Core

A dark matter particle is the simplest particle in our Universe [8]. It has been formed in the compression era of the universe, small “u”, by the integration of the simplest particle and energy into dark matter particles and dark energy. The compression era has created “Universe” in a vast universe and transformed a definite volume of matter into “Matter”. Dark matter is the simplest form of Matter in the Universe. Energy conveys itself through Matter. Individual dark matter particles cannot store dark energy in excess of the energy stored upon their formation in the compression era. Dark energy requires building up dark matter particle structures in order to colonize them. The core of black holes consists of dark matter particles in structures that hold weak attraction dark matter particles together. The energy stored in dark matter particles is not enough to keep such particles attracted to each other to form structures or objects.

The energy carried in by the energy ripple waves builds structures of dark matter particles. The amount of energy and matter available in the affected location defines the complexity of these structures as conveyed in **Figure 3**.

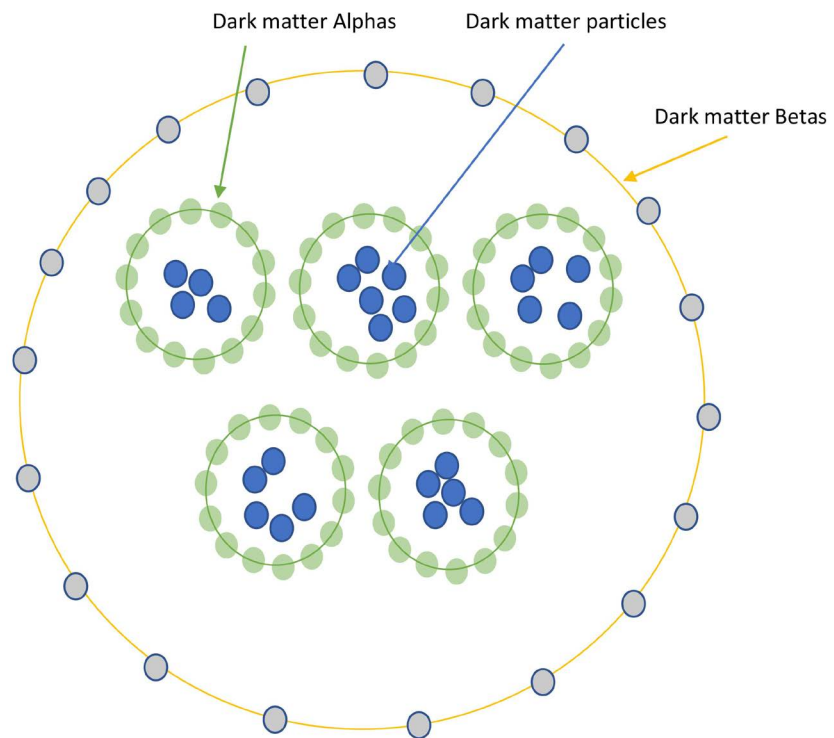


Figure 3. Dark matter structures.

The composition of the processing core is an identity determinant of a black hole. The core consists of a mixture of dark matter particles and simple structures built by these particles. The identity of a black hole varies with the variation of the number of the dark matter particles (D_p) compared to the total number of structured particles (D_s) in the processing core (D_p/D_s). Another defining character is the percentage of each structure in the core per total number of particles (P_t). For alpha particles, for example, it is D_{ap}/P_t . The processing core maintains equilibrium as it continuously processes objects trapped and driven in. The core that consists mainly of alpha particles during equilibrium, will be referred to as “alpha core”. As the flow of trapped objects decreases, and the energy in the location is consumed, dark matter particles decompose the Alpha-particles and D_p/D_s increases. As D_p/D_s increases beyond a threshold, the processing core “collapses” into a primitive core, totally consisting of dark matter particles. The composition of the core of the black hole defines the composition of the event horizon. The same applies for a betta-core as it collapses to an alpha core.

Dark energy in the core renders it turbulent, agitating, and rotating. Dark energy integrates dark matter structures that are crushed and formed again. If enough energy is available, the core integrates from primitive to Alpha particle core or beyond, in a process to store energy for future consumption. Amounts of dark energy escape the core via integrated vehicles of dark matter. If the core is not fed with the required amount of energy to maintain its structure, it will collapse from a Betta core to Alpha core or to a primitive core.

Dark matter particles might have different spins around different axes. In two-dimensions, the spin is either clockwise or anticlockwise. When two particles of the same spin are forced by energy to join, they form a larger structure that preserves the same spin. Momentum is preserved. Other structures of the same spin can join, by energy, to form larger structures with the same spin. Particles of the same spin can join together or repel each other if not able to join. They resemble, more or less, two mechanical gears of the same spin as they approach each other.

At the compression era, when the dark matter particles were formed, part of them had a clockwise spin and the other part a counterclockwise spin, in a two-dimensional perspective. When the expansion era started, and the particles scattered in the Universe, the particles with opposite spins were not distributed equally in all directions. As such, at any given location, one of the spins will prevail. So, at a certain location where the energy ripples hit, and as energy builds dark particles into structures and then objects, the location ends up with two objects of different spins, and with enormous energy colonies, attracting each other, forming the core of the black hole.

The core would be split into two semi-cores with a dominant one (**Figure 4**). The domination is for the larger semi-core. The resultant spin of the two semi-cores would be the spin of the surrounding material extending beyond the event horizon, into the trap horizon.

As the two semi-cores rotate in opposite directions, around two parallel axes, and attracting each other, they suck in material in their direct vicinity (**Figure 5**) from one side, process them, and eject part of them from the other side. The broken material structure would be the same as or smaller than the core particles. If the core is a beta, then the material would be broken into beta, alpha, and dark matter particles. Some of the new energy may be sucked into the core upgrading it, from alpha to beta, or will be stored inside some of the structures by upgrading them into alpha or beta, for example.

Some of the new energy ejects, in their matter built vehicles, out of the black hole and into space (**Figure 6**). The matter vehicles may be structures built from dark matter particles but still smaller than alpha structures in size, for example semi-alpha structures.

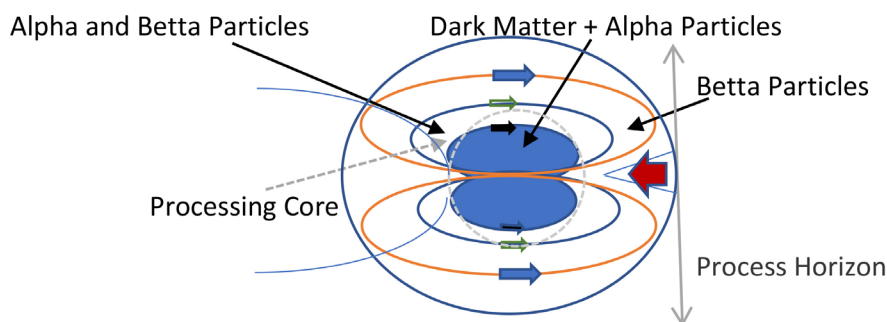


Figure 4. Alpha-core black hole.

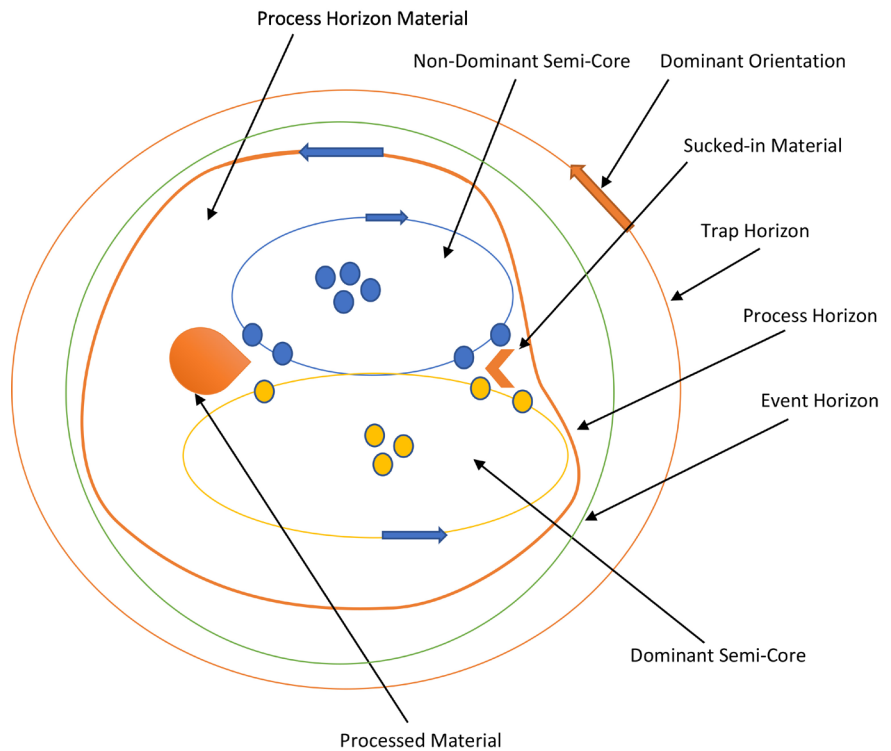


Figure 5. The core of a black hole.

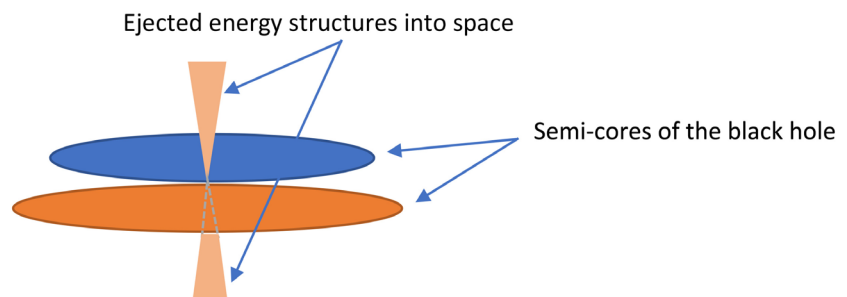


Figure 6. Ejected energy structures from black hole into space.

3.5. The Space of Horizons

The space around the black hole in which objects are subjected to direct and severe impact will be referred to as “area of severe impact”. This area is composed of three main spaces called “horizons” (**Figure 5**). The first is the “process horizon” which comprises material in the direct vicinity of the processing core and rotating around it. These materials are sucked in between the two rotating semi-cores to be decomposed and ejected into space or back into the process horizon for further processing. The material of the processing horizon is what falls in through the well-known event horizon.

The event horizon, in this paper, is the furthest space around the black hole that traps photons. Photons are colonized structures that energy uses as vehicles of transportation [8]. As the energy tends to accumulate mass for further struc-

tural development, photons are attracted to black holes. They penetrate the surrounding horizons until they reach a space comprised of denser structures, a sea of denser structures, on which photons float. That space is called event horizon.

Photons remain rotating in that space till they are broken down by the rotating material into denser structures that can drown further towards the processing horizon. In this case, some energy may escape or get ejected into space in less dense structures than the photons. The event horizon is the “trap horizon” of the photon. The trap horizon is the furthest space around the black hole that traps objects. The trap horizon comprises material orbiting around the black hole. These materials trap and decay passing objects in a particle-blasting effect. The particle-blasted materials sink into the horizons as per their respective densities. The trap horizon radius differs with the densities of the trapped objects. Objects are trapped at different distances from a black hole depending on their particle structures and densities.

For an object to approach a black hole, the buoyancy of the object should be less than force of attraction of the energy. The object, in this case, sinks through the seas of particles towards the black hole. Objects may sink towards black holes in one of several cases. The object may collapse into a heavier object and thus sinks into the sea the object was floating in or on. The object sinks also if the density of the sea the object is floating in or on decreases due to a dying black hole, for example. Another reason for a sinking object toward a black hole may be due to the formation of a new black hole in which a new system of seas is formed.

As the object sinks closer towards the black hole, it reaches a proximity, the trap horizon, where the rotating particles around the black hole particle-blast the object (**Figure 7**). The blasted material rotates around the event horizon. The particle-blasting process continues until the object is totally decomposed. The decomposed material rotates in the trap horizon where parts of it with densities

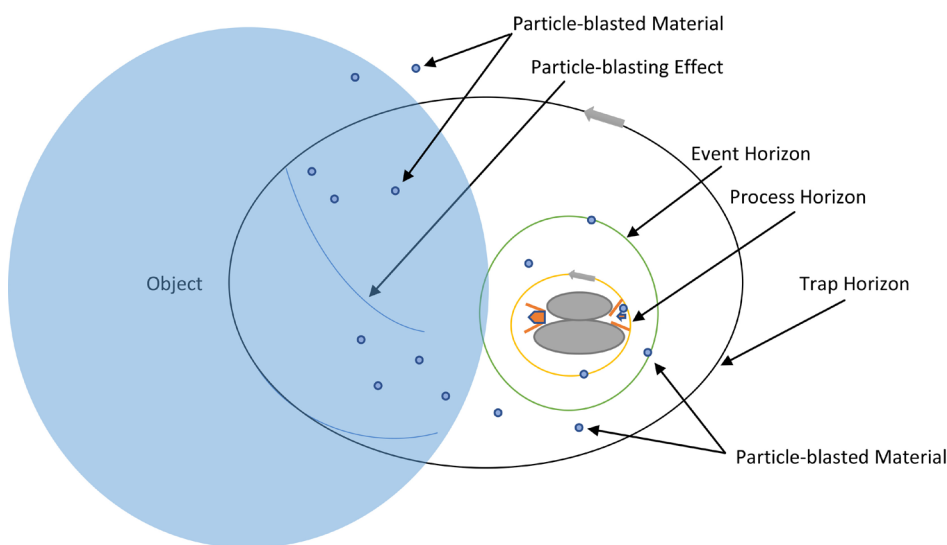


Figure 7. Particle-blasting effect.

much lower than the density of the trap horizon material may float away into space. Some parts may remain rotating within the trap horizon for long periods becoming part of it. Other parts of the material with high densities may sink to the event horizon or the process horizon and into the processing cores.

4. Theoretical Model

1) Energy colonizes matter. Energy accumulates matter forming higher complexity structures through different energy forms and thus greater capacity for energy colonization.

2) Black holes form, organize, and preserve the different density zones, recycle debris, and maintain equilibrium in the newly formed environment, the galaxy.

3) A black hole stratifies the space around it into seas of matter. Matter of similar densities float in the same sea. The seas of matter float over each other as a function of their densities.

4) Black holes are a necessary condition for the formation and survival of galaxies.

5) They define the galactic shape through the formation of the density zones, the seas.

6) The black hole core is split into two semi-cores that rotate in opposite directions.

7) The composition of the processing core and the percentage of each structure in the core per total number of particles (Pt), among others contribute to the identity determinant of a black hole.

8) The area around a black hole is composed of three main spaces called “horizons”: The first is the “process horizon”, then the “event horizon”, then the “trap horizon”.

9) The rotational speed and orientation of the process horizon is defined by the resultant in speed and orientation between the two semi-cores.

10) Primitive core cannot survive.

11) Energy fields are created by the affinity of energy to accumulate mass for further structure development. These structures are developed and colonized by more energy.

12) Photons are trapped by some event horizons depending on their size, else they pass to the process horizon. In the event horizon, photons remain until broken down.

13) Trap horizons differ with different objects. The distance that objects are trapped by a black hole varies according to their structures.

5. Hypothesis

1) Black holes are a necessary condition for the formation of galaxies.

2) Black holes stratify the surrounding space into seas of matter.

3) Black holes have split cores.

4) The cores consist of structures of black matter.

6. Discussion

This paper presents a complete model that, on one hand, explains numerous findings related to black holes, and on the other hand, refutes other related adopted ideas. In spite of the elusiveness of the subject, nature can only be perceived and thought of as an integrated logic. As such, black holes, and as part of nature, can be depicted through their functions, in a simpler endeavor than to comprehend their essence.

Black holes do not reveal themselves to direct observation but rather through their effect on their surrounding [26]. An example is the supermassive black holes at the centre of galaxies in Active Galactic Nuclei [26] [27]. Such black holes are probably the initial ones created as prerequisites for galaxies, as proposed by this paper. Other smaller black holes are scattered through galaxies [9]; as they give the galaxies their shapes through stratification of seas of matter.

Accepted indications of the presence of black holes are the concentration of masses in small spaces; they are assumed to form via collapsing star cores [10] [27]. As energy tends to accumulate matter for integration into more complex structures; and as the dark matter particles are integrated by energy in the ripple clash vicinity into more complex structures; cores of the black holes are formed of compacted dark matter structures.

When a black hole forms after a collapse of two black holes of different sizes, it initially looks like a chestnut, “with a cusp on one side and a wider, smoother back on the other” [28]. Scientists conjectured that black holes are spherical in shape, if they are non-rotating or form due to a gravitational collapse of a non-rotating star. If the black hole is rotating, then it bulges outward near its equator. [10] The chestnut shape of a black hole is depicted in **Figure 5**. It includes the processing cores and the processing horizon.

The probable merger of two black holes initiated gravitational waves detected in 2015 with the Laser Interferometer Gravitational Wave Observatory (LIGO) [29]. This occurrence is explained in this paper as the energy tendency to attract and accumulate matter.

Another phenomena explained by this paper are some of the findings of the Event Horizon Telescope (EHT), namely, what is referred to as the “photon nut” where photons “neither escape to infinity nor fall across the event horizon” [30]. These are photons floating on the event horizon until they are broken into denser structures, and thus fall into the process horizon. They can also be transformed into lighter structures that float with the colonizing energy back into space. This paper explains also the bright ring of emission around the black hole [31], to be the sucked-in and ejected material in the process horizon via the semi-cores of the black hole.

7. Conclusions

There is a limited comprehension among researchers of black holes, in essence, in role and in function. Present tools and instruments of science have not been

able to investigate black holes in essence. These illusive objects are only perceived through their assumed effects on their surroundings.

This paper has invested the power of the mind to explore black holes that, till lately, have only been variables in mathematical equations. A detailed model that respects laws of nature while refuting generally accepted theories has been presented. The model satisfies the necessary universal functions required for an optimizing nature. Then, the structure of the object required to perform those necessary functions has been proposed. The conditions and means for the formation of such objects, namely the black holes, have been presented.

The model to perform has to be structured by milestones defined by a theoretical model that states the main essential ideas for the whole model to work. Statements of the theoretical model can be revisited or modified for an enhanced understanding of black holes. The hypothesis presents the founding ideas for the model. Modification of these statements implies a major modification in the model itself. This research philosophy in its own right can be considered as a road map for empirical research.

Most importantly, this paper has transformed black holes from a set of scattered and vague ideas into structured objects of defined and necessary universal roles. Their necessary correlation with observed phenomena has been explained. Galaxies can only form in the presence of black holes. Multiple black holes define the shapes of galaxies. They also distribute formed stars and planets among the seas of matter the black holes form. Black holes are born and may die and decompose. Subtracting black holes from the Universe renders a chaotic and non-sustainable reality.

Scientific capabilities are still too modest to overcome their limitations in the near future. Mathematical equations can only reflect the limitations of the mind to identify the entailed variables. This paper belongs to a series of research that calls for releasing the human mind from materialistic constraints when it comes to understanding the Universe.

The limitations of the study are in the tools to empirically test and verify the proposed model. The validity of the proposed model may be obtained from the coherence of its ideas. There are some relevant data available; however, the interpretation is still speculative.

The human mind is the most powerful tool for discovering the Universe. Human's comprehension of such a complex system is complemented by one's understanding of its integrated subsystems. Empirical scientists are encouraged to confirm or negate the model building ideas in order to refine it further.

Conflicts of Interest

The author declares no conflicts of interest regarding the publication of this paper.

References

- [1] Smeenk, C. and Ellis, G. (2017) Philosophy of Cosmology. In: Zalta, E.N., Ed., *The*

- Stanford Encyclopedia of Philosophy* (Winter 2017 Edition), The Metaphysics Research Lab, Stanford.
<https://plato.stanford.edu/archives/win2017/entries/cosmology>
- [2] Gale, G. (2019) Cosmology: Methodological Debates in the 1930s and 1940s. In: Zalta, E.N., Ed., *The Stanford Encyclopedia of Philosophy* (Summer 2019 Edition), The Metaphysics Research Lab, Stanford.
<https://plato.stanford.edu/archives/sum2019/entries/cosmology-30s>
 - [3] Milne, E.A. (1934) *Philosophy*, **9**, 19-38.
<https://doi.org/10.1017/S0031819100030564>
 - [4] Milne, E.A. (1929) *The Aims of Mathematical Physics*. Oxford University Press, Oxford.
 - [5] Eddington, A.S. (1939) *The Philosophy of Physical Science*. Macmillan, New York.
 - [6] Whittaker, E.T. (1941) *Proceedings of the Royal Society (Edinburgh)*, **61**, 160-175.
<https://doi.org/10.1017/S0080454100006166>
 - [7] Daher, W. (2017) *International Journal of Sciences: Basic and Applied Research*, **32**, 116-133.
 - [8] Daher, W. (2017) *Global Journal of Science Frontier Research*, **17**, 29.
 - [9] Hamilton, A.J.S. (2020) General Relativity, Black Holes, and Cosmology.
http://timethefinalfrontier.weebly.com/uploads/1/9/7/5/19751121/special_relativity_and_applications.pdf
 - [10] Hawking, S. (1996) *The Illustrated a Brief History of Time*. Bantam Books, New York.
 - [11] Penrose, R. (1965) *Physical Review Letters*, **14**, 57-59.
 - [12] Schwarzschild, K. (1916) *Sitzungsberichte der Königlich Preussischen Akademie der Wissenschaften*, **7**, 189-196.
 - [13] Israel, W. (1986) *Canadian Journal of Physics*, **64**, 120-127.
<https://doi.org/10.1139/p86-018>
 - [14] Israel, W. and Poisson, E. (1990) *Physical Review D: Particles and Fields*, **41**, 1796-1809. <https://doi.org/10.1103/PhysRevD.41.1796>
 - [15] Taylor, E.F. and Wheeler, J.A. (2000) *Exploring Black Holes: Introduction to General Relativity*. Addison Wesley, Boston.
 - [16] Kerr, R.P. (1963) *Physical Review Letters*, **11**, 237-238.
<https://doi.org/10.1103/PhysRevLett.11.237>
 - [17] Misner, C.W., Thorne, K.S. and Wheeler, J.A. (1973) *Gravitation*. W. H. Freeman, San Francisco, 875-876.
 - [18] Zloshchastiev, K.G. (2005) *Physical Review Letters*, **94**, Article ID: 121101.
<https://doi.org/10.1103/PhysRevLett.94.121101>
 - [19] Hawking, S.W., Perry, M.J. and Strominger, A. (2016) *Physical Review Letters*, **116**, Article ID: 231301. <https://doi.org/10.1103/PhysRevLett.116.231301>
 - [20] The Noble Prize (1993) *The Noble Prize in 1993*: Press Release.
 - [21] Chandrasekhar, S. (1931) *Monthly Notices of the Royal Astronomical Society*, **91**, 456-466. <https://doi.org/10.1093/mnras/91.5.456>
 - [22] Oppenheimer, J.R. and Snyder, H. (1939) *Physical Review*, **56**, 455-459.
<https://doi.org/10.1103/PhysRev.56.455>
 - [23] Mathur, S.D. (2008) *Journal of Computational and Theoretical Nanoscience*, **2**, No. 2.

- [24] Maldacena, J. (2011) Black Holes and the Information Paradox in String Theory.
<https://www.ias.edu/ideas/2011/maldacena-black-holes-string-theory>
https://doi.org/10.1142/9789814374552_0004
- [25] Polchinski, J. (1995) *Physical Review Letters*, **75**, 4724-4727.
<https://doi.org/10.1103/PhysRevLett.75.4724>
- [26] Seyfert, C.K. (1943) *The Astrophysical Journal*, **97**, 28-40.
<https://doi.org/10.1086/144488>
- [27] McClintock, J.E. (2011) Measuring the Spins of Accreting Black Holes.
- [28] Calderon Bustillo, J., *et al.* (2020) *Communications Physics*, **3**, 176.
- [29] Abbott, *et al.* (2016) *Physical Review Letters*, **116**, Article ID: 061102.
<https://doi.org/10.1038/s42005-020-00446-7>
- [30] Johnson, M.D., *et al.* (2020) *Science Advances*, **6**, eaaz1310.
- [31] Akiyama, K., *et al.* (2019) *The Astrophysical Journal Letters*, **875**, L1.
<https://doi.org/10.1126/sciadv.aaz1310>

Detection and Determination of the Variation of the Speed of Time

Robert M. L. Baker¹, Bonnie Sue Baker², Fangyu Li³

¹Gravwave LLC, Playa del Rey, USA

²Transportation Sciences Corporation, Gravitational-Wave Department, Playa del Rey, USA

³Department of Physics, Chongqing University, Chongqing, China

Email: drrobert@gravwave.com, bonniesuebaker@gmail.com, fangyuli@cqu.edu.cn

How to cite this paper: Baker, R.M.L., Baker, B.S. and Li, F.Y. (2021) Detection and Determination of the Variation of the Speed of Time. *Journal of Modern Physics*, 12, 761-780.

<https://doi.org/10.4236/jmp.2021.126049>

Received: March 2, 2021

Accepted: May 9, 2021

Published: May 12, 2021

Copyright © 2021 by author(s) and Scientific Research Publishing Inc. This work is licensed under the Creative Commons Attribution International License (CC BY 4.0).

<http://creativecommons.org/licenses/by/4.0/>



Open Access

Abstract

Steadily increasing time is involved in most scientific analyses. Like other dimensions in spacetime we suggest that there can be a variation rate of time's progress or speed of time in the time dimension. We study speed-of-time variation observational data in three processes: muon decay, galaxy rotation (related to dark matter) and the separation speed of celestial objects as our Universe progresses (related to dark energy). Each of these processes will have an "observed value" of their time of completion P_o from an observation of the process at time t_1 and an "expected value" P_e of that time at time t_2 . Their difference is attributed to the variation of the speed of time. We provide a possible explanation for the anomalous separation of the observed and the expected galactic velocity curves. Our conclusion is that it is unnecessary to introduce dark matter or dark energy.

Keywords

Early Universe, High-Frequency Gravitational Waves, High-Frequency Relic Gravitational Waves, Primordial Gravitational Waves, Cosmology, Speed of Time, Dark Matter, Dark Energy, Galactic Velocity Curves

1. Introduction

We believe that although time, as a steadily increasing independent variable, is involved in almost all scientific analyses, time's rate of change (speed of time) and the variation of that speed should also be involved. We suggest that time, like the motion of objects moving in the three space dimensions, can increase or decrease at a variable rate. Similar to the hands of a watch moving fast or slow, this change in the speed of time could be almost trivially small or very large. In

the standard cosmological model, the early universe was very smooth (homogeneous), but we suggest that since the beginning of our Universe entropy's evolution should be inhomogeneous, that is the rate of entropy increase cannot be uniform. Because the direction of the time arrow depends on the "direction" of entropy increase, the speed of time should also depend on the "speed" of entropy increase. In this case, if the entropy of the whole Universe has been increasing and entropy's speed is slowing down, then the speed of time is also slowing down! Here we apply the speed-of-time concept to observational data concerning three different physical processes: muon decay time, the rotational speed of the observable portions of a galaxy (related to dark matter) and the separation speed of celestial-objects as our Universe progresses (related to dark energy).

We also suggest that the detection of High-Frequency Gravitational Waves (HFGWs) is an essential observational tool for examining the speed-of-time concept:

1) Unlike the low-frequency gravitational waves (e.g., the gravitational waves generated by the merger of black holes or neutron stars) HFGWs are generated less than a nanosecond after the beginning of our Universe. We believe these primordial or relic HFGWs were generated by processes occurring when the speed of time in our early Universe was extremely fast.

2) Today almost all mainstream cosmological inflation models expect that the upper limit of the frequencies of primordial HFGWs should be GHz or higher. This means that the period of the primordial HFGWs is about 10^{-9} seconds or less. That time may be about the time necessary to complete an oscillation or essentially the time to complete some activity or process in our early Universe.

3) We contend that primordial or relic HFGWs were propagated before our Universe became transparent to electromagnetic radiation. If such primordial HFGWs can be detected by the HFGW detector, discussed in connection with our analyses of Muon decay, then their observations may not only contain information on the speed of time, but information, gained by means of the analyses of the HFGW frequency spectrum produced by the processes themselves.

4) In the future detection of primordial high-frequency gravitational waves, it seems necessary to distinguish what is the increase of the wavelength of the primordial gravitational waves due to the possible expansion of the Universe (*i.e.*, the decrease of the frequency), and what is the decrease of the frequency due to the decrease of the speed of time, as our Universe ages. This determination may not only be a challenge, but also an important opportunity in the study of cosmology.

5) The observed speed of the stars comprising the periphery of nearby galaxies can be overestimated. Such an overestimates may be caused by the Doppler observation of stars beyond in spacetime the galaxy being miss-associated to be an actual peripheral galactic star. Since a star beyond the nearby galaxy would be further from the Earth than the galaxy and closer to the beginning of our Universe, they would be in a spacetime region of higher time speed and therefore higher apparent star speed relative to the observer on our Earth. Thus we may be fooled into associating them with the galactic stars and thereby overestimating the observational average speed of the peripheral galactic stars.

We will also discuss processes that do not depend internally on the three space dimensions and are independent of the time-varying flow of time in our Universe. We call them Non-Varying-Rate-of-Time (NVRT) processes and suggest muon decay as an example of a NVRT process.

Most processes depend upon various parameters and variables, such as a , b , c ... and time, but here we single out time as the variable of interest. We propose that the best way to determine the speed of time is to compare the same physical process at two different times. Each process, P , will have an “observed value” of the process’ time of completion, P_o , from an observation of the process at time t_1 and an “expected value” of P_e as the process time is expected to be at another time t_2 . Time t_2 is usually considered in this discussion to be a time in the past when the photons left the process P . Or in the case of muon decay, when the process time, P_0 was obtained and recorded in the past at a time t_1 . If time is not progressing steadily and uniformly, then we attribute any variation of the expected Process $P_e(t_2)$ time from the Process time we actually observe or actually record, $P_o(t_1)$, to a variation of the speed of time. The fundamental equation relating $P_o(t_1)$ and $P_e(t_2)$ to determine the variation of the speed of time, V_{st} is:

$$V_{st} = [P_o(t_1) - P_e(t_2)] / (t_1 - t_2). \quad (1)$$

If the observed time for a single cycle or for the completion of a Process, P_o is exactly the same as the expected time for such a process, P_e then time running smoothly with no variation, in which case is the Variation of the Speed of time is zero.

The Processes of interest and our expectations for them are:

- 1) The expected duration of muon decay at t_2 , $P_e(t_2)$, is equal to the last measured value of muon decay time in picoseconds, at t_1 .
- 2) The inverse of the expected speed of a portion of the visible disk of a galaxy at t_2 , $P_e(t_2)$, in seconds as based upon conventional Astrodynamics [1] [2].
- 3) The expected value of the speed of separation of a celestial object at t_2 , $P_e(t_2)$, is established by a “proposed” expansion theory of our Universe, here taken to be that the separation speed should be the same everywhere in our Universe (also that the Hubble “constant” is approximately 70 km/s per Mpc or 2×10^{-18} [m/s per meter] or approximately $1/5 \times 10^{17}$ seconds) therefore we express the expected cosmic object’s speed in fractions of the Hubble “constant” in seconds, to be equal everywhere in our Universe.

2. Muon Decay Time to Measure the Variation of the Speed of Time

The most accurate time measurements of Process time in a laboratory on Earth were found to be the decay time of Muon’s as measured by atomic or nuclear clocks. Muons are produced when cosmic rays strike atomic nuclei of molecules in the air and quickly decay over a fixed time interval. Muons can also be produced in a two-step process at large research facilities. High energy protons (>500 MeV) generated by a particle accelerator collide into a carbon or beryllium target and generate Muons.

The earliest measurement of muon decay time that we found was made in 1946 of 2,330,000 ps [3]. A more accurate measurement of muon-decay time found was 2,202,000 picoseconds (ps) by Eckhause, *et al.* in 1963 as part of the Olive, Particle Data Group [4] findings. The most accurate muon-decay time found so far was made by Webber and a group called the *MuLan Collaboration* in 2011 of 2,196,980 ps [5].

After further search of the literature a mysterious trend appeared: the duration of muon decay, which should be a constant, appears to shorten gradually, perhaps irregularly (including pauses and acceleration or lengthening), from 1946 to 2017 from very roughly 2.330 microseconds (1946) to very roughly 2.202 microseconds (1962-1963) by Lindy [6] and could be a basis for the detection and determination of the variation of the speed of time effect in laboratories on Earth independent of relativistic effects, that is if it is found that the shortening of muon decay time continues to be observed.

All of these observable data are exhibited in **Table 1** and graphed in **Figure 1**.

The 1946 *Conversi, et al.* measurement's estimated error was so large as to be eliminated, except as Clive Woods suggested, "... that if outliers were eliminated, then any possible trend might be masked." Therefore, if we include the 1946 *Conversi, et al.* measurement, we take the decay-time difference between both

Table 1. Review of length of apparent muon decay time versus time.

Date of Measurement	Apparent Muon Decay Time (Picoseconds)	Estimated Error (Picoseconds)	Muons at Rest or in high-speed Cosmic-ray generated Motion?	Reference
1946.0	2,330,000	±150,000	At Rest	Conversi, Pancini, Piccioni [3]
1962.0	2,203,000	±4000	At Rest	Lindy [6]
1963.0	2,202,000	±3000	At Rest	Eckhause, <i>et al.</i> [4]
1973.0	2,197,300	±300	At Rest	Duclos in Olive. [4]
1974.0	2,197,110	±80	At Rest	Balandin in Olive. [4]
1984.0	2,196,950	±60	At Rest	Giovanetti in Olive. [4]
1984.0	2,197,078	±73	At Rest	Bardin in Olive. [4]
2007.0	2,197,013	±21	At Rest	Chitwood in Olive. [4]
2008.0	2,197,083	±32	At Rest	Barczyk in Olive. [4]
2008.5	2,197,030	± 40	At Rest	Coan & Ye in Olive [4]
2009.5	2,196,980.3	±2.2	At Rest	Webber/MuLan [5]
2013.0	2,196,980.3	±2	At Rest; a copy of 2009.5 measurement	Tischchenko [7]
2015.0 ²	2,110,000	±70,000	Fast, Cosmic Ray	Barazandeh [8]
2015.0 ²	2,165,000	±403,000	Fast, Cosmic Ray	Barazandeh [8]
2016.0	2,078,000	±11,000	At Rest	Physics OpenLab [9]
2017.0	2,080,000	± 11,000	At Rest	Adams [10]

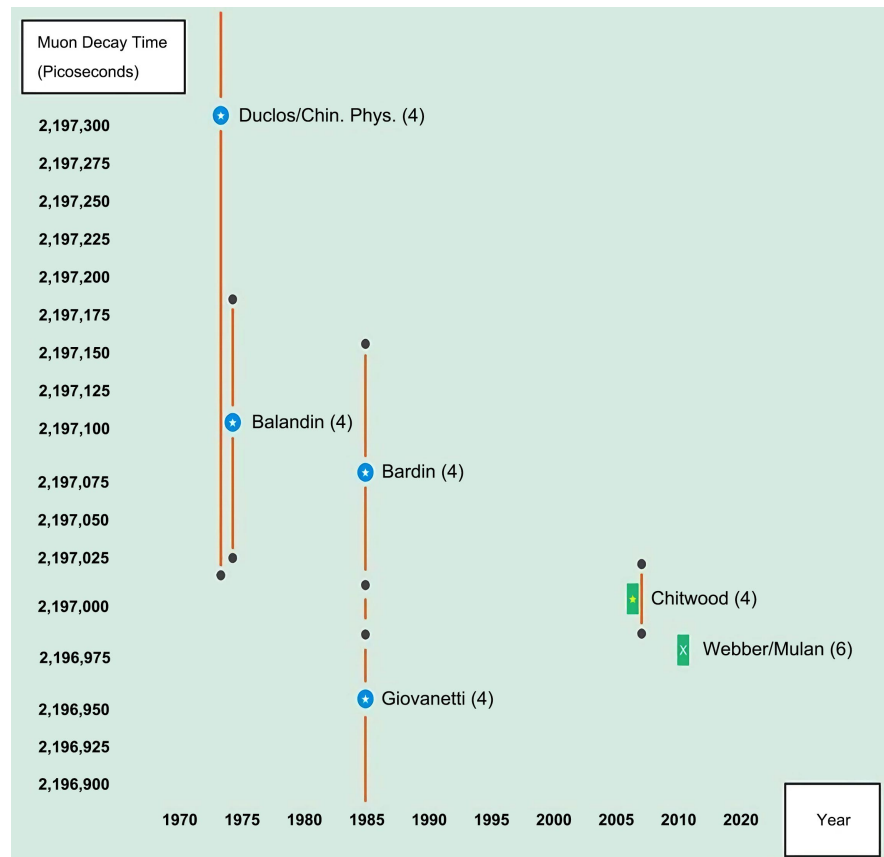


Figure 1. Data from **Table 1** and Fig. 1a, page 63 of [1]).

outliers, with $P_e = 2,330,000$ ps (we expect it to be exactly as measured most recently) and $P_o = 2,080,000$ ps (most recent 2017 measurement) over the time interval of $t_2 - t_1 = 2017 - 1946 = 71$ years, then the variation of the speed of time from Equation (1) would be

$$(2080000 - 2330000)/71 = -3521 \text{ ps/year} . \quad (1a)$$

If the outliers are eliminated and only the more accurate MuLan data utilize, then $P_e = 2,197,013$ ps [4] and $P_o = 2,196,980.3$ ps [5] over the time interval of $t_2 - t_1 = 2009.5 - 2007 = 2.5$ years, then the variation of the speed of time from Equation (1) would be

$$(2196980.3 - 2197013)/2.5 = -13 \text{ ps/year} . \quad (1b)$$

In any event, the **Table 1** exhibits most of the more accurate muon-decay times found and their estimated error. We recognize that the slowdown of clocks in ps per year, probably itself decreases or increases as time increases. Therefore, there may have been an actual “accelerated or decelerated slowdown” after the beginning of our Universe! However prior to this analysis, there was no a priori observational data of muon-decay time analyzed to indicate with certainty either a constant or a varying slowdown or speedup of the rate of time.

Under the supposition or working hypothesis that the aforementioned decrease in muon-decay time shortens as time increases, an interesting conjecture

immerses: that the muon-decay process operates with a different “clock” or change in the speed of time, compared with the clock with which the rest of our Universe operates! Is there a possibility that muon decay has a clock that runs without variation at a fast or slower pace as time progresses? Under this assumption or working hypothesis the rate of slowdown of the time in our Universe is computed to be very roughly (not enough data to support a valid estimate of error) of between very approximately -13 ps per year (or -4.1×10^{-19} s/s) and -3500 ps per year (or -1.1×10^{-16} s/s) during the 71 year period between 1946 and 2017. Since we have no other muon-decay times to analyze, we will make the provisional assumption that the muon-decay rate of time change in our Universe does not remain a constant, but becomes smaller as the time in our Universe increases! There are 2.2×10^9 seconds in 71 years so the rate of the assumed rate of change is $([3500 - 13] \times 10^{-12} \text{ seconds}) / 2.2 \times 10^9 \text{ seconds} = -1.6 \times 10^{-19} \text{ s/s}$. Therefore in this case, with the 71 years centered about 1981, or approximately 4.32×10^{17} seconds since the beginning of our Universe. These slowdowns per second over 71 years are very approximate and call for more Muon-decay measurements having higher accuracy as well as more data on muon-decay-time found from other past times.

Figure 2 is a Notional plot of the change in the speed of time variation as a

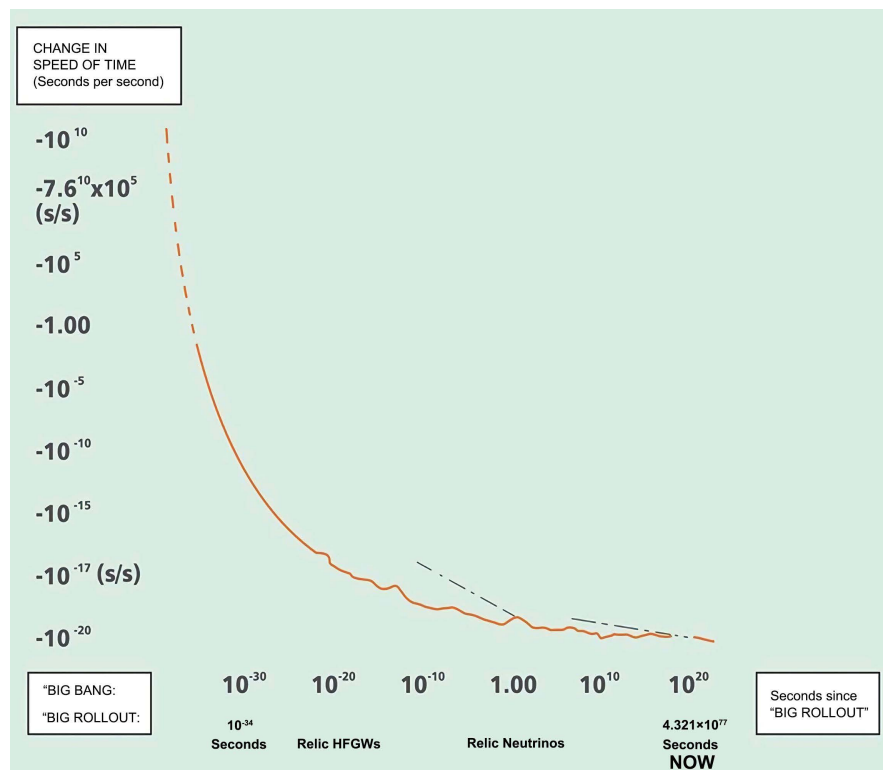


Figure 2. Notional graph from Fig. 3 of [11] of the change-of-speed-of-time variation with today’s time dimension. The Figure is only a schematic and not intended for detailed analyses. Notice different slopes (tangents) and irregularities and the current time rate of about 10^{-17} seconds per second between 10^{-15} and 10^{-20} seconds per second shown by the expanded graduation scale on the ordinate near the “BIG BANG” or “BIG ROLLOUT”.

function of the time since the “Big Bang” or “Big Rollout” taken from Fig. 3 of [11]. It is only schematic and not intended for detailed analyses. The substantial increase in the speed of time value in the Notional and schematic graph of **Figure 2**, a nanosecond or less after the beginning of our Universe, is based upon our Rollout Theory of the beginning of our Universe and the high speed of time near the beginning of our Universe proposed by Baker [12]. The detection of High-Frequency Gravitational Waves (HFGWs) generated by processes occurring less than a nanosecond after the beginning of our Universe would provide the most important fundamental data for the formulation of a theory on the variation of the speed of time! The specific data points on the very approximate curve, quite close in time to our Universe’s beginning would be disclosed by a study of the HFGWs emanating from the early Universe. Such a study could be obtained through utilization of the effect found by Li [13] and the Li-Baker HFGW Detector [14] as well as the analysis of the sensitivity and utilization of that Detector [15] [16] [17].

We assert that the Rollout Theory for our Universe [12] is simpler than some portions of the conventional Theory for the Big Bang: such as “...that the nascent Universe passed through a phase of exponential expansion soon after the Big Bang, driven by a positive vacuum energy density” (see Fig. 1 of [12]). Whereas the proposed Rollout Theory depends upon the simple concept that our Universe is similar to an ordinary clock or wristwatch that is slowing down as it ages, therefore by Occam’s razor the Rollout Theory is preferable.

Although it would not affect the correctness of the theorized Theory of our Universe [12], more accurate measurements of muon decay time are needed in order to actually calculate an accurate local variation of the speed of time on Earth or indicate that muon decay time does not change with time and does not have its own “clock.” The speed of time and/or the speed of time’s variation may well depend upon “where” one measures the variation on the fabric of spacetime and/or the local mass distribution of matter or some other feature of our Universe! There may be a number of alternatives to this slowing-of-time analysis, but since time slowing in our Universe has some bearing on two other processes to be considered in this study, we will continue with it.

3. Rotational Speed of a Portion of the Visible Disk of a Galaxy to Measure the Variation of the Speed of Time

If the rate of time was greater in the past (these observations come from photons produced by galaxies millions or billions of years ago), then galaxies would **appear** to us today, with our slower clocks, to be rotating faster just as a watch in the past, if seen today, would appear to be moving its hands faster than our slower clocks as seen today as in **Figure 3**.

As discussed on pages 71-72 of [11] the galaxies do not rotate like a solid top. Rather the galactic stellar material rotates at different rates depending primarily upon their radial distance from the galaxy’s center. In **Figure 4** the grey dashed

Galaxies APPEAR to rotate faster in the past if time was moving faster then. Astronomers have attributed this to a lot more mass or matter in them that holds them together so they can rotate fast and not pull apart. They call it “dark matter”



Figure 3. Rotational rate of galaxies.

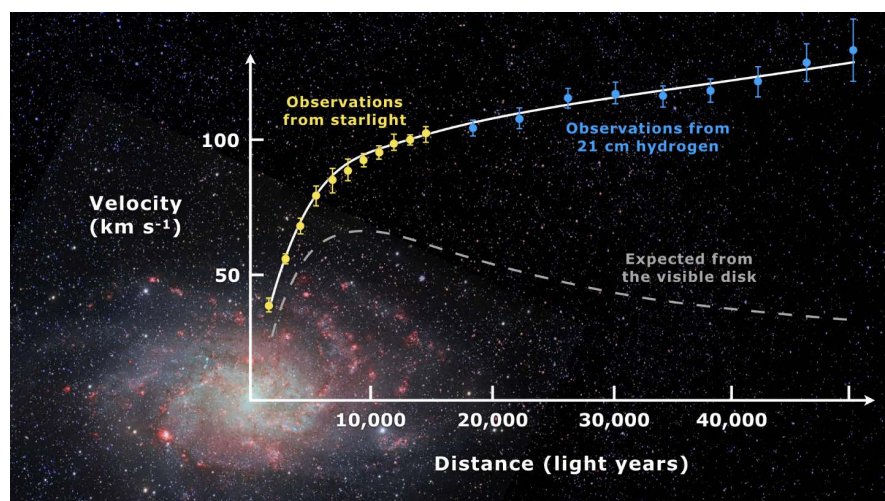


Figure 4. Typical galactic velocity curves. The upper-solid white-line curve is the observational data from galactic starlight (yellow data points) and radio-astronomy spectral analysis (blue data points) of the observed speed of galactic portions at various radial distances out from the galactic center of a typical galaxy such as Messier 33. The lower dashed-grey-line (speed) curves exhibit the expected speed, at the same radial distances, utilizing Astrodynamics [1] [2].

line exhibits the magnitude of the vector velocity in kilometers per second of stars in the galactic disk. It is obtained by Astrodynamics analyses [1] [2] of various galactic stars as a function of their radial distance in light years. The observed speed from the portion of the visible disk of a galaxy as measured from the Doppler Effect utilizing spectral data is shown by the solid white curve in **Figure 4**.

Consider the observational data for the galaxy, Messier 33, about 2.73 million light years away from the Earth as shown graphically in **Figure 4**. We will extract approximate values of the pertinent data from measurements of the drawing. This nearby galaxy is about the same distance from the beginning of our Universe as is the Earth. Consider a Doppler speed observation, P_o , of the luminous matter that shows the observed (by Doppler spectral analyses) tangential speed of “rotation” of a portion of the arms of the galaxy to be about 100 km/s at about

10,000 light years distant from the center of that galaxy. We will initially consider that distance from the galactic center for calculation since this observable part of a galaxy is moving at the maximum speed of galactic material approximately shown in **Figure 4**. The circumference of the assumed circular orbit of a galactic star (turns out to be a very poor assumption as will be discussed) at this 10,000 light year distance or 9.46×10^{16} km radius, is $2\pi \times 9.46 \times 10^{16}$ km = 5.94×10^{17} km. Therefore as observed, this requires 5.94×10^{17} km/(100 km/s) = 5.94×10^{15} seconds to complete one revolution or one orbital period of a star's circular orbit. The calculated and expected tangential speed, derived by applying conventional gravitational or Astrodynamic theory, is $(65/100) \times 5.94 \times 10^{15} = 3.86 \times 10^{15}$ seconds to complete one revolution or one orbital period. In order to compute Equation (1), we insert the difference between these two times and divide by the number of years for the photons to reach the Earth, $t_1 - t_2 = -2.73 \times 10^6$ years. Therefore the speed of time change at this position on the galaxy is $(5.94 \times 10^{15} - 3.86 \times 10^{15}) / 2.73 \times 10^6 = 6.52 \times 10^8$ seconds per year! Compared to muon-decay computed speed of time on the Earth, this is extremely large. As will be emphasized later, such an enormous speed of time is based upon a completely erroneous, although interesting, assumption of a circular galactic orbit and will be discarded. Furthermore, from **Figure 4**, the speed of time would appear to increase in a very anomalous fashion, even more so out nearer the periphery of the Messier 33 galaxy! As will be discussed, due to an increase in the speed of time in the past and miss-associated "background" stars measured, there may well be an over estimate of the speed of the galactic stars and especially miss association of these distant in spacetime apparently fast-moving stars with the galactic stars. Therefore in **Figure 4**, the upper solid line of observed Doppler-Effect observations could in actuality be much slower and closer, but might not overlap the lower estimated value of galactic rotational speed based upon conventional gravitational or Astrodynamic theory. The speed of stars beyond the 40,000 light-year radius are no doubt unrelated to Messier 33 and are observed from our Earth as having higher apparent speeds as our universe rolls out. In this case, the actual 21-cm spectral-line-shift observational data of **Figure 4** show those apparent stellar speeds due to the predicated slowdown of time from very high speeds, on average approach about 150 km/s in the region of observable spacetime near Messier 33 and supports the new Rollout Theory [12].

To measure the rotation of a galaxy, observations must take into consideration the average shift of the spectrum of the galaxy. This will almost always result in a net spectral redshift for galactic stars, since it includes the expansion of the universe, and also our solar system's motion around the galaxy we are observing (the rotation of our planet, our orbit around the Sun, the Sun's motion around the galaxy, and the galaxy moving through the universe). The more rapidly the galaxy rotates the more the red shift. Distant stars in spacetime, further and older than a given galaxy, show a larger red shift the faster time is moving in their spacetime region. Therefore, if mistaken for galactic stars then an erroneous higher galactic

rotational rate and “velocity curve” is mistakenly observed for the galaxy.

We must realize however, that the assumption of circular orbits for the observed stars is incorrect! We have no good information about how those orbits really are shaped. A far more fundamental concern is that “speed” is a scalar and not dependent on the trajectory of the speeding object. An analogy is that a 4-minute-mile Track Runner’s speed at a given point is not measured by “distance per mile run per 240 seconds” or for a marathon runner not measured by “26.2 miles in so many seconds” or for a galactic star not measured by “single orbit distance per orbital period.”! No, it is actually based upon the inverse of the time to move a given reference distance. In measuring the speed with which stars move in a galaxy it is for example the number of seconds to move a kilometer or a meter. Therefore, the P_0 observed process time shown in **Figure 4** is approximately 1/100 km/second or 0.01 seconds “per kilometer” and the P_e expected process time also roughly measured from **Figure 4** is approximately 1/64 km/second or 0.0156 seconds “per kilometer”. The expected process takes about 2.73 million years to reach the Earth, so $t_1 - t_2 = 2.732.73 \times 10^6$ years and Equation (1) is

$$\begin{aligned} & (0.010 - 0.0156) / 2.732.73 \times 10^6 \\ & = -2.08 \times 10^{-9} \text{ seconds per year or } -2.080 \text{ ps per year} \end{aligned} \quad (1c)$$

A big difference from the orbital-period approach, but probably within the possible error of the relatively nearby Earth’s muon decay speed-of-time determination of -13 ps/year to -3521 ps/year. Also this rate of time determined by spectral analyses is possibly underestimated because of time dilation plus gravitational potential!

As already emphasized, the significant departure of the observed speed of galactic portions from the expected speed in **Figure 4** is important and supports the Rollout Theory of our Universe. The expected speed is based upon orbital analyses. The motion of the stars in a galaxy is considered to be an n -body problem discussed, for example, in Section 2.1 of (2). There exist no general analytical solutions for $n > 2$, therefore *General Perturbations* do not apply and one must utilize *Special Perturbations* or numerical integration as discussed in Chapter 3 and Appendix D of (2). Presumably such techniques, including the effects of special and general relativity, GS and GR, were employed in the generation of the expected curve in **Figure 4**. The observed curve in **Figure 4** involves the variation of the speed of time. We consider that curve at about a 40,000 light year radial distance. We discussed the rather startling departure of the observed speed and the “expected” speed for this very nearby Galaxy. Therefore, the P_0 observed process time shown in **Figure 4** for radial distances less than 30,000 light years is very approximately 1/120 km/second or 0.000,008,3 seconds “per meter” and the P_e expected process time also roughly measured from **Figure 4** is very approximately 1/40 km/second or roughly 0.000,025 seconds “per meter”. Note that in this case we use the standard meter not the kilometer for analysis! Therefore, from Equation (1)

$$\begin{aligned} & (0.000,0083 - 0.000,025) / 2.73 \times 10^6 \\ & = -6.12 \times 10^{-12} \text{ seconds per year} = -6.12 \text{ ps/year} \end{aligned} \quad (1d)$$

But, of course, we should not jump to conclusions since the speed of the stars at the periphery of the Galaxy may include Doppler observations of those stars at a greater distance OBSERVED THROUGH the periphery of the Galaxy and operating in a higher-speed-of-time spacetime region of our Universe! However also recall that possibly the variation of the speed of time may also be dependent on the density of surrounding matter of the galaxy or other characteristics of the nearby features of spacetime. Like calculations based upon other observational data, this apparent increase the speed of time or cosmological effect (CE) must be taken into account in any comprehensive Theory developed for the change in the speed of time in our Universe. As has been pointed out, so far there is no *a priori* means to establish the speed of time. Let the observational data be our guide to a Theory of Time!

4. Separation Speed of Celestial Objects to Measure the Speed of Time

The Hubble Space Telescope (HST) observations of the stellar-object-separation speed of very distant supernovae showed that, a long time ago (billions of years ago), the universe was actually expanding more slowly than today. So the expansion of the universe apparently has not been slowing due to gravity, as it should! The expansion has apparently been accelerating! No one expected this since gravity should be slowing speeds down. No one knew how to explain the situation except to invent some invisible “dark energy” caused acceleration. So far no one has been able to detect this dark energy-truly a mystery! But wait! How is the speed of these very distant celestial objects’ relative to our Earth measured? Again, like the speeds of portions of a galaxy, the speed is measured by the Doppler Effect!

According to our working hypothesis [12], the speed of time was greater in the past. Since we can only see stars as they were in the past, we suggest that speed of time was greater in the vicinity of those stars we observe and greater and greater the farther away they are (their photons taking longer to reach us). The situation is just like viewing a scene with a variable-rate movie projector. In an old movie projection suppose the film was moving faster through the movie projector than usual, like the time moving faster. The situation is that the people on the movie scene appeared to be moving fast, but their actual speed was the same, usual speed! In order to illustrate this point, let’s consider another situation: From an observatory here, violin strings in a billions of light-year distant place with time running fast, would appear to vibrate faster and, if it were possible to hear the violin, then the violin’s pitch would appear to be higher (like a spectrum showing a higher frequency and being more blue and less red). However, inside that billions of light-years away concert hall the violin strings would not appear to vibrate faster and violin’s pitch would be unchanged! In fine, as we have just discussed, if time is running faster in a receding star’s vicinity, then the reddening of stars will appear

to be less since their spectra appears to move toward the bluer, higher frequency end and diminishes the observed Doppler-Effect-determined speed (as already noted, time dilation and gravitational potential have the opposite, *i.e.*, cause a more reddening, effect). The situation would seem to a casual observer that the higher speed of time in the past would make the receding speed of celestial objects increased or seem faster. This is not the case, the receding speed appears decreased as measured with a Doppler-measurement due to increased speed of time! That is, due to an increased speed of time, the star's receding speed is actually larger than the spectral, Doppler-determined, receding speed shows! We will now explain in more detail this situation by the following story: A scientist sits in a train station and requests the station manager to tell him how fast the trains are moving when a receding train reaches a mile-away point. Like the recessional speeds of celestial objects, the scientist only considers the recessional speed of the trains. The first train to pass is going at a 30 mph, recessional speed at the mile-away point down the track. The scientist notes in his log book that the receding train's-whistles frequency drops a little from the whistle's normal frequency at the one-mile distance point. Of course this frequency drop seems reasonable, since the whistle's sound waves are stretched out a little as the train recedes. The second train to pass is moving at 60 mph and the receding train's whistles frequency drops at the mile down-track point even more since the sound waves are stretched out even more by the rapidly receding train's whistle. The scientist records the whistle frequencies in his log of train-whistle frequencies for train receding at different speeds. He observes that receding train Whistle's frequencies drop more for faster receding trains since the sound waves are even more stretched out. The next day another train passes and the scientist wants to test out his work. The scientist tells the station manager that according to his log he expected that, from the frequency of the whistle, the currently receding train is going 30 mph. "No" says the station manager "...from my actual observations the train is moving at 60 mph mile at the down the track point from you." The scientist exclaims "But the sound waves are not stretched out as much and their frequency is not low enough for 60 mph". The station manager states that the actual pitch or frequency of this train's whistle had been changed by the Mechanics last night to a much higher frequency so the sound waves seem STRETCHED OUT like a 30 mph train! In the case of a receding stellar object, the increase in frequency is not accomplished by the Mechanics' whistle-increase modification, BUT BY THE INCREASED SPEED OF TIME INCREASING THE STELLAR OBJECTS APPARENT FREQUENCY! Or in the other by the story, like the violin sound's apparent increased frequency when heard from a distance.

The apparent increase in recessional speed (acceleration) between the Cosmic Microwave Background (CMB) very near the beginning of our Universe (at about 380,000 "years" after our Universes' beginning), of $6.75 \pm 0.05 \times 10^4$ m/s per Mpc [18] and [19] to those of the Cepheid Variables (at about 163,000 light years distant, of $7.4 \pm 1.5 \times 10^4$ m/s per Mpc (Table 5 of [18])) is simply due to the possibly high speed of time back at the time of the CMB. The Doppler-de-

terminated speed would be less than the true higher recessional CMB speed (producing a deceleration when compared to the Cepheid Variables speed) and agrees with a slowing due to gravity! No dark energy need be assumed!

The Hubble constant, H_0 , is approximately $H_0 = 70$ [km/sec/Mpc]. But can be expressed as the inverse of the time, T , in seconds for a celestial object to move an Mpc or $(3.09 \times 10^{22} \text{ [m/Mpc]}) / (70,000 \text{ [m/sec]}) = 4.4 \times 10^{17} \text{ [seconds]}$.

For calculations of the Process times, T , of celestial objects given their speeds of recession, we utilize the equation

$$T = 4.4 \times 10^{17} \times (S/70) \text{ (seconds)} \quad (2)$$

where S is the recessional speed of the celestial object in [km/sec/Mpc].

The CMB has a Speed, S of 74 [km/sec/Mpc]. Therefore Time, $T = 4.4 \times 10^{17} \times (74/70) = 4.65 \times 10^{17}$ seconds for celestial objects, such as the CMB fairly near the beginning of our Universe, to separate a “given distance” of a Megaparsec. Under a “popular” Theory of our Universe (not however, proposed in [12]) that the separation speed of objects in our Universe should remain a constant, this number of seconds would be expected everywhere in our Universe, therefore $P_e = 4.65 \times 10^{17}$ seconds.

Likewise for the more nearby Large Magellanic Cloud Cepheid's, which have an observed speed, S , of 67.5 [km/sec/Mpc] Time,

$T = 4.4 \times 10^{17} \times (67.5/70) = 4.24 \times 10^{17}$ seconds $= P_0$. Of course, the reference or “given distance” is huge as is the time interval between observations of the separation speed of these celestial objects in our Universe. An alternative approach would be to define the “given distance” as simply the MKS meter as was utilized for the galactic measurements. Of course a kilometer could also have been chosen as the “given distance”, so the choice is rather arbitrary. In the case of the galactic star's measurement, a galactic star's orbital period was not a valid, constant or unique “given distance”, therefore the meter was selected as the reference or “given distance.” In the case of the separation speed of celestial objects the Megaparsec in meters is a definitive unit of distance in MKS units and the same for all celestial objects under consideration. Also the assumption of a constant speed of recession is simply a popular concept and not involved in the working hypothesis Theory [12]. Therefore these calculations should be considered to be extremely provisional and needs to be examined very carefully!

Other “given distances” or “expected times” values for P_e might in future be realized better utilizing, Fast Radio Bursts (FRBs), Soft Gamma ray Repeaters SGRs, pulsars, double star orbits, etc. If these measurements disclose that their frequency or periodicity increase slightly as they or their sources are measured to be further and further from our Earth, that is older and older, then their measurements might provide good, more detailed data on our Universes' variation of the speed of time.

From Equation (1), the variation of the speed of time between the CMB and the Large Magellanic Clouds, in which there are about 13 billion or 1.3×10^{10} years between these observations or $t_1 - t_2 = 1.3 \times 10^{10}$ years is:

$$\begin{aligned} & [P_o(t_1) - P_e(t_2)] / (t_1 - t_2) \\ &= [4.24 \times 10^{17} \text{ seconds} - 4.65 \times 10^{17} \text{ seconds}] / 1.3 \times 10^{10} \text{ years} \quad (1e) \\ &= -3.15 \times 10^6 \text{ seconds per year} \end{aligned}$$

$= -3.15 \times 10^{18}$ ps per year or about -0.1 s/s. Therefore over hundred trillion or more times larger compared to the muon-decay-time derived variation of the speed of time of -13 ps per year to -3500 ps per year values. This CMB value is extremely large and subject to considerable scrutiny but is still in keeping with our working hypothesis [12] that the speed of time was far greater in the distant past near the beginning of our Universe than today! Essentially both time and the space-dimension spacetime of our Universe commence expanding at the speed of light according to [12].

The CMB is close to the beginning of our Universe, nevertheless the CMB is not close enough to be particularly useful in developing a Theory for the variation of the speed of time. For that we require information from the HFGWs created at least a nanosecond nearer in time to the beginning of our Universe. What really happens at the “point” where time and space commence must await the analysis of the HFGW spectrum of the early Universe. But recall that the variation of the speed of time after that commencement “point” may well also depend upon “where” one measures the variation of time on the fabric of spacetime, the local mass distribution of matter or some other feature of our Universe!

5. Muon-Decay Time Revisited and Non-Varying Rate of-Time (NVRT) Processes

Is there something more fundamental going on concerning muon-decay time? Not just “muon decay operates with a different ‘clock’ or time than the clock the rest of us and our Universe uses.” As discussed in Section 4 of [20], perhaps muon-decay time is a different kind of process. Let us explain the situation with another story: We will utilize the fictitious tale of a tribe called the “Muons” who originated billions of years ago near the beginning of time and exist even today. The Muons all have the unique capability to consistently run a mile in exactly four minutes. Recently a Muon runner came to my mile-long track. She asked if she could borrow my watch since she had misplaced hers. I agreed and handed over my watch with the admonition that my watch only showed the correct speed of time in my location at this specific local time. She looked at the watch and exclaimed: “...it is absolutely identical to the watch that I and my entire Muon tribe had used for billions of years ... my watches’ rate of time is exactly the same, not too fast and not too slow, as the watch I had always had and lost!” If there is one thing these Muons know about, it is time!

The Muon runner ran my mile-long track and at the track’s end, while looking at her “new” watch, she exclaimed “Perfect! My wristwatch shows exactly four minutes!” She told me that the Muons could not actually “see” the track – as a matter of fact, they could not judge or “see” any distance! “We Muons cannot recognize or even comprehend the three dimensions of space—we only recognize the time di-

mension.” Also she stated that I should be careful using the wristwatch that I replaced the one I had given her. “Perhaps your replacement wristwatch was not perfect!” She said: “After looking at your replacement wristwatch I discovered it is flawed in that it seems to slow down with time, whereas the one you gave does not!”

What else does this story apply to? Let us suppose that, say, Nucleosynthesis is similar to muon decay and is a Non-Varying Rate of-Time (NVRT) Process and marches to the Nucleosynthesis own drum as it were. We make the very provisional assumption that there is no actual motion of the nuclei in space; that these high-energy collisions among nucleons only occur with a certain process-duration time just like muon decay! If we were able to observe this Nucleosynthesis process in operation today, then the process like muon decay would appear to take less and less time to be completed as our Universe’s time slows down as measured by a Timer’s stopwatch. Like the 4-minute-mile Muon runner, whose inherent “wristwatch time” seems moving faster than the current Universe time of a Timer. She stops her mile run before the Timer’s stopwatch of today reaches the 4-minute point. Therefore, the Timer believes that she has run for a shorter time to complete the mile run (that is, to complete her “process”)! In a sense we are observing compressed time from a vantage point of uncompressed time. So as we might observe Nucleosynthesis from afar through our telescopes today, the process would appear to occur more and more quickly over the years of observation just like the process of muon decay! If that does not occur, then Nucleosynthesis is not a NVRT process otherwise the process is a NVRT process!

There may be other transient processes or subsystems that involve one or more quantum-mechanical sub-reactions, some well understood and some not well understood, that in total comprise a complete, possibly multiple-step process having a well-defined beginning and end. This is the proposition:

Proposition (page 65 of [11]) that some complex processes or sub systems are “marching” to their own intrinsic” time” or timeframe that is independent of the flow of “time” in our Universe. (We call them Non-Varying Rate of-Time (NVRT) Processes.)

That is, besides muon decay there may be other such process that we define as the Non-Varying Rate of-Time (NVRT) Processes. Such processes do not “go with flow” of time slowing in our Universe. Such NVRT processes, according to our working hypothesis, may include those that generate Big-Bang Nucleosynthesis (BBNs) generation of Oh My God (OMG) very high-speed particles, Fast Radio Bursts (FRBs), Soft Gamma ray Repeaters SGRs (the latter two possibly from Magnetars) and perhaps weak nuclear reactions of proton-proton chain (affecting stellar luminosity but far more likely not to be NVRT processes since they probably are “space-coordinate” dependent in their operation). We will concentrate the following analyses on muon decay since we have studied that process in some detail. By the way, galactic motion, black-hole mergers, Nova and other more extensive in motion in the three space coordinates and less quantum-mechanical in operation are not NVRT processes. Unlike the hypothetical Muon runners they recognize the three space dimensions. Also their time varies as time

mainly does in our Universe—they “go with the flow!”

It is important to understand that the Non-Varying Rate of-Time (NVRT) Processes working hypothesis or concept is not directly related to the Rollout of the Universe Theory [12], multiuniverses, special or general relativity, hyperspace, parallel universes, etc. the NVRT process is a very new and different concept!

Let us continue the discussion by using a standard muon-decay illustration as shown in **Figure 5**.

The very most important property of this standard diagram of muon decay

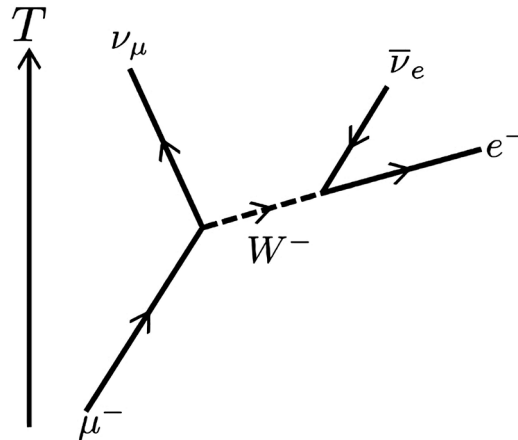


Figure 5. Standard diagram of muon decay.

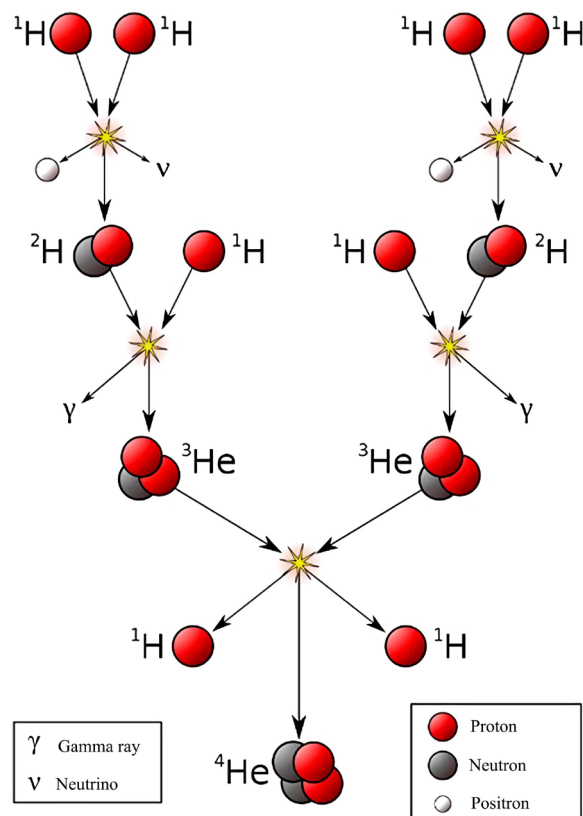


Figure 6. Standard diagram of proton-proton chain reaction.

shown in **Figure 5**, is that there is only one dimension involved: T or time. No space dimensions at all! We contrast this with the standard diagram of proton-proton chain reaction, which generates stellar luminosity, shown in **Figure 6**.

In this case an “alarm clock” that signals the beginning (when the alarm clock is set off by an experience e.g., a collision with a cosmic ray) and simply signals the end of the muon decay process when the alarm clock “rings”! Hydrogen and helium atoms move and physically collide with each other. They actually move through the dimensions of space! The idea is that *NVRT* processes, such as muon decay, are in a sense not actually a part of the spacetime continuum! Specifically, they have their own clock, that alarm clock time interval is completely independent of where in space the collision occurs or especially any “space change” in the Muon’s decay process during that process!

Do the Non-Variable Time Rate (*NVRT*) processes, like muon decay processes, relate to processes such as production of new elements and those that are involved in the mysterious core-collapse of supernova [21] happening billions of years ago? If such is the case, then we may have another mysteries solved!

6. Conclusions

An equation is presented involving the observed time for a process to be completed and the expected time for the process to be completed. The difference between these two times is attributed to a change in the speed of time. For the Process of muon decay the speed of time is found to decrease at the rate of between -13 picoseconds, ps, per year and -3521 ps/year at about the date of 1981 on Earth. Although it would not affect the correctness of the theorized Theory of our Universe [12], more accurate measurements of muon decay time are needed in order to actually calculate an accurate local speed of time on Earth or indicate that muon decay time does not change with time and is not a *NVRT* process. For a galaxy, such as Messier 33, the variation of the speed of time appears there to be -6.12 ps/year to at most -2080 ps/year (at the galaxies’ outskirts) as a very provisional determination. However this speed of time for Messier 33 may actually be caused, at least in part, by the Doppler shift of stars observed beyond the Galaxy in spacetime regions of higher speed of time and apparent higher speed or some other effect. However, no dark matter need be assumed. From the speed of separation of celestial object as our Universe progresses, we find that in the time between the observations of the receding speeds of the CMB and the Large Magellanic Cloud Cepheid’s of approximately thirteen billion year, there is a speed of time change of -3.15×10^{18} ps per year or about -0.1 s/s. This calculation is in keeping with the theorized very much higher speed of time in the past of the CMB near the beginning of our Universe, predicted by [12] and the much slower speed of time in our current observations of the relatively nearby (in time and distance) Large Magellanic Cloud Cepheid speed. There is no acceleration of the speeds of these celestial objects speed of separation. Those separation speeds

are decreasing as usually predicted by gravity and by using our speed-of-time theory, so that dark energy is not required!

Other determinations of the variation of the speed of time, and independent of special and general relativistic effects, might be by utilizing the Processes involving Fast Radio Bursts (FRBs), Soft Gamma ray Repeaters (SGRs), pulsars, double star orbital periods, etc.; of course only if these measurements are precise enough to disclose that their frequencies or rates appear to increase slightly as they or their sources are measured to be further and further from our Earth.

Other possible indicators of the variation in the speed of time besides muon decay time, quite valuable because they are independent of special and general relativity effects, might be found in meteoritic composition change over hundreds of thousands or millions of years. The research by Turner, *et al.* [22] found time differences in meteoritic-composition analyses that might relate to the speed of time: They found “... that the fluid-mobile uranium ion U^{64} moved within the past few 100,000 years ... This time scale is less than the cosmic-ray exposure age... when they were ejected into space. Fluid flow occurred after melting of ice” by impact heating (ablation) or solar heating. Or possibly, the effect was the result of the change in the speed of time right after the Earth was formed and today. The process here is the melting of the ice, the time it would be expected to occur and the time when it actually occurred.

With regard to galactic data to be utilized to compute the speed of time; in Section 3 we have computed the difference between the velocity curves in **Figure 4** of the nearby Messier 33 galaxy would lead to a speed of time between about -2 and $-2,000$ ps/year. However, galaxies closer to the beginning of our Universe might also lead to estimates of the speed of time. As summarized by Wardlow [23] “... key features of a mature galaxy arose more rapidly than has been thought.” Lelli, *et al.* [24] state “We conclude that massive bulges and regularly rotating disks can form more rapidly in the early Universe than predicted by of galaxy formation.” Therefore the speed of time may be roughly computed by differencing the expected time and the observed time that features of galaxy formation appear.

We concluded with a study of Processes like muon decay, which may operate with a “different clock,” a clock that does not participate in the variation in the speed of time that the rest of our Universe does—we call these Processes Non-Varying Rate of Time or NVRT processes.

The speed of time and/or the speed of time’s variation may well depend upon “where” one measures the variation on the fabric of spacetime and/or the local mass distribution of matter or some other feature of our Universe.

In order to establish a Theory for the origin and variation of the speed of time, we conclude that HFGW detection is required to understand the activity of Processes at a nanosecond or less after the beginning of our Universe [16]. We contend that primordial or relic HFGWs were propagated before our Universe became transparent to electromagnetic radiation. If such primordial HFGWs

can be detected by the Li-Baker HFGW detector, discussed in connection with our analyses of Muon decay, then their observations may not only contain information on the speed of time, but information, gained by means of the analyses of their frequency spectrum, concerning the processes themselves.

Acknowledgements

Andy Beckwith, Nagib Callaos, Paul Murad, R. Clive Woods, Eric Davis, Gary Stephenson and Giorgio Fontana have provided encouragement for many of our “out of the box” ideas including our theory of the variable speed of time. Mounir Belgacem has given valuable assistance with the preparation of the figures.

Funding

All funding for this paper was exclusively and personally provided by the authors and no external funding was utilized.

Authors' Contributions

Conceptualization and all analyses: R.M L B., Jr and B. S. B. and introduction of entropy and many HFGW-detection concepts FY L.

Conflicts of Interest

There were no competing interests of any author.

References

- [1] Herrick, S. (1971) *Astrodynamics: Orbit Determination, Space Navigation, Celestial Mechanics*, Volumes 1 and 2. Van Nostrand, Princeton.
- [2] Baker Jr., R.M.L. (1967) *Astrodynamics: Applications and Advanced Topics*. Academic Press, New York.
- [3] Conversi, M., Piccioni, O. and Pancini, E.P. (1946) Pancini, Piccioni (CPP) Experiment. Slide 10.
http://www0.mi.infn.it/~neri/HomePage/Teaching_files/Esperimento_CPP.pdf
- [4] Olive, K.A. (2014) *Chinese Physics C*, **38**, 648ff.
<https://doi.org/10.1088/1674-1137/38/9/090001>
- [5] Webber, D.M. (2011) *Physical Review Letters*, **106**, Article ID: 041803.
<https://doi.org/10.1103/PhysRevLett.106.041803>
- [6] Lindy, R.A. (1962) *Physical Review*, **125**, 1686-1696.
<https://doi.org/10.1103/PhysRev.125.1686>
- [7] Tischchenko, V. (2013) *Nuclear Physics B—Proceedings Supplements*, **225-227**, 232-235. <https://doi.org/10.1016/j.nuclphysbps.2012.02.048>
- [8] Barazandeh, C. (2016) *Journal Physics Conference Series*, **770**, Article ID: 012050.
<https://doi.org/10.1088/1742-6596/770/1/012050>
- [9] Physics OpenLab. (2016) Cosmic Ray Meeting, February, 2017, Slide 10: $2.050 \pm 0.040 \mu\text{sec}$, Slide 11: $2.080 \pm 0.110 \mu\text{sec}$, Slide 12: $1.90 \pm 0.190 \mu\text{sec}$ (2017).
<http://physicsopenlab.org/2016/01/10/cosmic-muons-decay>
- [10] Adams, M. (2017) Cosmic Ray Meeting. February, 2017, Slide 10, Slide 11, Slide 12.

- <https://indico.cern.ch/event/596002/contributions/2463437/attachments/1410577/2157296/Adams-Rome.pdf>
- [11] Baker Jr., R.M.L. (2019) *Journal of Space Science and Technology*, **25**, 60-77.
<https://doi.org/10.15407/knit2019.03.060>
 - [12] Baker Jr., R.M.L. (2020) *Journal of High Energy Physics, Gravitation and Cosmology*, **6**, 1-16.
 - [13] Li, F. and Baker Jr., R.M.L. (2007) *International Journal of Modern Physics B*, **21**, 3274-3278. <https://doi.org/10.1142/S0217979207044366>
 - [14] Baker Jr., R.M.L. (2001) Gravitational Wave Detector. Chinese Patent No. 018144223.0.
 - [15] Clive Woods, R., Baker Jr., R.M.L., Li, F., Stephenson, G., Davis, E. and Beckwith, A.W. (2011) *Journal of Modern Physics*, **2**, 498-518.
<https://doi.org/10.4236/jmp.2011.26060>
 - [16] Beckwith, A.W. and Baker Jr., R.M.L. (2019) *Journal of High Energy Physics, Gravitation and Cosmology*, **6**, 103-122.
 - [17] Li, F.-Y., Wen, H., Fang, Z.-Y., Li, D. and Zhang, T.-J. (2020) *The European Physical Journal C*, **80**, 879. <https://doi.org/10.1140/epjc/s10052-020-08429-2>
 - [18] Aghanim, N., Akrami, Y., Ashdown, M., Aumont, J., Baccigalupi, C., Ballardini, M., Banday, A.J., Barreiro, R.B., Bartolo, N., Basak, S., Benabed, K., Bernard, J.P., Bersanelli, M., Bielewicz, P., Bock, J.J., Bond, J.R., Borrill, J., Bouchet, F.R., Boulanger, F., Bucher, M., Burigana, C., Butler, R.C., Calabrese, E., Cardoso, J.F., Carron, J., Casaponsa, B., Challinor, A., Chiang, H.C., Colombo, L.P.L., Combet, C., Crill, B.P., Cuttaia, F., De Bernardis, P., De Rosa, A., De Zotti, G., Delabrouille, J., Delouis, J.M. and Di Valentino (2020) *Astronomy & Astrophysics*, **641**, 56.
<https://doi.org/10.1051/0004-6361/201936386>
 - [19] Riess, A.G., Stefano, C., *et al.* (2019) *The Astrophysical Journal*, **876**, 217-243.
<https://doi.org/10.3847/1538-4357/ab1422>
 - [20] Baker Jr., R.M.L. and Baker, B.S. (2021) *Journal of Systematics, Cybernetics and Informatics Special Issue "Rigor and Inter-Disciplinary Communication"*, **18**, 217-243.
 - [21] Burrows, A. and Vartanyan, D. (2021) *Nature*, **589**, 29-39.
<https://doi.org/10.1038/s41586-020-03059-w>
 - [22] Turner, S., McGee, L., Humayan, M., Creech, J. and Zanjda, B. (2021) *Nature*, **371**, 164-167. <https://doi.org/10.1126/science.abc8116>
 - [23] Wardlow, J. (2021) *Science*, **371**, 674-675.
<https://doi.org/10.1126/science.abg2907>
 - [24] Lelli, F., Di Teodoro, E.M., Fraternali, F., Man, A.W.S., Zhang, Z.-Y., De Breuck, C., Davis, T.A. and Malolino, R. (2021) *Science*, **371**, 713-716.
<https://doi.org/10.1126/science.abc1893>

Reconstruction Method in $F(G)$ Gravity: Stability Study and Inflationary Survey

C. Aïnamon¹, M. J. S. Houndjo^{1,2}, A. A. L. Ayivi³, M. G. Ganiou³, A. Kanfon^{2,3}

¹Institut de Mathématiques et de Sciences Physiques (IMSP), Porto-Novo, Bénin

²Faculté des Sciences et Techniques de Natitingou, Natitingou, Bénin

³Département de Physique, Université d'Abomey-Calavi, Calavi, Bénin

Email: ainamoncyrille@yahoo.fr, sthoundjo@yahoo.fr, ayiviluc@yahoo.fr, moussiliou_ganiou@yahoo.fr, kanfon@yahoo.fr

How to cite this paper: Aïnamon, C., Houndjo, M.J.S., Ayivi, A.A.L., Ganiou, M.G. and Kanfon, A. (2021) Reconstruction Method in $F(G)$ Gravity: Stability Study and Inflationary Survey. *Journal of Modern Physics*, 12, 781-797.

<https://doi.org/10.4236/jmp.2021.126050>

Received: March 21, 2021

Accepted: May 10, 2021

Published: May 13, 2021

Copyright © 2021 by author(s) and Scientific Research Publishing Inc. This work is licensed under the Creative Commons Attribution International License (CC BY 4.0).

<http://creativecommons.org/licenses/by/4.0/>



Open Access

Abstract

The present paper is devoted to reconstruction and cosmological study in modified $F(G)$ theory of gravity. Our reconstruction scheme is based on Friedmann metric induced equations in modified $F(G)$ theory by supposing a power law form for the scale factor of Friedmann metric. Firstly, we deal with the stability study, the obtained model. This survey reveals that for appropriated choice of the reconstructed model parameter, this model is stable under two cosmological evolutions namely the de Sitter and the power law evolutions symbolized by the appropriated scale factor. Secondly, we investigate the inflationary survey by fitting the model with the inflation observables. These observables are determined and their comparison with Planck's results leads to a special inflationary $F(G)$ model. We prove that this model especially obtained for radiation domination evolution develops an instability, so can fall to ordinary matter domination era or dark energy domination era. This is the key of graceful exit from inflation.

Keywords

Modified Gravity, Inflation, Stability, Gauss-Bonnet

1. Introduction

Cosmology aims to study the universe as a whole [1]. It is based on Einstein's theory of gravity, General Relativity which has brilliantly succeeded some experiment tests. But some recent observations such as the *Ia* type supernova [2] [3] and the Cosmic microwave background [4] [5] impose new constraint on the current Universe content. These observations allow us to affirm that the Universe is in a phase of accelerated expansion. Thus, an alternative attempts to

provide a plausible explanation to the present of our Universe in accordance with these observations, several theoretical approaches have emerged. These approaches can be classified into two categories [6]. The first brings together those which maintain the General Relativity as a gravitational theory and modify the content of the Universe by introducing new exotic forms of matter fields either as an inflaton field or as dark matter. The second category is made up of approaches that modify gravity theory by building theories that limit General Relativity, but with additional degrees of freedom that can lead to accelerated expansion of the Universe. The latter is called the theory of modified gravity which we quote among others: $F(R)$ theory, $F(T)$ theory, $F(R, T)$ theory, $F(T, T)$ theory, $F(G)$ theory, $F(R, G)$ theory, $F(G, T)$ theory where R, T, T , denote respectively the scalar curvature, the scalar torsion and the trace of the energy-momentum tensor. Note that these modified theories of gravity have been the subject of attention of several researchers in recent years. A special modified General Relativity has recently been used for several interesting works [7] [8] [9]: the $F(G)$ theory is a modified theory of Gauss-Bonnet where $F(G)$ is a generic function of the Gauss-Bonnet invariant G which is inspired by string theory and takes the form:

$$G = R^2 - 4R^{\mu\nu}R_{\mu\nu} + R^{\mu\nu\rho\sigma}R_{\mu\nu\rho\sigma} \quad (1)$$

The Gauss-Bonnet term plays an important role because it makes it possible to avoid phantom contributions and helps to regulate the action of gravitation [10] [11] [12]. This 4-dimensional Gauss-Bonnet term is a topological invariant and therefore has no dynamic effect if it is added linearly to the Lagrangian. To introduce an additional dynamic, we can associate the Gauss-Bonnet term with a scalar field, as it naturally appears in the effective actions using low energy chains [13] [14]. For exponential coupling with a scalar field potential, this model can produce a period dominated by matter followed by an accelerated period [15] [16].

Several other interesting works have been done so far in this theory. The Gauss-Bonnet scalar and the $F(G)$ theory were considered to reconstruct theories favorable to the expansion of the universe [11]. In [17], the conditions of existence and stability of cosmological solutions of the power law, when the Einstein-Hilbert action is modified by inclusion of a Gauss-Bonnet function $F(G)$, have been established. The cylindrical symmetry in $F(G)$ gravity was studied and it was shown that only three choices of $F(G)$ models are compatible with the exact solutions [18]. The same authors obtained in [19] a perfectly symmetrical and cylindrical solution in modified Gauss-Bonnet theory. A description of the deceleration-acceleration cosmological transition has been made in modified $F(G)$ and $F(R)$ theory [20] where it has been shown that a solution containing the Big-Bang and Big-Rip singularities can be reconstructed using only the auxiliary field formalism. The cosmography in modified $F(G)$ gravity theory has been studied in [21] and the authors have reconstructed the present values of $F(G)$, of its derivatives as well as those of the cosmographic parameters by

considering a homogeneous and isotropic universe on a large scale. A cosmological study was carried out in modified Gauss-Bonnet theory [22] to account for the recent accelerated expansion of the universe. In their work, C. Bömher and F. Lobo analyzed the stability of Einstein's static universe by considering linear and homogeneous perturbations in the context of the modified Gauss-Bonnet theory [23]; by use of a generic function $F(G)$, they showed that the region of stability of such a universe is governed by the parameter of equation of state ω and the second derivative of the model $F(G)$.

This success of the $F(G)$ theory has motivated us to take an interest in it and solving some current riddles in cosmology. The present work constitutes a contribution going in the same direction as the points previously mentioned. In addition to the benefit of being able to explain the present Universe acceleration of the by modifying standard theories of gravity, another major issue which will hopefully be explained in the next two decades, is the primordial post-quantum gravity era of our Universe. To date there are two candidate descriptions for this primordial era, the inflationary scenario [24]-[32] and the bouncing cosmology scenario [33] [34] [35]. Thus, in our present study, we will endeavor first to reconstruct a model in modified $F(G)$ gravity theory. Then, we aim to investigate the stability of the reconstructed model in order to check its possibility to render account some Universe evolution phases. Nowadays, inflation survey reveals as an excellent tool to investigate dynamical property of a cosmological model. This justifies the second part of this work where the inflationary observables will be addressed with the reconstructed model.

The paper is organized as follow. After providing the basic equations of the gravitational $F(G)$ theory in Section 2, we deal with the reconstruction program through the Section 3. The stability of the reconstructed model is achieved in the Section 4. The model is put at the heat of cosmological inflationary survey via the Section 5. The final section 6 is devoted to the conclusion.

2. Basic Equations of the Gravitational $F(G)$ Theory

The action in dimension 4 of $F(G)$ gravity theory is given, as in [36] [37], by:

$$S = \frac{1}{k} \int \sqrt{-g} \left[\frac{R}{2} + F(G) \right] d^4x + S_m \quad (2)$$

where R is the Ricci scalar curvature, $F(G)$ is a generic function of the Gauss-Bonnet topological invariant G , $k^2 = 8\pi G$ et S_m is the action of matter.

By varying this four-dimensional action with respect to the metric, we obtain the equation of the field which is written [36] [37]:

$$G_{\mu\nu} + 8 \left[R_{\mu\rho\nu\sigma} + R_{\rho\nu} g_{\sigma\mu} + \frac{1}{2} (g_{\mu\nu} g_{\sigma\rho} - g_{\mu\sigma} g_{\nu\rho}) R - R_{\rho\sigma} g_{\nu\mu} \right. \\ \left. - R_{\mu\nu} g_{\sigma\rho} + R_{\mu\sigma} g_{\nu\rho} \right] \nabla^\rho \nabla^\sigma F'(G) + (GF'(G) - F) g_{\mu\nu} = T_{\mu\nu}^m \quad (3)$$

where $G_{\mu\nu}$ is Einstein's tensor, $T_{\mu\nu}^m$ the energy-momentum tensor of matter. In this work, we consider that $k^2 = 8\pi G = 1$ and the prime represents the ordinary derivative with respect to G . For the Robertson-Walker flat space metric which is written as:

$$ds^2 = -dt^2 + a(t)^2 \sum_i dx_i^2 \quad (4)$$

we have:

$$R = 6(\dot{H} + 2H^2); \quad G = 24H^2(\dot{H} + H^2) \quad (5)$$

where H is the Hubble parameter and the dot means $()$ the time derivative.

Considering that the universe is flat and filled with a perfect fluid, Friedmann equations for the modified gravity $f(G)$ are written:

$$3H^2 = GF'(G) - F - 24H^3\dot{F}'(G) + \rho_m \quad (6)$$

$$-2\dot{H} = -8H^3\dot{F}'(G) + 16H\dot{H}\dot{F}'(G) + 8H^2\ddot{F}'(G) + \rho_m \quad (7)$$

The continuity equation is given by:

$$\dot{\rho} + 3H(\rho + P) = 0 \quad (8)$$

$$\dot{\rho} + 3H\rho(1 + \omega) = 0 \quad (9)$$

where ω is the energy parameter.

The equations which constitute the basis of the theory being established, we will now design our model.

3. Reconstruction of $F(G)$ Model

In this section, we will reconstruct a $F(G)$ model. To do this, we choose a scale factor $a(t)$ obeying the power law and which is in the form:

$$a(t) = a_* \left(\frac{t}{t_*} \right)^p \quad (10)$$

where a_* is the value that takes a at the time t_* and p is a constant. In this case, the Hubble parameter satisfies the following relations:

$$H = \frac{p}{t}; \quad \dot{H} = -\frac{p}{t^2}; \quad H^2 = \frac{p^2}{t^2} \quad (11)$$

Then, the GB invariant takes the form:

$$G = \frac{24p^3(p-1)}{t^4}, \quad (12)$$

leading to

$$t = \left[\frac{24p^3(p-1)}{G} \right]^{\frac{1}{4}} \quad (13)$$

From the continuity Equation (9), we obtain:

$$\rho = \rho_0 \left[\frac{24p^3(p-1)}{G} \right]^{\frac{-3}{4}p(1+\omega)} \quad (14)$$

Taking into account the Equations (11)-(13), the first Friedmann equation becomes:

$$\frac{4}{p-1}G^2F''(G) + GF'(G) - F(G) - \left[\frac{3pG}{8(p-1)} \right]^{\frac{1}{2}} + \rho_0 \left[\frac{G}{24p^3(p-1)} \right]^{\frac{3}{4}p(1+\omega)} = 0 \quad (15)$$

This equation takes the form:

$$CGF''(G) + F'(G) - F(G) - \sqrt{A}G^{\frac{1}{2}} + \rho_0 \frac{G^\alpha}{B\alpha} = 0 \quad (16)$$

$$\text{with: } C = \frac{4}{p-1}; \quad A = \frac{3p}{8(p-1)}; \quad B = 24p^3(p-1) \quad \text{et} \quad \alpha = \frac{3}{4}p(1+\omega).$$

It is a differential equation in term of G which, after solving, gives the solution:

$$F(G) = -\frac{4\sqrt{A}G^{\frac{1}{2}}}{2+C} - \frac{\rho_0 G^\alpha}{B^\alpha(-1+\alpha)(1+\alpha C)} + C_1 G^{\frac{1}{C}} + C_2 G \quad (17)$$

that we write more simply:

$$F(G) = DG^{\frac{1}{2}} + EG^\alpha + C_1 G^\beta + C_2 G \quad (18)$$

$$\text{where: } D = -\frac{4\sqrt{A}}{2+C}; \quad E = \frac{-\rho_0}{B^\alpha(-1+\alpha)(1+\alpha C)}; \quad \beta = -\frac{1}{C}; \quad C_1 \text{ and } C_2 \text{ being}$$

integration constants. The model (18) is a general model. The reason is that for appropriate choice of its parameters namely the parameters $C, p, \omega, \rho_0, C_1$ et C_2 , the viable $F(G)$ models investigated in [9] can be recovered. Such models have the properties to describe not only cosmological evolutions leading by dark matter and the ordinary matter and also the transition between the two evolutions. To verify this expected property of the model, we will deal with its stability in the coming section.

4. Stability of the $F(G)$ Model

In this section, it is about the study of the stability of the $F(G)$ model constructed. To achieve this, we use de Sitter solutions and power law solutions which are techniques generally used in cosmology as shown by the work [17] [38] [39] [40] [41]. We will consider both the perturbation of matter and geometry in the general equations of motion. In the same approach with the work [42] [43], the geometric and the matter perturbations will be led respectively by the following equations

$$H(t) = H_b(t)(1 + \delta(t)), \quad (19)$$

$$\rho(t) = \rho_b(t)(1 + \delta_m(t)) \quad (20)$$

where $H_b(t)$ and $\rho_b(t)$ correspond respectively to the Hubble parameter and to the energy density of basic ordinary matter. By making an analogy with the continuity Equation (9), we can write:

$$\dot{\rho}_b(t) + 3H_b(t)\rho_b(t)(1+\omega) = 0 \quad (21)$$

whose solution is:

$$\rho_b(t) = \rho_0 e^{-3(1+\omega)\int H_b(t)dt} \quad (22)$$

whith ρ_0 , an intégration constant.

In order to study the linear perturbation of $H(t)$ and $\rho(t)$, we carry out a development of the model $F(G)$ in series of $G_b = 24H_b^2(\dot{H} + H_b^2)$ as following:

$$F(G) = F^b + F_G^b(G - G_b) + O^2 \quad (23)$$

On the one hand, we substitute the Equations (19), (20) and (23) in Equation (6) which is the first Friedmann equation, and we obtain after simplification:

$$\begin{aligned} \dot{\delta}(t) & \left[24H_b^3(24H_b^2\dot{H}_b + 24H_b^4)F_{GG}^b - 24H_b^3F_G^b - 576H_b^6(48H_b\dot{H}_b^2 \right. \\ & + 24H_b^2\ddot{H}_b + 96H_b^3\dot{H}_b)F_{GGG}^b \left. \right] + \delta(t) \left[(24H_b^2\dot{H}_b + 24H_b^4)(72H_b^2\dot{H}_b \right. \\ & + 96H_b^4)F_{GG}^b - (72H_b^2\dot{H}_b + 96H_b^4)F_G^b - 72H_b^3(48H_b\dot{H}_b^2 + 24H_b^2\ddot{H}_b \\ & + 96H_b^3\dot{H}_b)F_{GG}^b - 24H_b^3(48H_b\dot{H}_b^2 + 24H_b^2\ddot{H}_b + 96H_b^3\dot{H}_b)(72H_b^2\dot{H}_b \\ & + 96H_b^4)F_{GGG}^b - 6H_b^2 \left. \right] + \rho_b\delta_m(t) = 0 \end{aligned} \quad (24)$$

On the other hand, the substitution of the Equations (19) et (20) in Equation (9) leads to:

$$\delta(t) = \frac{-\dot{\delta}_m(t)}{3(1+\omega)H_b(t)} \quad (25)$$

By eliminating $\delta(t)$ from combination of Equations (24) and (25), we get the differential equation:

$$\begin{aligned} \frac{d\delta_m(t)}{\delta_m(t)} & = 3(1+\omega)\rho_b \left[24H_b\dot{H}_bF_G^b - 24H_b\dot{H}_b(24H_b^2\dot{H}_b + 24H_b^4)F_{GG}^b \right. \\ & + 576H_b^4\dot{H}_b(48H_b\dot{H}_b^2 + 24H_b^2\ddot{H}_b + 96H_b^3\dot{H}_b)F_{GGG}^b + (24H_b\dot{H}_b \\ & + 24H_b^3)(72H_b^2\dot{H}_b + 96H_b^4)F_{GG}^b - (72H_b\dot{H}_b + 92H_b^3)F_G^b \\ & - 72H_b^2(48H_b\dot{H}_b^2 + 24H_b^2\ddot{H}_b + 96H_b^3\dot{H}_b)F_{GG}^b - 24H_b^2(48H_b\dot{H}_b^2 \\ & + 24H_b^2\ddot{H}_b + 96H_b^3\dot{H}_b)(72H_b^2\dot{H}_b + 96H_b^4)F_{GGG}^b - 6H_b \left. \right]^{-1} dt \end{aligned} \quad (26)$$

whose general solution is written in the form:

$$\delta_m(t) = C_0 \exp \left\{ 3(1+\omega) \int C_H dt \right\} \quad (27)$$

where C_0 is an intégration constant and C_H has for expression:

$$\begin{aligned} C_H & = \rho_b \left[24H_b\dot{H}_bF_G^b - 24H_b\dot{H}_b(24H_b^2\dot{H}_b + 24H_b^4)F_{GG}^b \right. \\ & + 576H_b^4\dot{H}_b(48H_b\dot{H}_b^2 + 24H_b^2\ddot{H}_b + 96H_b^3\dot{H}_b)F_{GGG}^b + (24H_b\dot{H}_b \end{aligned}$$

$$\begin{aligned}
& + 24H_b^3 \Big(72H_b^2 \dot{H} + 96H_b^4 \Big) F_{GG}^b - \Big(72H_b \dot{H}_b + 92H_b^3 \Big) F_G^b \\
& - 72H_b^2 \Big(48H_b \dot{H}_b^2 + 24H_b^2 \ddot{H} + 96H_b^3 \dot{H}_b \Big) F_{GG}^b - 24H_b^2 \Big(48H_b \dot{H}_b^2 \\
& + 24H_b^2 \ddot{H}_b + 96H_b^3 \dot{H}_b \Big) \Big(72H_b^2 \dot{H}_b + 96H_b^4 \Big) F_{GGG}^b - 6H_b \Big]^{-1}
\end{aligned} \quad (28)$$

From the Equations (25) et (27), we obtain:

$$\delta(t) = -\frac{C_0 C_H}{H_b} \exp \left\{ 3(1+\omega) \int C_H dt \right\} \quad (29)$$

In the rest of our work, we will use the stability of de Sitter solutions as well as that of power law solutions in order to appreciate the convergence of each of the perturbation terms.

4.1. Stability of de Sitter Solutions

De Sitter's solutions are well known in Cosmology because they constitute a perfect approximation of the exponential expansion of the Universe during its primordial inflation [44]. They are described by a constant Hubble parameter. In this context, the Hubble parameter and the associated scale factor correspond to:

$$H_b(t) = H_0 \Rightarrow a(t) = a_0 e^{H_0 t} \quad (30)$$

So the expression (22) becomes:

$$\rho_b(t) = \rho_0 e^{-3(1+\omega)H_0 t} \quad (31)$$

And C_H takes the form:

$$\begin{aligned}
C_H = \rho_b \Bigg[& -3D(24)^{\frac{1}{2}} H_0 + 4\alpha(-2+\alpha)E(24)^\alpha H_0^{4\alpha-1} \\
& + 4\beta(-2+\beta)C_1(24)^\beta H_0^{4\beta-1} - 96C_2 H_0^3 - 6H_0 \Bigg]^{-1}
\end{aligned} \quad (32)$$

Moreover, from the differentiation of each member of the Equation (31), we express dt which allows us to write:

$$\int C_H dt = -\frac{1}{3(1+\omega)H_0} \int \frac{C_H}{\rho_b} d\rho_b \quad (33)$$

which give:

$$\begin{aligned}
\int C_H dt = & -\frac{\rho_b}{3(1+\omega)} \Bigg[-3D(24)^{\frac{1}{2}} H_0^2 + 4\alpha(-2+\alpha)E(24)^\alpha H_0^{4\alpha} \\
& + 4\beta(-2+\beta)C_1(24)^\beta H_0^{4\beta} - 96C_2 H_0^4 - 6H_0^2 \Bigg]^{-1}
\end{aligned} \quad (34)$$

By substitution of this previous expression in the relations (27) et (29), we obtain respectively:

$$\begin{aligned}
\delta_m(t) = & C_0 \exp \left\{ -\rho_b \Bigg[-3D(24)^{\frac{1}{2}} H_0^2 + 4\alpha(-2+\alpha)E(24)^\alpha H_0^{4\alpha} \right. \\
& \left. + 4\beta(-2+\beta)C_1(24)^\beta H_0^{4\beta} - 96C_2 H_0^4 - 6H_0^2 \Bigg]^{-1} \right\}
\end{aligned} \quad (35)$$

and

$$\begin{aligned} \delta(t) = & -C_0 \rho_b \left[-3D(24)^{\frac{1}{2}} H_0^2 + 4\alpha(-2+\alpha)E(24)^\alpha H_0^{4\alpha} \right. \\ & \left. + 4\beta(-2+\beta)C_1(24)^\beta H_0^{4\beta} - 96C_2 H_0^4 - 6H_0^2 \right]^{-1} \\ & \times \exp \left\{ -\rho_b \left[-3D(24)^{\frac{1}{2}} H_0^2 + 4\alpha(-2+\alpha)E(24)^\alpha H_0^{4\alpha} \right. \right. \\ & \left. \left. + 4\beta(-2+\beta)C_1(24)^\beta H_0^{4\beta} - 96C_2 H_0^4 - 6H_0^2 \right]^{-1} \right\} \end{aligned} \quad (36)$$

4.2. Stability of Power Law Solutions

In this study, we are interested in the solutions described by the power law of the scale factor. They are also initiated in Cosmology to describe a power law type inflation [41]. Thus, the scale factor changes according to a power of time t . And we have:

$$a(t) \propto t^n \Rightarrow H_b(t) = \frac{n}{t} \quad (37)$$

Note that by posing $n = p$, the scale factor of (37) corresponds to that of the Equation (10). The density of ordinary energy given by the relation (22) and the Gauss-Bonnet invariant given by (5) take the respective forms:

$$\rho_b(t) = \rho_0 t^{-3n(1+\omega)} \quad (38)$$

and

$$G_b = \frac{24n^3(n-1)}{t^4} \quad (39)$$

Then the relation (28) expressing the magnitude C_H becomes here:

$$\begin{aligned} C_H = \rho_0 \left\{ -48n^2(2n-1) \left[\frac{1}{2} Dk^{\frac{1}{2}} g_b^{\frac{1+q}{4}} + \alpha E k^{\alpha-1} g_b^{\frac{\alpha+q-1}{4}} + \beta C_1 k^{\beta-1} g_b^{\frac{\beta+q-1}{4}} \right. \right. \\ \left. \left. + C_2 g_b^{\frac{3+q}{4}} \right] + 2(24)^2 n^5 (n-1)(2n-7) \left[-\frac{1}{4} Dk^{\frac{3}{2}} g_b^{\frac{1+q}{4}} \right. \right. \\ \left. \left. + \alpha(\alpha-1) E k^{\alpha-2} g_b^{\frac{\alpha+q-1}{4}} + \beta(\beta-1) C_1 k^{\beta-2} g_b^{\frac{\beta+q-1}{4}} \right] \right. \\ \left. + 8(24)^3 n^8 (n-1)(2n-1) \left[\frac{3}{8} Dk^{\frac{5}{2}} g_b^{\frac{1+q}{4}} + \alpha(\alpha-1)(\alpha-2) E k^{\alpha-3} g_b^{\frac{\alpha+q-1}{4}} \right. \right. \\ \left. \left. + \beta(\beta-1)(\beta-2) C_1 k^{\beta-3} g_b^{\frac{\beta+q-1}{4}} \right] - 6n g_b^{\frac{1+q}{4}} \right\}^{-1} \end{aligned} \quad (40)$$

$$\text{avec } q = -3n(1+\omega); \quad k = 24n^3(n-1) \quad \text{et} \quad g_b(t) = \frac{G_b(t)}{k}$$

Taking into account the Equation (39), we deduce: $dt = -\frac{1}{4} g_b^{-\frac{5}{4}} dg_b$.

It follows:

$$\begin{aligned}
 \int C_H dt = & -\frac{\rho_0}{4} \int \left\{ -48n^2(2n-1) \left[\frac{1}{2} Dk^{-\frac{1}{2}} g_b^{\frac{q+6}{4}} + \alpha Ek^{\alpha-1} g_b^{\frac{\alpha+q+4}{4}} \right. \right. \\
 & + \beta C_1 k^{\beta-1} g_b^{\frac{\beta+q+4}{4}} + C_2 g_b^{\frac{q+8}{4}} \left. \right] + 2(24)^2 n^5 (n-1)(2n-7) \left[-\frac{1}{4} Dk^{-\frac{3}{2}} g_b^{\frac{q+6}{4}} \right. \\
 & + \alpha(\alpha-1) Ek^{\alpha-2} g_b^{\frac{\alpha+q+4}{4}} + \beta(\beta-1) C_1 k^{\beta-2} g_b^{\frac{\beta+q+4}{4}} \left. \right] \\
 & + 8(24)^3 n^8 (n-1)(2n-1) \left[\frac{3}{8} Dk^{-\frac{5}{2}} g_b^{\frac{q+6}{4}} + \alpha(\alpha-1)(\alpha-2) Ek^{\alpha-3} g_b^{\frac{\alpha+q+4}{4}} \right. \\
 & \left. \left. + \beta(\beta-1)(\beta-2) C_1 k^{\beta-3} g_b^{\frac{\beta+q+4}{4}} \right] - 6n g_b^{\frac{q+6}{4}} \right\}^{-1} dg_b
 \end{aligned} \quad (41)$$

Note that we have not found an analytical solution for the integral of the relation (41), then a numerical study will be carried out in order to obtain the perturbation functions and to discuss their convergence.

4.3. Stability Analysis

In this part of the work, we will deal with the evolution survey of the solutions obtained as a time function. We emphasize here that in the case of the study of de Sitter's solutions, an explicit analytical expression of each of the perturbation functions $\delta_m(t)$ and $\delta(t)$ is obtained respectively in (35) and (36) respectively. And we can easily notice that for an appropriate choice of parameters, the quantities $\delta_m(t)$ and $\delta(t)$ converge. Indeed, when t straightens forward to infinity, the fonction $\rho_b(t) = \rho_0 e^{-3(1+\omega)H_0 t}$ tends to 0 for positive or zero ω . Then, for $\rho_b(t)$ tending to 0, we see that $\delta_m(t)$ tends to C_0 (which is an arbitrary constant) and $\delta(t)$ tends to 0. Hence these two functions converge. In the case the power law solutions, the idea was to calculate the integral given by the Equation (41) then introduce the result in each of the Equations (27) and (29) in order to obtain the respective expressions of $\delta_m(t)$ and $\delta(t)$. But, it turns out that the analytical solution of the Equation (41) is not easy to get, so we proceeded to a numerical study. Thus, our approach at this level consists to plot the perturbation functions $\delta_m(t)$ and $\delta(t)$ without having obtained their analytical expressions; which can permit us to appreciate their convergence. These curves are those of **Figure 1** and **Figure 2** below. They show the behaviors of $\delta_m(t)$ and $\delta(t)$ respectively for a Universe dominated by ordinary matter ($\omega = 0$) and for a Universe dominated by radiation ($\omega = 1/3$). We also note that these disturbance functions are convergent.

The convergence of these quantities for different values of the parameters of the reconstructed model, according to the de Sitter approach and the power law approach, proves that this model is stable. It is therefore conducive to the reproduction of the stage dominated by matter, radiation and also the phase characterized by de Sitter inflation [42].

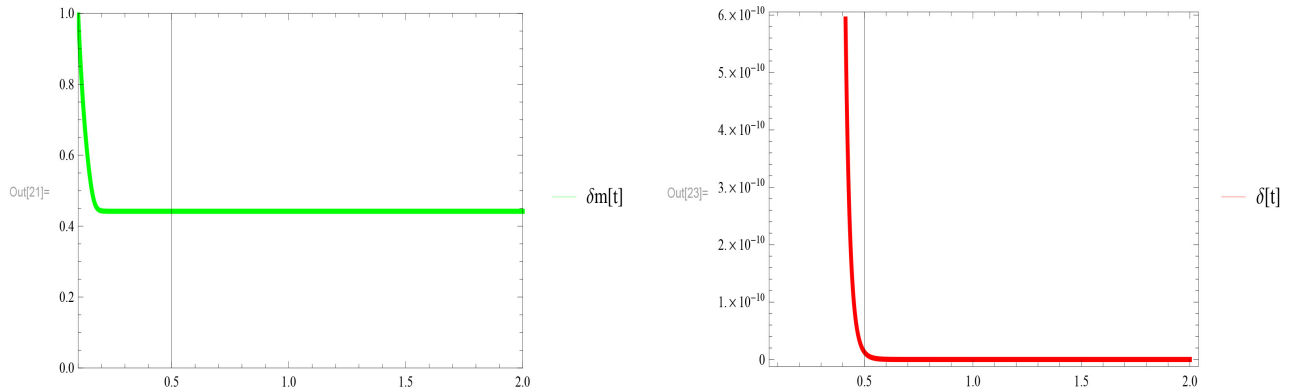


Figure 1. The perturbation functions of matter (green curve) and geometry (red curve), for: $\omega = 0$, $n = 8$; $\rho_0 = 10^{-9}$; $C_1 = 30$ and $C_2 = 100$.

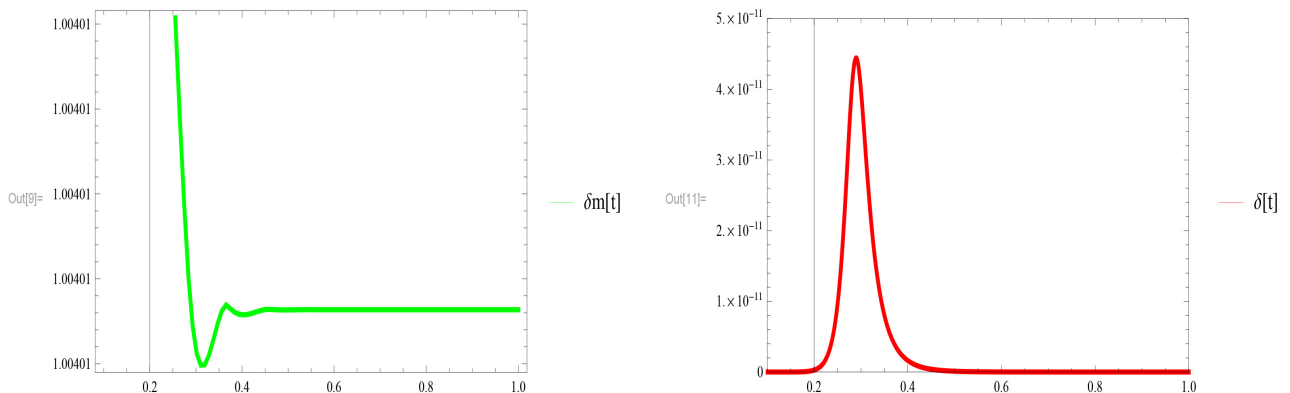


Figure 2. The perturbation functions of matter (green curve) and geometry (red curve), for: $\omega = 1/3$, $n = 8$; $\rho_0 = 10^{-9}$; $C_1 = 30$ and $C_2 = 100$.

5. Cosmological Inflation

In this section of our work, we study cosmological inflation. In particular, we will determine the values of the observables of the inflation phenomenon within the framework of a scale factor obeying the power law. Taking into consideration the Planck's results, we will deduce a family of models $f(G)$ capable of describing inflation.

5.1. Slow-Roll Parameters and Inflationary Observables

In cosmological inflation survey, several works have always been based on the study of the inflationary observables [38]. These are the scalar spectral index of the curvature perturbations n_s , the running $\alpha_s \equiv \frac{dn_s}{d \ln k}$ of the spectral index n_s where k is the absolute value of the wave number k , the spectral index n_T of the tensor and the ratio r .

From the scalar potential denoted $V(\phi)$ characterizing inflation and its derivatives, the parameters of the slow-roll are defined as follows [39] [40]:

$$\varepsilon \equiv \frac{M_p^2}{2} \left(\frac{1}{V} \frac{dV}{d\phi} \right)^2 \quad (42)$$

$$\eta \equiv \frac{M_p^2}{2} \frac{d^2 V}{d\phi^2} \quad (43)$$

$$\xi^2 \equiv \frac{M_p^4}{V^2} \frac{dV}{d\phi} \frac{d^3 V}{d\phi^3} \quad (44)$$

Note that the inflation ends when $\varepsilon = 1$.

We have the approximate expressions of the inflation observables as a function of the slow-roll parameters relative to the potential. They are written according to [39] [40]:

$$r \approx 16\varepsilon \quad (45)$$

$$n_s \approx 1 - 16\varepsilon + 2\eta \quad (46)$$

$$\alpha_s \approx 16\varepsilon\eta - 24\varepsilon^2 - 2\xi^2 \quad (47)$$

$$n_T \approx 16 - 2\varepsilon \quad (48)$$

Let us specify that in modified theory of gravity, it is not possible to exploit the conformal transformation of the Einstein theory because one cannot define neither a scalar potential, nor the parameters of the slow-roll relating to it. We then introduce the Hubble slow-roll parameters ε_n which are defined by:

$$\varepsilon_{n+1} \equiv \frac{d \ln |\varepsilon_n|}{dN} \quad (49)$$

with $\varepsilon_0 \equiv H_{ini}/H$ and $N \equiv \ln(a/a_{ini})$ the e-folding number and where a_{ini} is the scale factor at the start of inflation and H_{ini} is the corresponding Hubble parameter. It follows:

$$\varepsilon_1 \equiv \frac{\dot{H}}{H^2} \quad (50)$$

$$\varepsilon_2 \equiv \frac{\ddot{H}}{\dot{H}H} - \frac{2\dot{H}}{H^2} \quad (51)$$

$$\varepsilon_3 \equiv (\ddot{H}H - 2\dot{H}^2)^{-1} \left[\frac{\ddot{H}\dot{H}H - \ddot{H}(\dot{H}^2 + \ddot{H}H)}{\dot{H}H} - \frac{2\dot{H}}{H^2} (\ddot{H}H - 2\dot{H}^2) \right] \quad (52)$$

Thus, we obtain as in [39] [40] the inflation observables which are written:

$$r \approx 16\varepsilon_1 \quad (53)$$

$$n_s \approx 1 - 2\varepsilon_1 - 2\varepsilon_2 \quad (54)$$

$$\alpha_s \approx -2\varepsilon_1\varepsilon_2 - \varepsilon^2\varepsilon_3 \quad (55)$$

$$n_T \approx -2\varepsilon_1 \quad (56)$$

These observables thus expressed can be easily determined. Particularly within the framework of our study where we considered a scale factor evolving according to the power law.

5.2. Inflationary $F(G)$ Model in Agreement with Planck's Results

Recall that our model (18) was reconstructed from the first Friedmann equation. By ejecting this model into the second Friedmann equation, we get the following differential equation

$$\begin{aligned}
 & 2\dot{H}(1+\omega) \left[\frac{(-1+p)p^3}{H^2 + (H^2 + \dot{H})} \right]^{-\frac{3}{4}p(1+\omega)} + 4608H^4 \left\{ - \left((1+\omega) \left[-2 + \frac{3}{4}p(1+\omega) \right] \right. \right. \\
 & \times \left. \left[\frac{H^2 + (H^2 + \dot{H})}{(-1+p)p^3} \right]^{\frac{3}{4}(-4+p+p\omega)} \right) \left[18432(-1+p)^2 p^8 (-1+p(4+3\omega)) \right]^{-1} \\
 & - p \left[6144(1+p)H^2 (H^2 + \dot{H})^2 \sqrt{\frac{pH^2(H^2 + \dot{H})}{-1+p}} \right]^{-1} \left\{ \left[2\dot{H}^2 (2H^2 + \dot{H}) + H\ddot{H} \right]^2 \right. \\
 & + \left. \left\{ p \left[\left[2 - 2p(4+3\omega) \right] H^4 - 2[-1+p(4+3\omega)]H^2\dot{H} + (-1+p^2)(1+\omega) \right. \right. \right. \\
 & \times \left. \left[\frac{H^2(H^2 + \dot{H})}{(-1+p)p^3} \right]^{\frac{3}{4}p(1+\omega)} \sqrt{\frac{pH^2(H^2 + \dot{H})}{-1+p}} \right) \left[4H^4\dot{H} - 6\dot{H}^3\ddot{H} - 8H\dot{H}\ddot{H} - H^2(18\dot{H}^2 \right. \\
 & \left. \left. \left. + H^3 \right) \right] \right\} \left[4(1+P)[-1+p(4+3\omega)]H^2(H^2 + \dot{H})^2 \sqrt{\frac{pH^2(H^2 + \dot{H})}{-1+p}} \right]^{-1} = 0 \quad (57)
 \end{aligned}$$

The Equation (57) is a differential equation in $H(t)$ which admits for solution

$H(t) = \frac{p}{t}$. Thus, from relations (50)-(52), we obtain:

$$\varepsilon_1 = \frac{1}{p} \quad (58)$$

$$\varepsilon_2 = 0 \quad (59)$$

$$\varepsilon_3 = \frac{1}{p} \quad (60)$$

then, the relations (53)-(56) lead to:

$$r \approx \frac{16}{p} \quad (61)$$

$$n_s \approx 1 - \frac{2}{p} \quad (62)$$

$$\alpha_s \approx 0 \quad (63)$$

$$n_T \approx -\frac{2}{p} \quad (64)$$

These are the values of the observables of power law inflation. We will now de-

termine a $F(G)$ model capable of describing such inflation and which is in agreement with Planck's results.

According to Planck's results, we have: $0.962 \leq n_s \leq 0.974$ and by virtue of equality (62), we obtain: $52.632 \leq p \leq 76.923$.

By posing for example $p = 60$, we obtain: $r = 0.266$, $n_s = 0.966$, $\alpha_s = 0$ and $n_r = -0.033$ which are values actually in agreement with Planck's results. Considering that just after inflation, the universe is essentially dominated by radiation, we have $\omega = 1/3$ and the model becomes:

$$F(G) = C_2 G^{\frac{-59}{4}} - \frac{3\sqrt{590}}{61} \sqrt{G} + C_1 G - \frac{\rho_0}{4.042 \cdot 10^{511}} G^{60} \quad (65)$$

Note that it is possible to derive a $F(G)$ model family describing inflation and in perfect agreement with Planck's results by suitably choosing the values of the parameter p of our model.

The question that is actually to be asked consists in checking if the inflationary model (65) extols the exit from inflation.

5.3. Graceful Exit from Inflation

Several approaches are used to study the exit from inflation. Based on the dynamic of the Hubble parameter, the exit from inflation are successfully performed through the type VI singularity survey [45] and through the dynamic of the slow-roll parameters [46] [47]. For the first time, the authors in [48] have performed the exit from inflation by involving quantum effects coming from trace anomaly equation and giving a de Sitter solution whose instability scores the graceful exit from inflation. In [49], from an autonomous dynamical system reconstructed from $f(R)$ motion equation and assisted by scalar field, they numerically provide a de Sitter attractor which becomes unstable for e-fold number $N = 60$ (end of inflation), proof of a graceful exit from the inflationary era. The actor of this exit is the scalar field because in their previous analysis [50] without scalar field, the obtained de Sitter solution is eternally stable. This last result is confirmed in $f(T)$ theory by [51]. One can conclude from these last approach that the instability in a dynamical evolution is a source of graceful exit.

Recently, the authors in [9] have analysed an intrinsic dynamic in $f(G)$ theory where some conditions for the cosmological viability of $f(G)$ dark energy models have been performed. Through an approach based on autonomous dynamical system depending from two single parameters m and r , they provide natural conditions in the $f(G)$ gravity to describe a ordinary matter or radiation epoch, the dark energy epoch and the transition between the both epochs. The fundamental required condition is that the $m(r)$ curve should pass through $(-1/2; -1/2)$ in the $m-r$ plane. This means the same point $(-1/2, -1/2)$ corresponds to ordinary matter or radiation domination and the dark energy domination. So the critical points manifesting this property must be unstable in order to pass from matter or radiation domination epoch to the dark matter domination epoch. Such instability is reached when the parametric function

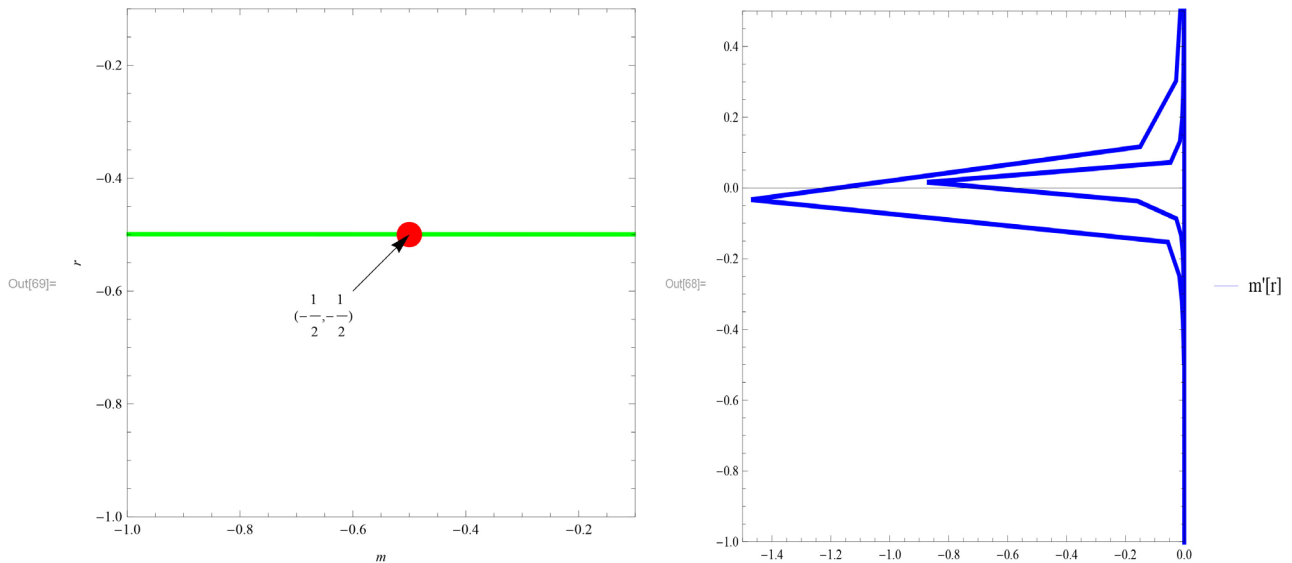


Figure 3. Evolution of $m(r)$ (green curve at left) and its first derivative $m'(r)$ (blue curve at right) for model (65) with $\rho_0 = 10^{200}$, $C_1 = 1.39727 \times 10^{45}$ and $C_2 = 1.14346 \times 10^{138}$.

$m(r)$ satisfies the condition $m'(-1/2) > -1$. The parameter m and r are given by

$$m(G) = \frac{Gf''(G)}{f'(G)} \quad \text{and} \quad r(G) = -\frac{Gf'(G)}{f(G)} \quad (66)$$

without providing the functional form of $m(r)$ and $m'(r)$ in the framework of the inflationary model (65), their parametric plot leads to the **Figure 3**. The green curve shows clearly the key point $(-1/2, -1/2)$ is reached meaning that this model can truly lead the radiation domination era. The condition of transition from the radiation domination era to ordinary matter domination era or dark energy domination era is clearly appreciable via the blue curve in the same **Figure 3** because it shows $m'(-1/2) > -1$. Such instability is qualified graceful exit from inflation [52].

6. Conclusion

During this study, we devoted to the reconstruction of a model in the modified theory of gravity $F(G)$. From well elucidated processes, we have conducted the study of its stability. The results obtained clearly show that the reconstructed model is stable for the both de Sitter and the power-law evolutions. Therefore, this model is potentially suitable for dealing with cosmological questions such as the inflation of the Universe, the explanation of the different phases of the evolution of the Universe, and many others. In this work, the question of the Universe inflation was also approached. The study made it possible to find the observables within the framework of a scale factor evolving according to the power law. This study also made it possible to determine a model describing the inflation of the universe and which is in agreement with Planck's results. Our analy-

sis shows that the obtained top model develops clearly the graceful exit from the inflation.

Conflicts of Interest

The authors declare no conflicts of interest regarding the publication of this paper.

References

- [1] Fabris, J. (2004) Introduction à la cosmologie. Ecole Internationale sur les Structures Géométriques et Applications, Dakar.
- [2] Riess, G., Filippenko, A.V., Challis, P., et al. (1998) *The Astronomical Journal*, **116**, 1009. <https://doi.org/10.1086/300499>
- [3] Perlmutter, S., Aldering, G., Goldhaber, G., et al. (1998) *The Astrophysical Journal*, **517**, 565.
- [4] Komatsu, E., Dunkley, J., Nolta, M.R., et al. (2008) *The Astrophysical Journal Supplement Series*, **180**, 330.
- [5] Komatsu, E., Smith, K.M., Dunkley, J., et al. (2011) *The Astrophysical Journal Supplement Series*, **192**, 18.
- [6] Bamba, K., Capozziello, S., Nojiri, S. and Odintsov, S.D. (2012) *Astrophysics and Space Science*, **342**, 155-228. <https://doi.org/10.1007/s10509-012-1181-8>
- [7] Nojiri, S. and Odintsov, S.D. (2005) *Physics Letters B*, **631**, 1.
- [8] Cognola, G., Elizalde, E., Nojiri, S., Odintsov, S.D. and Zerbini, S. (2006) *Physical Review D*, **73**, 084007. <https://doi.org/10.1103/PhysRevD.73.084007>
- [9] Zhou, S.Y., Copeland, E.J. and Saffin, P.M. (2009) *Journal of Cosmology and Astroparticle Physics*, **2009**, JCAP07(2009)009. <https://doi.org/10.1088/1475-7516/2009/07/009>
- [10] Chiba, T. (2005) *Journal of Cosmology and Astroparticle Physics*, **2005**, 8. <https://doi.org/10.1088/1475-7516/2005/03/008>
- [11] Cognola, G., Elizalde, E., Nojiri, S., Odintsov, S.D. and Zerbini, S. (2007) *Physical Review D*, **75**, 086002. <https://doi.org/10.1103/PhysRevD.75.086002>
- [12] De Felice, A., Hindmarsh, M. and Trodden, M. (2006) *Journal of Cosmology and Astroparticle Physics*, **8**, 5. <https://doi.org/10.1088/1475-7516/2006/08/005>
- [13] Amendola, L., Charmousis, C. and Davis, S.C. (2006) *Journal of Cosmology and Astroparticle Physics*, **12**, 020. <https://doi.org/10.1088/1475-7516/2006/12/020>
- [14] Motaharfara, M. and Sepangi, H.R. (2016) *The European Physical Journal C*, **76**, Article No. 646. <https://doi.org/10.1140/epjc/s10052-016-4474-1>
- [15] Koivisto, T. and Mota, D. (2006) *Physics Letters B*, **644**, 104-108. <https://doi.org/10.1016/j.physletb.2006.11.048>
- [16] Sanyal, A.K. (2007) *Physics Letters B*, **645**, 1-5. <https://doi.org/10.1016/j.physletb.2006.11.070>
- [17] Uddin, K., Lidsey, J.E. and Tavakol, R. (2009) *General Relativity and Gravitation*, **41**, No. 12.
- [18] Houndjo, S., Rodrigues, M., Momeni, D. and Myrzakulov, R. (2013) *Canadian Journal of Physics*, **92**, 1528-1540.
- [19] Rodrigues, M.E., Houndjo, M.J.S., Momeni, D. and Myrzakulov, R. (2013) *Canadian Journal of Physics*, **92**, No. 2. <https://doi.org/10.1139/cjp-2013-0414>

- [20] Nojiri, S., Odintsov, S., Toporensky, A. and Tretyakov, P. (2010) *General Relativity and Gravitation*, **42**, 1997-2008.
- [21] Setare, M.R. and Mohammadipour, N. (2012) Cosmography in $F(R)$ Modified Gravity. arXiv:1206.0245v1 [physics.gen-ph].
- [22] Li, B., Barrow, J.D. and Mota, D.F. (2007) *Physical Review D*, **76**, 044027. <https://doi.org/10.1103/PhysRevD.76.044027>
- [23] Boehmer, C.G. and Lobo, F.S.N. (2009) *Physical Review D*, **79**, 067504.
- [24] Guth, A.H. (1981) *Physical Review D*, **23**, 347. <https://doi.org/10.1103/PhysRevD.23.347>
- [25] Linde, A.D. (1983) *Physics Letters B*, **129**, 177-181. [https://doi.org/10.1016/0370-2693\(83\)90837-7](https://doi.org/10.1016/0370-2693(83)90837-7)
- [26] Bamba, K., Nojiri, S., Odintsov, S.D. and Sáez-Gómez, D. (2014) *Physical Review D*, **90**, 124061.
- [27] Bamba, K., Nojiri, S. and Odintsov, S.D. (2014) *Physics Letters B*, **737**, 374-378. <https://doi.org/10.1016/j.physletb.2014.09.014>
- [28] Gao, Q. and Gong, Y. (2014) *Physics Letters B*, **734**, 41-43. <https://doi.org/10.1016/j.physletb.2014.05.018>
- [29] Odintsov, S.D. and Oikonomou, V.K. (2018) *Physical Review D*, **98**, ID: 044039.
- [30] Kleidis, K. and Oikonomou, V.K. (2018) *International Journal of Geometric Methods in Modern Physics*, **15**, 1850137. <https://doi.org/10.1142/S0219887818501372>
- [31] Kleidis, K. and Oikonomou, V.K. (2018) *International Journal of Geometric Methods in Modern Physics*, **15**, 1850212. <https://doi.org/10.1142/S0219887818502122>
- [32] Odintsov, S.D. and Oikonomou, V.K. (2018) *Physical Review D*, **98**, 024013. <https://doi.org/10.1103/PhysRevD.98.024013>
- [33] Odintsov, S.D. and Oikonomou, V.K. (2015) Big-Bounce with Finite-time Singularity: The $F(R)$ Gravity Description. arXiv:1512.04787 [gr-qc].
- [34] Odintsov, S.D., Oikonomou, V.K., Fronimos, F.P. and Fasoulakos, K.V. (2010) Unification of a Bounce with a Viable Dark Energy Era in Gauss-Bonnet Gravity. arXiv:2010.13580.
- [35] Houndjo, M.J.S. (2017) *The European Physical Journal C*, **77**, Article No. 607. <https://doi.org/10.1140/epjc/s10052-017-5171-4>
- [36] Rudra, P. (2014) *International Journal of Modern Physics D*, **24**, No. 2.
- [37] Nojiri, S. and Odintsov, S. (2005) *Physics Letters B*, **631**, 1-6. <https://doi.org/10.1016/j.physletb.2005.10.010>
- [38] Nojiri, S., Odintsov, S.D. and Oikonomou, V.K. (2017) *Physics Reports*, **692**, 1-104. <https://doi.org/10.1016/j.physrep.2017.06.001>
- [39] Bamba, K., Odintsov, S. and Saridakis, E. (2017) *Modern Physics Letters A*, **32**, Article ID: 1750114.
- [40] Houndjo, S. (2017) *The European Physical Journal C*, **77**, 607.
- [41] Goheer, N., Goswami, R., Larena, J., Dunsby, P.K.S. and Ananda, K. (2009) *AIP Conference Proceedings*, **1241**, 898. <https://doi.org/10.1063/1.3462731>
- [42] De Felice, A. and Tsujikawa, S. (2009) *Physics Letters B*, **675**, 1-8.
- [43] de la Cruz-Dombriz, A. and Sáez-Gómez, D. (2012) *Classical and Quantum Gravity*, **29**, 245014.
- [44] Cai, Y., Capozziello, S., De Laurentis, M. and Saridakis, E. (2015) *Reports on Progress in Physics*, **79**, 106901.

- [45] Odinstov, S.D. and Oikonomou, V.K. (2015) Singular Inflationary Universe from $F(R)$ Gravity. arXiv: 1510.04333[gr-qc].
- [46] Odintsov, S.D. and Oikonomou, V.K. (2015) *Physical Review D*, **92**, 024058.
- [47] Odintsov, S.D. and Oikonomou, V.K. (2015) *Physical Review D*, **92**, 124024.
<https://doi.org/10.1103/PhysRevD.92.124024>
- [48] Bamba, K., Nojiri, S. and Odintsov, S.D. (2014) *Physics Letters B*, **731**, arXiv: 1401.7378v1[gr-qc].
- [49] Kleidis, K. and Oikonomou, V.K. (2018) Autonomous Dynamical System Description of de Sitter Evolution in Scalar Assisted $f(R)-\phi$ Gravity. [arXiv:1808.04674 [gr-qc]].
- [50] Odintsov, S.D. and Oikonomou, V.K. (2017) *Physical Review D*, **96**, Article: 104049. [arXiv:1711.02230v1[gr-qc]]. <https://doi.org/10.1103/PhysRevD.96.104049>
- [51] Ganiou, M.G., Logbo, P.H., Houndjo, M.J. and Tossa, J. (2019) *The European Physical Journal Plus*, **134**, Article No. 45.
<https://doi.org/10.1140/epjp/i2019-12393-8>
- [52] Nashed, G.G.L., El Hanafy, W. and Ibrahim, Sh.Kh. (2014) Graceful Exit from $f(T)$ Gravity. arXiv:1411.3293[gr-qc].

Tensor and Effective Vector Approach to Gravitational Radiation in the Weak Field Limit

P. Christillin

Dipartimento di Fisica, Università di Pisa, Pisa, Italy
Email: paolo.christillin@unipi.it

How to cite this paper: Christillin, P. (2021) Tensor and Effective Vector Approach to Gravitational Radiation in the Weak Field Limit. *Journal of Modern Physics*, 12, 798-805.

<https://doi.org/10.4236/jmp.2021.126051>

Received: March 21, 2021

Accepted: May 10, 2021

Published: May 13, 2021

Copyright © 2021 by author(s) and Scientific Research Publishing Inc.
This work is licensed under the Creative Commons Attribution International License (CC BY 4.0).

<http://creativecommons.org/licenses/by/4.0/>



Open Access

Abstract

The purpose of the present paper is to enquire whether General Relativity (GR) is necessary for the prediction of gravitational waves. It will be shown that in the weak field limit the same predictions come also from the treatment of a zero mass, spin 2 gravitational scattering amplitude. This will also justify the simpler effective vector approach of the author, only the angular distribution differing from that of a tensor theory.

Keywords

Gravitational Waves, Weak Field Limit, Non GR Approaches

1. Introduction

The recent detection of gravitational waves has been indeed a great technological achievement. As regards its theoretical interpretation however some clarifying remarks are needed. As well known a considerable number of problems arose with the treatment of gravitational waves in the non linear formulation of GR which led Einstein [1] to deny their existence even in the linearized case. Those problems were finally overcome (they were even at the very beginning [2]) but the folklore survived of the “non existence of gravitational waves”. This probably explains the amount of enthusiasm for their actual detection. In any case their existence in the weak field case (binary system 1916 + 13) is out of question and justifies the validity of the linearized theory. They do indeed carry energy and the radiated power has been accounted in a simple way just from the e.m. analog [3]. Actually even in the LIGO/VIRGO experiment a linearized approach has been used to describe the detection plus a simulation for the strong emission process.

2. The Scattering Amplitude

A very simple and elegant approach for the weak gravitational waves case had been put forward by Feynman [4] but seems to have remained rather unnoticed. For that reason we want to resume it and underline that the GR results for wave detection in the weak field limit can be simply obtained from the propagation of a massless spin 2 object and Lorentz invariance of the amplitude for the exchange of a graviton. This approach reproduces at the same time other features which have been so far considered to be a crucial proof of GR, namely the factor of two for gravitational light deflection. In addition it backs up the results obtained from the “naive” gravitomagnetism approach to gravitation [3]. Let therefore follow Feynman’s approach [4] starting from the electromagnetic vector case.

In both cases the basic ingredient is the consideration of the scattering amplitude (respectively photon and graviton) instead of the treatment of the vertex via the proper Lagrangian.

As it will be shown this allows a considerable simplification, essentially due just to Lorentz invariance and the features of the virtual exchanged photon and graviton will be taken over to the on shell case.

The vector

The source of e.m. is the vector current j_μ related to the vector potential A_μ by

$$A_\mu = -1/k^2 j_\mu \quad (1)$$

or in coordinate space

$$A_\mu = -\square j_\mu \quad (2)$$

The interaction between a current and the field *i.e.* $j_\mu A^\mu$ yields the interaction between the currents in the scattering amplitude f

$$f = j'_\mu \frac{1}{k_\mu^2} j^\mu \quad (3)$$

which for the particular choice

$$k^\mu = (\omega, 0, 0, k) \quad (4)$$

here $k = |\vec{k}|$, reads

$$f = \frac{1}{\omega^2 - k^2} [j'_4 j_4 - j'_1 j_1 - j'_2 j_2 - j'_3 j_3] \quad (5)$$

Current conservation

$$k^\mu j_\mu = 0 \quad (6)$$

i.e.

$$j^3 = \omega/kj^4 \quad (7)$$

allows us to put the amplitude in the form

$$f = \frac{j'_4 j_4}{k^2} + \frac{1}{\omega^2 - k^2} (j'_1 j_1 + j'_2 j_2) \quad (8)$$

The first term represents the (Fourier transform of the) well known instantaneous Coulomb potential, whereas the second the two components of plane polarized propagating waves.

Such a “miraculous” separation has been obtained with the ingredients:

- 1) Zero mass photon;
- 2) Current conservation;
- 3) Lorentz invariance of the amplitude.

From the scattering amplitude, the form of the vertex, taken to be equal at production and at absorption, will be inferred.

The tensor

Let us then pass over to gravitation which will be treated along the same lines. We will assume the source to be given by the energy momentum tensor since gravity is determined by energy and not by mass. This will “perturb” the Minkowski metric $g_{\mu\nu}$ with the addition of $h_{\mu\nu}$ (for an extension to higher orders, which is not our concern here, see e.g. P. Menotti [5])

$$h_{\mu\nu} = -1/k^2 T_{\mu\nu} \quad (9)$$

or in coordinate space

$$h_{\mu\nu} = -\square T_{\mu\nu} \quad (10)$$

Current conservation is here replaced by energy momentum conservation

$$k^\mu T_{\mu\nu} = 0 \quad (11)$$

with the same choice

$$k^\mu = (\omega, 0, 0, k)$$

In the first term of the scattering amplitude

$$f = T'_{\mu\nu} 1/|k_\mu^2| T^{\mu\nu} - \alpha T'_{\mu\mu} 1/|k_\mu^2| T^{\nu\nu} \quad (12)$$

which contains all possible ($i, j = 4, 3, 2, 1$) terms, the previous energy momentum conservation condition is used to get rid of the terms with index 3 via

$$\omega T_{4\nu} = -k T_{3\nu} \quad (13)$$

separating again the instantaneous part from the propagating one. Thus of the initial 10 terms six remain, respectively 3 instantaneous and 3 retarded.

Focusing on the latter ones, this might seem to imply the existence of three polarization states. One of them is however eliminated by the trace condition which disposes of the spin zero contribution by adjusting the above coefficient α to be equal to $1/2$).¹

The final expression for the total amplitude then reads

$$f \simeq \frac{1}{|k|^2} \left[T'_{44} T_{44} (1 - \omega^2/k^2) + T'_{44} (T_{11} + T_{22}) + (T'_{11} + T'_{22}) T_{44} - 4T'_{41} T_{41} - 4T'_{42} T_{42} \right] + \frac{1}{\omega^2 - k^2} \left[(T'_{11} - T'_{22})(T_{11} - T_{22}) - 4T'_{12} T_{12} \right] \quad (14)$$

where the pole terms represent the two degrees of freedom of the propagating

¹It is easy to see that this term just corresponds to the addition of the term $-1/2 \eta_{\mu\nu} T$ to the vertex of the linearized theory. Thus Feynman’s approach elegantly bypasses all of the formal gauge requirements.

waves due to the transverse quadrupole components. *Exactly the GR result (see below)*. The ingredients used in the derivation of the amplitude are just

- 1) Zero mass of the graviton;
- 2) Energy momentum conservation;
- 3) No spin zero;
- 4) Lorentz invariance.

In this case too the vertex can be inferred only by assuming that also at the source we have a weak field production. Its structure is more involved than in the vectors case.

The first term corresponds to the usual Newtonian attraction plus a relativistic correction.

The term $T'_{44}T_{11}$ would lead in the case of the gravitational attraction by a fixed source (T'_{44}) of a relativistic particle, in particular a photon, to an additional factor of 2 with respect to the Newtonian result $T'_{44}T_{44}$. This is because $T_{11} = v^2/c^2 T_{44}$ so that “the energy of the photon and hence its attraction is doubled.” *Lorentz invariance is thus enough to produce twice the Newtonian light deflection by a fixed source.*

This can also be directly read from the form of the scattering amplitude. Indeed the counter term (spin zero) is manifestly zero for the photon whereas $= -1/2 \frac{m^2}{k^2}$ for a N.R. massive particle. Thus the amplitude for the photon is twice the latter.

All of the other terms except the 44 ones are $O(v^2/c^2)$. However only the terms T_{41}, T_{42} are linear in the velocities v_1, v_2 , thus of a vector-vector form, so only they correspond to the usual magnetic terms namely gravitomagnetic ones. In the approximate vector description of gravity they are responsible for magnetic effects which then lead via the displacement term to radiation. They enter with a factor of 4 which means that when rephrased as an effective vector interaction the current for gravitation is

$$j_G = 2mv \quad (15)$$

This might appear contradictory with the current conservation relation used above for the e.m. current but has been explicitly derived from SR arguments in an effective vector formulation of gravitation (EVG) in [3], showing that only with this factor the propagation velocity is c as explicitly used also in Feynman's formulation. The previous result comes about because once more the Lorentz constraint of the scattering amplitude allows *to this order*, to extract an “effective” form of the vertex. Notice also, that only for the quadrupole radiation (because of the absence of dipole) can radiation be accounted for by a true quadrupole (T_{11}) in the tensor formulation and by the retardation of the gravitomagnetic terms (T_{4i}) in the vector theory.

In conclusion the doubling of the attraction of a photon (with respect to the Newtonian case) and the doubling of the current obtained naively from the analogous electromagnetic one ($q \rightarrow m$) are a simple consequence of the tensor

nature of gravity and are not results peculiar to GR.

In short we can summarize it by saying that the (non Lorentz invariant, to this order) gravitational current (in an equivalent vector theory) of a photon can be taken to be

$$(2\hbar\omega, 2m\mathbf{v}) \quad (16)$$

where the gravitomagnetic terms are now responsible for radiation along the electromagnetic lines.

3. Quadrupole Radiation = Tidal Effects in Minkovski Space

Given the remarkable result that a number of supposed GR predictions can be reproduced alternatively in a much simpler way, let us now enquire also in this case what remains as a peculiar GR feature. As said before in the weak field limit just a tensor formulation yields GR results, so in this section we will be concerned only with the comparison with the effective vector approach.

In the e.m. formulation the angular distribution ($d\omega$) of the electric quadrupole radiation is proportional to

$$\int \left| \hat{\mathbf{r}} \times \frac{d^3 \vec{Q}_{ij}}{dt^3} \right| \frac{d\omega}{4\pi} = \frac{1}{5} \left| \frac{d^3 Q_{ij}}{dt^3} \right|^2 \quad (17)$$

[6] where

$$\vec{Q}_{ij} = \hat{r}_j Q_{ij}$$

and Q_{ij} stands for the usual traceless momentum tensor. Thus the quadrupole radiation is transverse, as it should, and is it only its angle average which is expressed in terms of the true quadrupole moment.

As regards gravitation, the traceless transverse (TT) gauge expresses the power as the time derivative of the strain tensor h_{ij}

$$h_{ij} \simeq \int \frac{d^3 x' T_{ij}}{r} \quad (18)$$

where T_{ij} stands for the transverse spacial components of the energy momentum tensor.

No explicit expression of T_{ij} is utilized but, by using conservation of the energy momentum tensor, the usual quadrupole expression is derived:

$$\int d^3 x' T_{ij} = \frac{1}{c^2} \frac{d^2}{dt^2} \int d^3 x T_{00} x_i x_j \quad (19)$$

this incorporates all of the dynamics, retardation etc. of $T_{\mu\nu}$ in the double derivative of the source and yields for the strain tensor h_{ij}

$$h_{ij} = \frac{2G}{3rc^4} \frac{d^2 Q_{ij}}{dt^2} \quad (20)$$

Thus the emitted power is given by its time derivative and hence by the third derivative of the quadrupole momentum tensor. This can be obtained in terms of the e.m one by replacing

$$W_G = W_{el} \left(\frac{1}{4\pi\epsilon_0} \rightarrow G, q \rightarrow 2m \right) \quad (21)$$

where the last substitution actually corresponds to the above mentioned “effective” gravitomagnetic current.

$$W = \frac{G}{45c^5} \left| \frac{d^3 Q_{ij}}{dt^3} \right|^2 \quad (22)$$

Thus the transverse e.m field and the transverse graviton enter the rate only as a function of the third derivative of the respective quadrupole moment.

Let us then pass over to consider differential effects so as to ascertain how much of the tensor nature of gravitation really comes into play. Let us first of all recall that

$$g_P \simeq \frac{G}{c^3 r} \frac{d^3 (Ml^2)}{dt^3} \simeq \frac{GMl^2 \omega^3}{c^3} \frac{e^{i\omega t}}{r} \simeq \frac{G}{c^3 r} \frac{Ml^2}{T^3} \quad (23)$$

where the term $k \cdot r$ in the exponential has already been used for the retardation necessary to derive the quadrupole, and

$$\frac{b}{c} \simeq \frac{G}{c^4 r} \frac{Ml^2}{T^2} \simeq \frac{GM}{c^2 r} \left(\frac{l}{cT} \right)^2 \quad (24)$$

is related to the strain tensor by

$$\frac{b}{c} \simeq \hat{r}_j \cdot h_{ij} \quad (25)$$

where

$$g = -\frac{db}{dt}$$

b being the velocity imparted by the wave to the apparatus. It is worth noticing the difference with respect to the static radial case. All the effect is governed by the transversality of the field. Because of the finite light velocity and its propagation time between the two extremes of the apparatus (the related laser signal)

$$t' \simeq t + L/c$$

time dependent tidal effects arise, thus correcting the conclusions of [7].

In effect consider now two generic points P and P' , the extremes of our apparatus of length L . They will be subjected to the gravitational acceleration of a gravitational wave which can be analyzed in sinusoidal components, so *both locally at rest in the respective free fall frames. However the acceleration at the time the gravitational wave reaches P and at the time elapsed for the photon to reach P' from P , distance covered by light in a first approximation in time $\Delta t = L/c$, are in general different simply because*

$$dg_P/dt \neq 0$$

In other words, considering for simplicity a transverse apparatus arm (to the propagation direction and hence collinear with the polarization vector) of length

L the time dependent acceleration at one extreme is not the same the other extreme experiences at time t' even at a wave front.

Thus by expanding in terms of $\omega L/c$, one gets for the differential acceleration

$$g_{P'} - g_P \simeq \left(\frac{dg_P}{dt} \right) \Delta t \simeq \frac{dg_P}{dt} \frac{L}{c} \quad (26)$$

In the (sub) Newtonian regime proper to interaction with matter, one can directly use $ma = F$

$$\frac{d^2 \Delta L}{dt^2} = \left(\frac{dg_P}{dt} \right) \frac{L}{c} \simeq - \left(\frac{d^2}{dt^2} b \right) \frac{L}{c} \quad (27)$$

so that

$$\frac{\Delta L}{L} = - \frac{b}{c} \quad (28)$$

In the general case a factor $1 - \cos \theta$ if L forms such an angle with respect to r intervenes.

Thus the equivalence principle in the case of radiation replaces the space tidal effects of the static case by the time dependent ones for waves

$$\Delta r/r \Rightarrow \simeq \Delta t/T \simeq L/cT$$

i.e. the relative variation of the radiation acceleration in the time of detection over the signal period. Notice that in this semi quantitative derivation (which is in any case totally consistent with the approximations of the standard GR treatment) nothing more than the time dependence of the acceleration and the finite velocity of light has entered.

In conclusion a time dependent tidal effect for gravitational waves is reproduced also by an effective vector theory and is again not a feature of GR, although only the (hardly measurable) angular distribution and the effects of the transverse polarizations are different in the two approaches.

4. Conclusion

It has been recalled that just a tensor approach to gravitation can account for gravitational waves in the weak field limit with the same GR results. The same outcome can also be obtained in an effective vector theory of gravitation. Only the angular distribution and the effects of the polarization are different and might thus provide in principle a test of the tensor approach to gravitation. In conclusion in addition to the effects (light deflection, red shift, perihelion precession) which have been regarded as peculiar to GR also the main features of radiation can be obtained with alternative simpler formulations.

Acknowledgements

It is a pleasure to thank G. Morchio for continuous discussions and for enlightening criticism throughout this work.

Conflicts of Interest

The author declares no conflicts of interest regarding the publication of this paper.

References

- [1] Einstein, A. (1916) *Annalen der Physik*, **354**, 769-822.
<https://doi.org/10.1002/andp.19163540702>
- [2] Denson, C. (2016) Hill and Pawel Nurowski. arxiv: 1608.08673v1[gr-qc].
- [3] Christillin, P. and Barattini, L. (2012) Gravitomagnetic Forces and Quadrupole Gravitational Radiation from Special Relativity. arXiv:1205.3514v3 [physics.gen-ph].
- [4] Feynman, R. (1964) Lectures on Gravitation. CRC Press, Boca Raton.
- [5] Menotti, P. (2017) Lectures on Gravitation. arXiv:1703.05155v1 [gr-qc].
- [6] Massachusetts Institute of Technology, Department of Physics (2005) Electromagnetic Radiation and Scattering. Physics 8.07.
<http://core.csu.edu.cn/NR/rdonlyres/Physics/8-07Fall-2005/9281A8EE-B595-43DB-BA3E-190BE126516D/0/radiation.pdf>
- [7] Christillin, P. (2015) *The European Physical Journal Plus*, **130**, 132.
<https://doi.org/10.1140/epjp/i2015-15132-3>

Inflation, Dark Energy, Acceleration, Missing Mass?

P. Christillin

Dipartimento di Fisica, Università di Pisa, Pisa, Italy

Email: paolo.christillin@unipi.it

How to cite this paper: Christillin, P. (2021) Inflation, Dark Energy, Acceleration, Missing Mass? *Journal of Modern Physics*, 12, 806-828.

<https://doi.org/10.4236/jmp.2021.126052>

Received: March 10, 2021

Accepted: May 10, 2021

Published: May 13, 2021

Copyright © 2021 by author(s) and Scientific Research Publishing Inc.

This work is licensed under the Creative Commons Attribution International License (CC BY 4.0).

<http://creativecommons.org/licenses/by/4.0/>



Open Access

Abstract

The black hole (b.h.) model based on the strong field treatment of the Newton potential is presented. The essential role of self energy both at the Planck level and for matter and radiation at later stages supports the picture of an expanding Universe necessarily accompanied by particle creation if energy conservation applies at every scale. This process is shown to provide a gravitational repulsive force which can counterbalance gravitational attraction thus allowing the possibility of a steady expansion. This black hole treatment of our Universe evolution, questions the necessity of inflation. The role of the critical density to dictate the fate of the Universe is replaced by the black hole condition which entails a different relation between Hubble parameter and density thus disposing of dark energy. Since its predictions provide a different time development of the Universe also the evidence for its acceleration is disputed. That seems to provide a coherent scheme for our picture of the Universe evolution, based on Hubble's law and backed up by the consideration of inertial forces. Newtonian angular momentum is also not conserved at cosmological scales. Finally we consider two coordinates systems. The conformally flat coordinates are shown to disprove inflation and the relevance of the Painleve-Gullstrand metric in providing global coordinates is underlined. The combined effect of Hubble expansion and of proper time also questions the existence of missing mass.

Keywords

Cosmogony, Black Hole, Particle Creation, Inflation, Dark Energy, Missing Mass

1. Introduction: The Origin of the Big Bang and Its Evolution

The present cosmological description is, to say the least, unsatisfactory. Essential

ingredients appear to be ad hoc recipes: inflation, missing mass and dark energy. The main ingredient is General Relativity (GR) [1] which however was founded before Hubble's [2] discovery, so that a theory essentially meant to describe a static Universe was forced to incorporate this revolutionary effect via the notorious cosmological constant. This artifact, of no physical origin, then entails in the first Friedman [3] equation (see below) the appearance of the even more mysterious dark energy, which has rightly eluded till now any experimental evidence. In addition great part of the dynamics, up to superclusters, has been described in Newtonian terms, which have thus legitimated the existence of missing mass. Let us also recall that two essential hypotheses are at the foundations of our theoretical framework: isotropy and homogeneity. Whereas the first is backed up by evidence, the second is a reasonable but disputable ingredient although it has the great advantage of allowing simpler calculations. It is more in the line of a Copernican line of thought. However this implies the absence of pressure gradients and this seems to represent another formidable problem. As a matter of fact whereas in Newtonian mechanics the repulsive role of pressure is paramount in the description of stellar formation, no such a role is played in GR. Quite on the opposite pressure adds up to ordinary matter density and increases attraction. But in the end fits demand it to be negative and hence curiously reminiscent of the "old" (Newtonian) repulsive pressure!

For our purposes the most relevant thing is the connection between the self energy and the mass which implies (following Feynman's conjecture [4]) that the energy to assemble from infinity many masses $M = \sum_i m(i)$ is zero when their self energy provides a deep enough potential well,

$$Mc^2 - \frac{GM^2}{R} = 0 \quad (1)$$

and the corresponding strong field parameter

$$\varepsilon = \frac{GM}{c^2 R} = 1$$

The above requirement is easily understood. A bound gravitational system of whichever form (photons or matter) increases its energy when the interaction distance increases. Since energy must be conserved this can happen only by allowing for matter (energy) creation to restore the energy balance, as it is actually the case. And this reflects in the strong field parameter. Of course this approach is highly speculative but "we must remember that here we are not dealing with an ordinary problem but with a cosmological problem" [4]. It is obviously based on the form of the Newtonian potential, probed in familiar contexts, implemented by the b.h. condition. This is, so to say, the opposite of the GR approach which is, in a sense, the extension of the weak field Newtonian limit.

Our aim will be to see whether this, Newton based, very simple model accounts for experimental facts without additional parameters. Indeed to make a long story short GR, at least in the form of Friedman [3] equations, essentially

reproduces Newtonian physics apart from the cosmological term.

In addition ε intervenes in the problem of inertial forces. Indeed the inertial and gravitational masses m_i and m_g are equal if

$$m_i c^2 = \frac{GMm_g}{r}$$

i.e.

$$\varepsilon = 1$$

This is only a qualitative argument which has been detailed for the different situations where inertial forces enter in Ref. s ([5] [6] [7] [8] [9]).

There is an additional relation which deserves attention, at least heuristically. Namely from the b.h. condition one can derive

$$W_U = E_U / t_U = m_U c^2 / t_U = c^5 / G = W_P$$

i.e. that the power to create matter in the Universe is constant and equal to that at the Planck time to create radiation. Interesting is also the fact that in the expression for the Planck power \hbar has disappeared. Of course this is balanced by an equal and opposite contribution from the self energy.

For the present Universe

$$\frac{GM_U}{c^2 R_U} \simeq 1$$

where $M_U = M_0$ and $R_U = R_0$ the subscript 0 standing for the present value of these quantities and when there is no possibility of misunderstanding simply M ad R .

It is obvious that in a Universe which has expanded, if the mass would have remained constant, as in the standard treatment where $\rho = 1/R^3$, the previous value would have become

$$\varepsilon' = \frac{GM_U}{c^2 R'_U} = \varepsilon \times \frac{R_U}{R'_U} \quad (2)$$

which implies in turn a negative total energy! To cure it we must admit that the total mass has varied, necessarily increasing by the same amount.¹

Such an approach for the varying mass problem has already been proposed in [11] which we follow here in an improved version.

It has been strongly emphasized [12] how close to the critical one the density in the course of the expansion must have been otherwise we would not be here. This reflects in the constancy of **the strong field parameter** ε . An additional argument why ε cannot depend on time is that the only reasonable possibility is

$$\frac{d\varepsilon}{dt} \simeq H(t)\varepsilon$$

Now since H is positive and $\varepsilon(\text{Planck}) = \varepsilon(U) = 1$, as it will be shown later,

¹Such a relation which realizes Mach's principle has also been used by [10] in considering the possibility of a G variation. This however has been experimentally disproved.

this eventuality is discarded.

Clearly *the constancy of ε implies the cancellation of the acceleration*. Indeed

$$\frac{d\varepsilon}{dt} = \frac{GdM}{Rdt} - \frac{GMdR}{R^2dt} = 0 \quad (3)$$

where the last term is proportional to the acceleration

$$a \cdot v = \frac{GMdR}{R^2dt}$$

cancelled by the mass variation

$$a = \frac{GdM}{RdR}$$

Thus the matter creation mechanism entering the black hole condition implies also a steady state expansion.

The present treatment will hence be based on Equations (1) and (3).

How the b.h. condition treated as an equation compares to the Einstein ones will also be elucidated in the following. The essential point seems to be its implementation of the strong field limit which appears to be realized in our Universe. How that happens will be shown explicitly for radiation.

2. The Planck Scenario

Vacuum fluctuations *i.e.* the appearance of virtual particles are an essential ingredient of our theoretical armory. For instance in QED the vacuum fluctuation of an e^+e^- pair lives because of the uncertainty principle

$$\Delta E \Delta t \geq \hbar \quad (4)$$

essentially for times

$$\Delta t \simeq 1/(2m_e c^2)$$

and the potential $V \simeq \frac{e^2}{r}$ modifies negligibly the previous argument.²

According to the prevailing picture the Planck fluctuation should last for times of the order of Planck's time $t_p \simeq 10^{-44}$ sec.

That this is not so can be seen by considering that the total Planck energy \mathcal{E}_p is zero

$$\mathcal{E}_p = E_p - GM_p^2/R_p = M_p c^2 - GM_p^2/R_p = 0 \quad (5)$$

³⁾ *i.e. the same condition which applies to our Universe.* The previous relation can be also easily proven with the explicit form of the Planck quantities.

This backs up one way of deriving the Planck quantities by requiring the Compton wavelength of a particle to coincide with its b.h. radius. Thus the Planck mass corresponds to the energy contained in the minimum quantum radius (because it cannot be of smaller dimensions without violating the uncertainty

²In this connection let us recall speculations [13] according to which in the QED strong field case also the previous relation might not hold true thus leading to pair creation.

³One should therefore probably re express the uncertainty relation as $\Delta \mathcal{E}_p \Delta t \geq \hbar$.

principle) *i.e.* to **the smallest quantum black hole**.

Such a configuration is not stable and can thus evolve.

Starting from the Planck scale, where dR cannot decrease, this bubble must have necessarily expanded. However an expanding gravitational system of given mass gains energy because of the interaction term as mentioned in the previous paragraph. Thus in order to conserve the total energy, and because of the different role of the mass in the two terms, such an expansion produces a mass increase *i.e.* mass must be created.

Notice also (by using $200 \text{ MeV fm} = 1$) that

$$E_p = kT_p R_p \simeq 10^{19} \text{ GeV} \times 10^{-35} \text{ m} = 10^{22} \text{ MeV} \times 10^{-20} \text{ fm} \simeq 1/2$$

which indicates a “strong interaction” relation between gravitational Planck quantities arising just from first principles.

The interesting thing is moreover that the black body total energy expression

$$E_p = kT_p (kT_p R_p)^3 \simeq kT_p$$

yields effectively an additional consistency relation, substantiating the previous relation (to within the above numerical approximations). The photon number is thus

$$N_p \simeq (kT_p R_p)^3 \simeq 1$$

The previous relation should be corrected by including the effective number of constituents which behave like photons above their respective threshold [14] and hence contribute a sizable amount of energy (ν, e^+e^- , hadrons). However the above connection between energy and photon number can be used as an effective result.

In conclusion ε_p is equal to 1 and Feynman’s [4] conjecture receives also a microscopic support.

3. The Time of Radiation. The Role of Pressure Gradient

The balance between gravitational attraction of the photon cloud and its pressure has also been considered by Weinberg [14] (“it is the balance between the gravitational field and the outward momentum of the contents of the universe that governs the rate of expansion of the universe”).

Let us start by considering early enough times *i.e.* when “photons” are in thermal equilibrium with hadrons through creation and destruction of (typically) nucleon-antinucleon pairs (short for hadrons like quarks.. etc and other degrees of freedom) which will add to photons, which however determine the typical orders of magnitude, particles masses being negligible. The photon energy density being

$$\varepsilon_{rad} = c^2 \rho \simeq (kT)^4 \simeq p$$

the radiation mass is

$$m_{rad} c^2 \simeq (kT)^4 R^3 \simeq kT (kTR)^3 = (kT) N_\gamma$$

Notice that these relations are based only on the Special Relativity treatment

of the black body. But its gravitational self energy in these extreme conditions cannot be neglected. We demand again the whole energy to be zero. The form of the self energy is dictated by the Newton potential⁴

$$Gm_{rad}^2/R = m_{rad}c^2$$

In sum energy conservation can be formulated for primordial “photons” as

$$\mathcal{E} \simeq (kT)^4 R^3 \left(1 - \frac{G(kT)^4 R^3}{c^4 R} \right) = 0 \quad (6)$$

The overall total “bare” energy factors our like the mass in the energy conserved Newtonian approach. We have

$$\frac{c^2}{R^2} = H^2 = G\rho = \frac{G(kT)^4}{c^2}$$

which is sort of a *relativistic Hubble-like relation for the dimensions of the Universe whose outer radius expands at velocity c*. This provides a tentative alternative description where the **critical density is halved and no dark energy enters** (see below Friedman equations). Since the Hubble parameter is seen to be determined by highly relativistic galaxies it seems also from an experimental point of view more adequate to resort to a relativistic description.

Indeed one has for $R = 10^{26}$ m

$$t_U = \frac{R}{c} \simeq 3 \times 10^{17} \text{ sec}$$

which is in line with the traditional value and also the well known relation between temperature and the age of the Universe

$$T^2 \simeq \frac{1}{t} \quad (7)$$

We can thus summarize our results:

1) total energy remains equal to zero

$$(KT)^4 R^2 \rightarrow \text{const}$$

and the temperature decreases.

2) bare mass increases

$$(kT)^4 R^3 \rightarrow R$$

3) photon number increases

$$(kT)^3 R^3 \rightarrow R^{3/2}$$

This provides repulsion. A huge generation of less energetic photons has taken place (because of the deep potential well) and a comparable number of nucleon-antinucleon pairs has been created which are in thermal equilibrium with them and which annihilate.

⁴Also Weinberg considered the balance between pressure and potential energy to determine the Jeans mass which at $T = 3000$ K resulted in too big globular clusters. That would roughly correspond in the present approach to the total Universe mass.

From the previous expressions it is immediate to get

$$d\rho/\rho = -2dR/R = 4dT/T$$

As mentioned in the introduction also the cancellation of the acceleration results.

Now

$$\begin{aligned}\frac{dM}{dR} &= \frac{(kT)^4}{dT} R^3 \frac{dT}{dR} + 3(kT)^4 R^2 \\ &= -2(kT)^3 R^3 (KT/R) + 3(kT)^4 R^2 \\ &= (kT)^4 R^2 = \frac{M}{R}\end{aligned}$$

which corresponds to Equation (3).

Therefore *the matter creation mechanism entering the black hole condition implies also a steady state expansion*. The previous equation also clarifies the role of the expansion (+) and of the temperature (−) in the varying mass. Also with a generic $\rho \simeq 1/R^2$, without an explicit T dependence, the result holds true.

Let us underlined once more that the N_γ behavior is the opposite of the classical black body spectrum where, at constant R a decreasing temperature implies a decreasing number of photons. The fundamental difference is however that the temperature decrease is due here to an expansion *i.e.* to an increase of the “box” and this will result in an increase of the photon number.

Here the black body treatment of primordial photons realizes and justifies the previous general results, at variance with GR.

We can conclude that pressure counterbalancing attraction seems to be proven for radiation (so that we do not think it justified to follow GR in adding pressure to the attraction) and for later times when hadrons are formed the dilution due to Universe expansion may be compensated by the increase of their number.

This approach differs from the steady state proposal by Hoyle [15] since for us the density variation is fundamental and we give a microscopic justification of particle creation. As mentioned the constancy of ε guarantees the constancy of the inertial mass and presumably disposes of the retardation problem.

4. The Universe Evolution. Baryogenesis

As repeatedly underlined the relevant point is that the self energy dependence on R is not the same as that of the energy so that this correction does not factorize. Thus self-energy can then act as a gauge in the reconstruction of the history of the Universe. **As a consequence its evolution will be dictated by the black hole condition and will be therefore different from the traditional one determined by the GR equations.** In particular it will affect the CMB treatment and its horizon determination. Also the ratio of nucleon to photon number will be shown not to be constant.

Indeed whereas in going backward in time the black body constraint on matter keeps being valid (apart from very early times where it has to be interpreted as “radiation”), for photons it begins to play a role when the photon energy increases reaching that limit at recombination and matches with the treatment of radiation of primordial times.

We try here to outline the behavior of radiation and matter in the course of time (recalling some of the results obtained in [11]). Of course both of them contribute to the gravitational field. Due to their different behavior it is however simpler to treat them separately. At present the matter contribution completely realizes the strong field limit whereas radiation, in spite of the numerical preponderance of photons yields a negligible contribution. Indeed the total matter energy in the Universe coming from Hubble’s law is

$$E_m \simeq 10^{80} \text{ GeV} \simeq 10^{80} m_p \quad (8)$$

depending on the nucleon energy density ε_m and the particle density n_m , as

$$\varepsilon_m = n_m (mc^2 + 3/2 kT)$$

m standing here for the nucleon mass and subscript m for matter. The present energy density of radiation, coming from the CBR, is

$$\varepsilon_\gamma \simeq (kT_\gamma)^4 \simeq 10^5 \text{ eV/m}^3 \quad (9)$$

This yields a total energy of radiation for the Universe at present

$$E_\gamma \simeq \varepsilon_\gamma (R_U)^3 \simeq 10^{74} \text{ GeV} \quad (10)$$

Thus matter dominates in energy over radiation

$$E_\gamma / E_m \simeq 10^{-6} \quad (11)$$

However the total number of photons is given by

$$N_\gamma = n_\gamma R^3 \simeq 10^{87}$$

The ratio of photons to nucleons is thus of the order

$$\frac{N_\gamma}{N_m} \simeq 10^7$$

where $N_m = n_m R^3$.

As regards matter their present dominance with $\varepsilon = 1$ is used to reconstruct their importance down to $T = 10^{13} \text{ K}$ where photons materialize in them. Therefore

- 1) $T = 10^{32} \text{ K}$, $t \simeq 10^{-44} \text{ sec}$, $R \simeq 10^{-35} \text{ m}$ the Universe begins
- 2) $T = 10^{13} \text{ K}$, $t \simeq 10^{-5} \text{ sec}$, $R = 3 \times 10^3 \text{ m}$

The number of photons at this temperature is roughly 10^{57} which is also pleasantly the number of nucleons in going from the present 10^{80} to 10^{57} at that time (radii being in a $\simeq 10^{26}/10^3$ ratio).

With these numbers we can give a more direct justification of baryogenesis. Indeed with the equality of the number of photons and nucleon antinucleons at

this temperature it would be enough an imbalance of $O(10^{-7})$ to justify the present nucleon dominance. So the explanation of baryogenesis is rather insensitive to the model, provided it reproduces the photon dominance.

$$3) \quad T = 10^9 \text{ K}, \quad t \simeq 10^3 \text{ sec}, \quad R = 3 \times 10^{11} \text{ m}$$

This is the temperature for electron positron threshold. Below they annihilate leaving a cold Universe where nuclei can start forming. The photon to nucleon

ratio is $\left. \frac{N_\gamma}{N_m} \right|_{t_{e^+e^-}} \simeq 10^4$. Customarily the photon density is regarded as a reliable

quantity. Its ratio to nucleon density is then used to determine the latter quantity and finally the present percentage of the critical density. Of course since the reconstruction history is different in the present model, also that number will differ. Indeed when the photon mean free path will become larger than the Hubble radius

$$\lambda = \frac{1}{n_m \sigma_e} > \frac{c}{H}$$

where $\sigma_e = 6.6 \times 10^{-29} \text{ m}^2$ and $n_m = n_e$, photons will decouple from the electrons and the Universe will become transparent. And this decoupling happens roughly at recombination. Moreover baryogenesis (and D production) can be accounted for only if the nucleon density is sufficiently low. In a standard context with constant nucleon number the density at that time would have turned out too big, *whereas in the present approach where the nucleon number varies with time this finds a natural explanation, contradicting the smallness of the present nucleonic percentage.*

4) $T = 3000 \text{ K}$ **recombination**, $t_{rec} \simeq 3 \times 10^{14} \text{ sec}$. (roughly one order of magnitude bigger than the traditional estimate based on $R \simeq t^{2/3}$), $R_{rec} = 10^{23} \text{ m}$.⁵

The remarkable thing is that at *recombination photon and the matter energy equalize*. Indeed $E_\gamma \simeq 3 \times 10^{77} \text{ GeV}$ whereas by enforcing the strong field limit for matter $M_m \simeq 10^{77} \text{ GeV}$. *Thus the remark by Weinberg [14] "It is striking that the transition from a radiation to a matter dominated universe occurred at just about the same time that the contents of the universe were becoming transparent to radiation, at about 3000 K. No one really knows why this should be so..." receives in this approach a natural explanation.*

Note also that the photon density n_γ is of the order of 10^9 at $T = 3 \text{ K}$ and of 10^{18} at $T = 3000 \text{ K}$. Thus N_γ is constant from $R = 10^{26}$ to $R_{rec} = 10^{23}$

corresponding to $z = 1000$. The photon to nucleon ratio is $\left. \frac{N_\gamma}{N_m} \right|_{rec} \simeq 10^9$

compared with the present estimate 10^7 showing that this ratio is not constant in time as usually said.

To summarize, back to R_{rec} we have conservation of N_γ but decrease of

⁵However at recombination the strong field limit is overcome by the previous value of the Universe radius so that in order to be consistent R must be determined from $R^2 = \frac{c^4}{G(kT)^4}$ which yields

$R \simeq 3 \times 10^{22}$, slightly altering the previous estimate.

N_m till the different energy equalize. In still former times but after $T = 10^{13}$ both energy densities increase in the same way because of the self energy constraint. But their number density varies as

$$\frac{n_\gamma}{n_m} \simeq \frac{m_p c^2 + 3/2 kT}{kT_\gamma} \quad (12)$$

In conclusions one has a linear connection between matter creation and the dimensions of the Universe throughout, and a linear dependence between the temperature of radiation and radius R back to recombination time and quadratic before, Equation (7)

$$T^2 \simeq 1/t = c/R$$

A totally different scenario from the prevailing one.⁶

5. On the Friedman Equations. Elementary Considerations

The Friedman equations with the cosmological term for a flat Universe read

$$H^2 = 8\pi/3 G\rho + \Lambda/3 \quad (13)$$

and

$$\dot{H} + H^2 = -4\pi/3 G(\rho + 3p/c^2) + \Lambda/3 \quad (14)$$

where $H = \dot{\chi}/\chi$ and χ is the scale factor. They are based on the LFRW metric which will be extensively treated in par. 7) and are the Einstein equations relevant to determine the velocity and acceleration of the Universe.

Let us first underline an obvious fact. *Thanks to the Lemaitre-Hubble relation the first two terms of the first equation are forced to have the same χ dependence. The dimensions of the sphere around the origin factorize. This means that ρ is independent of scale and may only depend on time.* Thus the fact that one obtains the same condition which is regarded as a property of an infinite universe, implies that one can use the metric and the equations locally also for the interior of the finite b.h. bubble.

Thus the fact that the previous equation seems to get a support from the Newtonian limit is utterly misleading. Indeed in that case a real constant can be added to the sum of the kinetic and potential energy determining the escape velocity. However no similar role can be attributed to Λ in the cosmological case (it is worth recalling that the cosmological term was indeed introduced in order to provide a stable non expanding Universe, that the solution was found by Friedman not to be stable and that the cosmological constant was “forced” after the Lemaitre-Hubble discovery to somehow reproduce a repulsive agent). Thus Equation (15) and Equation (16) are substantially different.

⁶This does not exhaust the treatment of photons. Indeed the CXB [16] shows the presence of an *additional* sizable energetic photon background due to the $T \simeq 10^7$ K $\simeq 30$ KeV photon emission from the core in the formation process of stars. Whether this can contribute to the baryonic black hole limit is an open question. In any case this more energetic photon component coming mainly from AGNs pertains to a later stage of the evolution.

$$V^2 - 2G\rho R^2 = \text{const} = E \quad (15)$$

$$H^2 R^2 - 2G\rho R^2 \neq \text{const}' = R^2 \Lambda \quad (16)$$

Put it another way one cannot add a constant term to a homogeneous equation without contradicting it.

Let us also remark that pressure enters GR⁷ so has to increase the effect of matter density but then in whichever form $(\rho + 3p/c^2)$ or in the cosmological term it turns out to be necessarily negative in order to account for experimental data. In this phenomenological approach it is attributed a repulsive role along the Newtonian picture, its gradient balances gravitational attraction and just from inspection of the previous equations this is consistent with the relativistic Hubble like equation without any dark energy. It has already been underlined that the b.h. condition halves the potential contribution to the first equation. Indeed as it is more transparent in Newtonian terms, in GR the coefficient of $G\rho$ comes essentially from a N.R. $v^2/2 = G\rho$ where of course v can never attain c , thus doubling the role of the density. This in spite of the fact that the Hubble parameter is essentially of relativistic character $H_o \simeq 10^{-18} \text{ sec}^{-1} \simeq c/R_U$ with a “reasonable” $R_U \simeq 10^{26} \text{ m}$. From the b.h. condition $c^2/R_U^2 = G\rho$ one immediately obtains a halved role of the density.

So dark energy exists only within the standard theoretical framework and its existence ironically recalls of ether. As a matter of fact the necessity of introducing the cosmological term in the acceleration equation implies an additional contribution of its potential energy. This does not happen for the b.h. model where the counter-acceleration follows from the varying mass in the energy equation.⁸

The role of the density in the b.h. model is different from that in the Friedman equations. Indeed according to our model the density is fixed by the equation and there is no critical density which determines the fate of the Universe which will expand for ever.

6. The Cosmological Term and Vacuum Energy. The Problem of Flatness

Let us consider the first (the energy) Friedman equation which can be rewritten as

$$1 = \Omega = \Omega_m + \Omega_\Lambda \simeq \frac{G\rho}{H^2} + \frac{\Lambda}{H^2}$$

⁷This does not question how pressure enters the energy momentum tensor nor GR, the problem simply being whether that theory accounts for reality or not.

⁸We give here an additional heuristic argument to show how one can reconcile the present approach with Friedman-like equations. As a matter of fact if we give Λ its correct dimensions c^2/R^2 in the second equation, by neglecting pressure and imposing zero acceleration $\frac{GM}{R^3} = \frac{\Lambda c^2}{R^2}$ with a unit value for Λ we have $\frac{GM}{c^2 R} = \Lambda = 1$. Thus a non constant cosmological term could realize the black hole condition. As mentioned, in going from the acceleration equation to the energy one the b.h. condition fixes the “integration constant”.

and said to be valid for all times (see e.g. [17]). It should constrain the amount of matter density and of the elusive dark energy associated to the cosmological constant. Now in the present matter dominated regime where $\chi \simeq t^{2/3}$ we have

$$\rho \simeq \chi^{-3} \simeq 1/t^2$$

and

$$H^2 \simeq 1/t^2$$

The same time dependent behavior of ρ results also for radiation era where $\chi \simeq t^{1/2}$ and with $\rho \simeq 1/R^2$ and $R \simeq c/t$ although with a different meaning of R (with respect to χ) and different consequences. This proves that $\rho = \rho(t)$ gives only the gross features of our expansion (in the sense that the two previous different solutions are both compatible) and that finer details can only be got from the behavior of χ .

Therefore if energy conservation (to which the previous condition essentially corresponds) has a meaning at all *i.e.* must be valid at any time and not by chance just at the present one, the term with *constant* Λ would increase due to the factor $1/H^2$ in the future and decrease in the past thus unmistakably violating the above equality.

In fact

$$\frac{d\Omega}{d\chi} = \frac{1}{\dot{\chi}} \frac{d\Omega}{dt} = 0 + \frac{1}{\dot{\chi}} \Lambda \frac{d(1/H^2)}{dt}$$

The previous relation is regarded as a test of no curvature and at the same time it raises the problem of why space-time, which is the strongest quantity in the Universe development [18], would have so dramatically changed in the course of time due to the time dependence of the second term. This has been overcome (see e.g. [19]) showing that the effect coming from the cosmological term can be cancelled only by a curvature effect in turn reexpressed through the second Friedman equation. Its deviation from 1 is then shown to depend on the parameter of the corresponding pressure which has been obliged to be again negative ($p \simeq -\rho$). This leads to the stability of the solution $\Omega \simeq 1$. *Thus space curvature peculiar to GR can be reconciled with flatness simply because self energy provides the appropriate counterterm.* In other words the popular picture of space deformation by gravity at a local level is completely discarded at universal scales.

It can be also easily recognized that the previous condition on Ω is equivalent to the time derivative of the b.h. condition.

Let us also underline that a void Universe $\rho = 0$ [20] would also produce $v = \text{const}$. That can be reconciled with our preceding result where $\rho \neq 0$ in the sense that the total zero energy requirement seems to be somewhat equivalent to the no matter case.

Finally Perlmutter's [21] worry about the fact that "it seems a remarkable and

implausible coincidence that the mass density, just in the present epoch, is within a factor of 2 of the vacuum energy density” finds a natural explanation. The two things are just the same: indeed the **(non existing)** cosmological term can be related at most to (a fraction of) the present matter density.

$$H_0^2 \simeq G\rho_U \simeq \frac{GM_U}{R_U^3} \simeq \frac{c^2}{R_U^2} = \frac{1}{t_U^2} \quad (17)$$

which when compared to the primordial quantities

$$H_p^2 \simeq G\rho_p \simeq \frac{GM_p}{R_p^3} = \frac{c^2}{R_p^2} = \frac{1}{t_p^2} \quad (18)$$

would yield

$$\frac{H_0^2}{H_p^2} = \frac{t_p^2}{t_U^2} \simeq 10^{-122} \quad (19)$$

and identifying Λ with a fraction of matter density

$$\Lambda_0/\Lambda_p \simeq H_0^2/H_p^2 \simeq 10^{-122} \quad (20)$$

Thus what is presented (if one assumes the constancy of Λ) as the well known most disastrous prediction of physics ever, unless various bosons, fermions etc. would conspire to cancel these 120 orders of magnitude, seems to find here a natural explanation. Λ could be interpreted **at best** as part of the rate of particle creation from the vacuum which “accompanies” a varying matter density of the universe. In other words we have to admit that the “Universe vacuum” may differ from the textbook one.

7. Different Metrics and the Horizon Problem. Inflation? Acceleration?

We now pass to see which conclusions can be reached in a more formal way. The local invariant interval of a *homogeneous isotropic* expanding Universe reads

$$ds^2 = c^2 dt^2 - \chi^2(t) dx^2 \quad (21)$$

where $\chi(t)$ is the **dimensionless** scale factor which is supposed to convey all of the time dependence of the expansion, x is the comoving coordinate and the angular dependence has been left over because of isotropy.

We will examine two different implementations:

- 1) the time dependence of $\chi(t)$ is reabsorbed in the term $c^2 dt^2$ via a rescaling of the invariant interval.
- 2) a “Painleve-Gullstrand like” one (or the Lemaitre-Hubble-Painleve-Gullstrand), where the same approach used in the central symmetric static case [22] will be extended to the “Hubble frame”. In other words like the free falling frame is used to dispose of gravity allowing the local use of SR, so it happens here for the (infinity of) frames which expand at the Hubble velocity.

Both approaches have advantages for different aspects of the problem and will help to elucidate which physical features are of course common to both and hence physical and which statements on the contrary have a significance only relative to a given metric.

1) Rescaled Minkovski interval or the conformally flat coordinates and causality. The problem of the horizon. Inflation?

The previous expression Equation (21) can be rewritten for $t \geq 0$ as

$$ds^2 = \chi^2(t) [c^2 d\tau^2 - dx^2]$$

where

$$d\tau = dt/\chi(t)$$

In terms of (τ, x) light velocity is always c but of course the flow of time is altered with respect to “ours”.

Notice that

$$\int dt/t$$

(non accelerated expansion) is divergent for early times unlike $\chi \simeq t^\alpha$ (decelerated expansion) for the α of the GR treatment. If χ is integrable, time has had a beginning and there are regions not causally connected to a common one in the past, if not this time is infinite in the past and any two finite regions have a common one in the past which they are causally connected to. This coordinate system is hence particularly suited for the discussion of causality since it is of the Minkovski form and it puts strong bounds on the behavior of the scaling factor χ .

Indeed light velocity is obtained as usual by putting to zero the previous invariant interval

$$\frac{dx}{dt} = \frac{c}{\chi(t)}$$

and in the present model $\chi = t/t_0$.

The interpretation of $\tau(t)$, the conformal time, is important. It represents the comoving distance traveled by light at time t . Since two points can communicate at most with light velocity it therefore represents the dimensions of the region causally connected at time t , thus defining the causal horizon.

This $1/t$ behavior which “stretches” early times with respect to the present ones, is enough to solve the problem of causality and the connected horizon problem. Indeed it reproduces naturally the inflationary explosion.

As a matter of fact in the present model the dimensions of the region causally connected and hence thermalized at decoupling $\Delta\chi_{dec}$ are much bigger than the comoving Hubble radius $\Delta\chi_H$ which determines (for us) the observable region (see **Figure 1**)

$$\Delta\chi_{dec} \simeq \int_{t_p}^{t_{rec}} dt/t \gg \Delta\chi_H \simeq \int_{t_{rec}}^{t_0} dt/t$$

$$14 - (-44) \gg 17 - 14$$

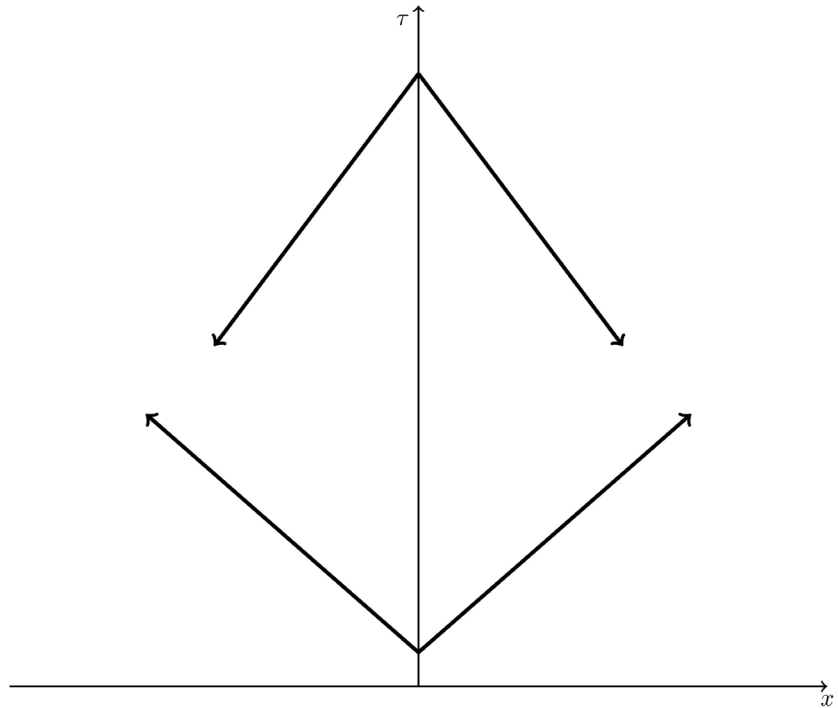


Figure 1. Starting at τ_p from a region of dimensions R_p whose worlds lines expand at velocity c all subsequent events are causally connected since they were at the Planck scale. τ is the comoving time.

The world we experience has always been in causal contact.

Moreover it gives us a measure of temperature fluctuations at decoupling time which appear at an angle of $O(1^\circ)$ degrees. That the previous relation yields

$$\frac{\Delta\chi_H}{\Delta\chi_{dec}} = \theta \simeq 3^\circ$$

should not be considered as a failure but on the contrary a spectacular semi-quantitative confirmation of the present approach over 60 orders of magnitude.

Let us now turn to the problem of the reported acceleration of supernovae. The comoving distance

$$\chi(a) = \int_{t(a)}^{t_0} dt'/t'$$

in the standard approach where $R \simeq t^{2/3}$ is given by [23]

$$2/H_0 \left(1 - 1/\sqrt{1+z}\right)$$

whereas for “our” $R \simeq t$ by

$$1/H_0 \ln(1+z)$$

As can be easily seen from **Figure 2**, they are equal for $z = 0.0026$ whereas for $z = 0.86$ they are respectively 0.52 [23] in the traditional approach and 0.60 in present one, and for higher z always bigger in the latter. This is easily explained. The Universe was decelerating for $R \simeq t^{2/3}$ and hence light took less time to reach us from distant stars; therefore distant objects would look brighter.

Thus in order to justify their apparent faintness one had to invoke an acceleration. On the contrary in the present approach, since expansion was a steady one, high z objects are actually farther apart than in the traditional scenario and hence fainter. We then see that the time evolution predicted by GR in a standard treatment can only be maintained at the price of introducing extra parameters (particularly dark energy), which are not necessary in the present description. One might object that one has replaced one parameter with another one. This is however not completely true in the sense that our “creation” mechanism has some microscopic justification particularly in the radiation era, and is predictive without further adjustments, in addition to accounting for causality whereas dark energy and inflation seem just questionable recipes.

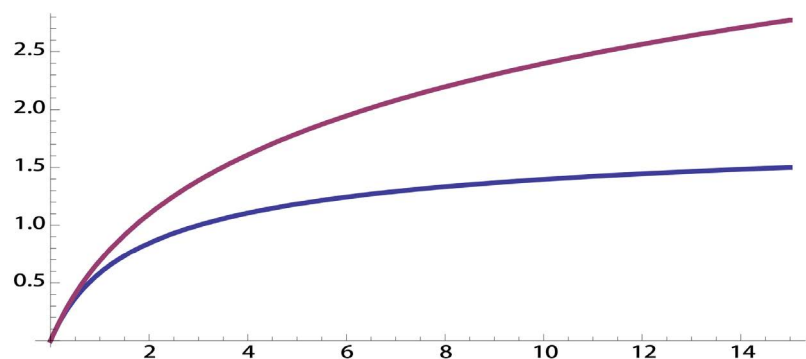


Figure 2. Comoving distance in the standard approach where $R \simeq t^{2/3}$ (lower curve) and in the present model where $R \simeq t$ (upper curve) vs. z . For given z comoving distances in the present approach are larger typically by some tens of a percent which correspond actually to differences between traditional predictions and measured luminosities.

The red shift is easily accounted for along standard lines. Indeed light emitted at former time t_1 is affected with respect to the present time t_0 where $\chi(t_0)=1$ by the factor $\chi(t_1)$ *i.e.* time runs slower. Hence the present time frequency is much slower than that at the time of emission

$$\frac{\omega(t')}{\omega(t_0)} = \frac{1}{\chi(t')} = \frac{\lambda_0}{\lambda'} = \frac{R_0}{R'}$$

To conclude the present $1/t$ evolution the Planck fluctuation disposes of inflation. The standard picture of an infinite Universe at the Planck time, which, because of the unexpected causal connections, necessarily has to shrink at the inflation “point” which then expands very rapidly for a very short time is thus over-ridden.

2) The Lemaitre-Hubble-Painleve-Gullstrand (LHPG) metric

Let us come to another relevant coordinate system: the Hubble-Painleve-Gullstrand (LHPG). This is reproduced by introducing in the invariant interval Equation (21)

$$ds^2 = c^2 dt^2 - \chi^2(t) dx^2 \quad (22)$$

$y = \chi x$ and the Hubble parameter $H = H(t) = \frac{\dot{\chi}}{\chi}$.

Thus

$$ds^2 = c^2 dt^2 - \chi^2(t) \left[\left(\frac{dy}{\chi} - \frac{\dot{\chi}}{\chi^2} y dt \right)^2 \right]$$

or

$$ds^2 = dt^2 \left(c^2 - (\dot{y} - Hy)^2 \right) \quad (23)$$

So the original space part of the invariant interval has been transformed in a velocity dependent one in contrast to what has been done in the case of the rescaled Minkovski interval.

Here

$$Hy = v(t, y)$$

represents the velocity of expansion of the point y at the time t .

We can [22] keep the invariant interval in the genuine Painleve'-Gullstrand form *i.e.*

$$ds^2 = c^2 dt^2 \left(1 - (Hy/c)^2 \right) - dy^2 + 2Hy dy dt + dy_{\perp}^2$$

At equal times ($dt = 0$) the radial y coordinate

$$ds = dy$$

measures *proper distances*.

We then have by putting $dy = 0$

$$ds^2 = d\tau^2 = c^2 dt^2 \left(1 - (Hy/c)^2 \right)$$

the proper time. Thus *we get a well known but nevertheless relevant result that the most distant the celestial objects under consideration the higher their velocity and consequently the smaller their time intervals. Thus far away objects live longer than naively expected with respect to our time.*

For transverse light propagation

$$\frac{dy_{\perp}}{dt} = c \sqrt{1 - (Hy/c)^2}$$

Radial light propagation is got by setting to zero the previous invariant interval

$$c = \pm (\dot{y} - Hy)$$

or in terms of y , $|y| = y$ in the (y, t) plane

$$\frac{dy}{dt} = H(t)y - c$$

where the case of backward propagation is considered in order to see objects in the past.

The first relevant result is that **the velocity of light, always c in the local frame changes in space-time** as the vector composition with the Hubble ex-

pansion velocity. Thus light was more and more deviated in the past because of the increasing role of $H(t)$ in the radial and transverse light propagation. This makes clear how the velocity of stars is of course composed of the recession velocity of the Hubble frame plus the intrinsic *subluminal* intrinsic velocity \dot{x} . This explains the so called “superluminal” behaviour of galaxies with high z .

The similarity with the P.G. metric ([22] and ref.s therein) used in the static spherically symmetric case is manifest. There the free falling frame carrying the absolute time of ∞ represented the inertial frame with the SR Minkovski interval locally eliminating gravity. Here the same happens for the outward Hubble velocity. **Therefore the LHPG metric represents an infinity of inertial frame and provides a dynamical extension of the Minkovski metric** more in the Einstein spirit, this time not “eliminating” gravity but expansion.

The connection between the rescaled and LHPG coordinate systems is immediate.

If we rewrite the basic equation in terms of the comoving coordinate

$$\frac{d\chi x}{dt} = \dot{\chi}x + \chi\dot{x} = \dot{\chi}x - c$$

we get

$$\frac{dx}{dt} = \frac{c}{\chi}$$

(where the proper sign of c has been chosen) just reproducing the light velocity of the previous paragraph.

Recently the most distant galaxies observed (GN-z11) and (EGSY8p7) with respectively $z = 11.1$ and 8.68 at a distance of 13.4 and 13.2 billions of years have caused particular concern because of their closeness to the very age of the Universe. This however depends again on the history reconstruction. *The present $t'/t_0 \simeq 1/z$ with respect to $t'/t_0 \simeq (1/z)^{3/2}$ of the usual treatment leaves us unworried since the time span between t' and the present t_0 is larger in this approach than in the standard one.*

This metric has manifestly the advantage, already clear in the static symmetric case, of evidentiating the connection between local and global coordinates in the propagation of light. The mirage effect in space-time, much bigger than in light deflection and in lensing, would alter our view of the past. This is illustrated in **Figure 3** and represents a *simple realization of the photon geodetics*, which near us can be well approximated by $y + c(t - t^2/t_0)$. Thus after decoupling which represents for us the frontier of visibility almost a straight line. This metric has however the advantage of explicitly showing that world lines originated in the primeval black hole.

Finally application of the Euler-Lagrange equations (which can be used also for galaxies) of motion in the N.R. limit

$$\delta \int L dt = \delta \int ds = \delta \int dt \sqrt{1 - \left[(\dot{y} - H(t)y)^2 \right]} = 0 \quad (24)$$

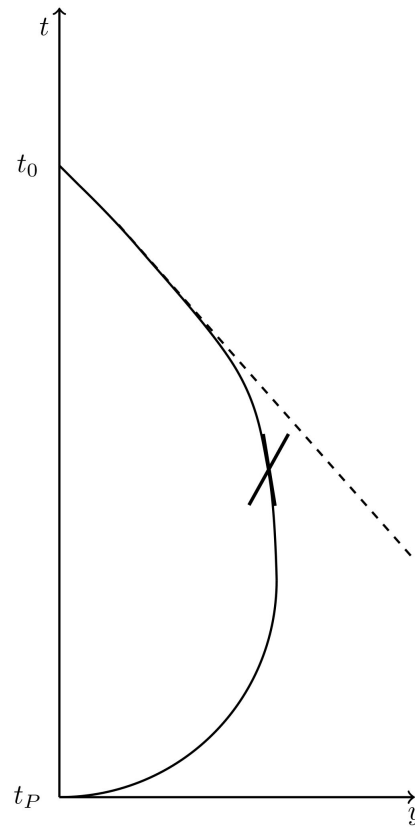


Figure 3. Light propagation in the (t, y) plane. Because of the vector composition of the local invariant light velocity c with the frame velocity determined by the varying Hubble parameter, light as observed at a given place (on Earth at present for example) in global coordinates deviates more and more when emitted at former times (with an analogous effect to light deviation in a static gravitational field). Not in scale.

yields

$$\ddot{y} = -(\dot{H} + H^2) \dot{y}$$

where the expression of the Universe acceleration enters. Thus the equivalence principle holds true if the Universe expansion is unaccelerated.

8. On Olbers's Paradox

We want briefly to reconsider the reasons why the night is not brilliant. The first qualitative argument is that the night is indeed bright but at the wavelength of CMB photons and not at wavelength of visible light.

Take a single star at a distance r from the earth of radius R . If it emits W photons per unit time, a fraction

$$W \frac{\pi R^2}{4\pi r^2}$$

is received from the earth. Consider then the whole Universe as composed of spherical layers of width dr with N stars per unit volume. The total contribution is then

$$W \frac{R^2}{4\pi r^2} 4\pi N r^2 dr$$

which, when integrated over all space appears to yield an infinite contribution. However, since distant stars have increasing velocity all of them outside of $r = GM/c^2$ do not contribute making the sum finite. Thus the same black hole condition enters again.

9. Hubble's Law, Angular Momentum and Missing Mass

An immediate consequence of Hubble's law is that since all points are equivalent the same expansion law should hold for all of them. Although this may appear trivial, *the expansion with respect to a privileged point i.e. the center of a system (galaxy) implies that the relative distance of the orbiting object varies, apart from the moving away of the whole system.*

In Newtonian mechanism angular momentum for central forces is conserved *i.e.*

$$\frac{d}{dt} \mathbf{L} = \frac{d}{dt} \mathbf{r} \times m\mathbf{v} = 0$$

However if Hubble's law is valid

$$\frac{d}{dt} \mathbf{r} \times m\mathbf{v} = H\mathbf{r} \times m\mathbf{v}$$

This implies non conservation of angular momentum

$$\frac{d}{dt} \mathbf{L} = H\mathbf{L}$$

Thus in addition to particle number conservation another cherished belief cannot be extrapolated from our limited space time experience to other scales proper to the Universe creation process.

One could as well reexpress the previous relation as

$$\frac{\Delta \mathbf{L}}{\mathbf{L}} \simeq HT$$

i.e. that the violation of angular momentum conservation for a central force is greater the bigger the dimensions and therefore the characteristic time (T) of the system, in line with the previous result.

This analysis has used Newtonian absolute time. It is therefore not correct, but it was just aimed at showing the limits of a Keplerian treatment.

Let us now turn to the missing mass problem. If one has a mass M with spherical symmetry orbiting ones obey Newton's law thus determining their acceleration and therefore

$$\frac{v^2}{r} = \frac{GM}{r^2}$$

Thus the velocity should fall as $v \simeq 1/\sqrt{r}$. This is not what one observe since the orbital velocity is greater or when a curve is measured it flattens out for large

distances. Well known examples are the Sun velocity, the external Hydrogen lines orbiting the galaxy M33 and M11 and the Coma cluster whose parameters have been reported in the accompanying table. The Keplerian approach is apparently justified since involved velocities are indeed non relativistic. To start with, given the quoted values for the velocities the respective periods are of the order of 10^8 y, 10^8 y and 10^9 y respectively. To trust our theoretical treatment over such periods when the star formation mechanism is not yet established is probably a bit presumptuous. This has lead, among other alternatives [24], to postulate the existence of missing mass. Its features, apart from peculiar gravitational properties, are a relative increase according to the dimensions of the system (Table 1).

Table 1. Astronomical parameters. Distances in meters. Velocities in km/s. In the final column the Hubble velocity $v_H = Hd$, calculated not at the present time t_0 but at $t' \simeq 10^{16}$ sec, time of structure formation, is reported.

star	distance r	dimensions d	velocity	Hubble velocity
sun		3×10^{20}	220	30
M_{33}	10^{14}	10^{20}	150	10
Coma	3×10^{24}	10^{22}	1500	1000

Thus the quantities for our Galaxy and M_{33} are similar but the distance of the latter is larger whereas for Coma all of them are bigger. For what has been said before we have H at the time of formation. The “Hubble” velocity which should add to that coming from the virial theorem and attributed to the visible mass is then almost ok for the sun, scanty for M_{33} and again ok for Coma. Moreover rotating external layers might influence the velocity of orbiting masses. This has been considered by Mizony [25] showing that this is indeed the case and that the usual treatment based on a symmetrical central mass is inadequate, thus disproving a missing mass halo. One further comment about the usual statement that dark matter is necessary to assure the necessary gravitational force to bind these systems otherwise they would have disappeared [26] To start with super-clusters are not seen nearer and therefore at later times, where they have evolved in smaller structures (galaxies) with higher symmetry. Therefore they have decayed. Second we have from the LHRW invariant interval the connection between distant objects and their proper time. That is **the farther the stars the slower their proper time**. For instance for the Coma cluster the factor $\sqrt{1-(Hy/c)^2}$ entering the proper time is close to zero with the present parameters. The ensuing picture is that of a competition between the Hubble effect which tends to disrupt and the slowing down of time which temporarily assures the stability of the gravitating system. This completely overturns the naive and peacefully picture of Newtonian systems and alters our view of the past. Therefore we might conclude that the existence of missing mass is at least questioned.

10. Conclusions

As summarized in the introduction the present theoretical situation is commonly dramatically presented as: some 90 percent of our world is in the form of unknown entities (dark matter and dark energy) with, to say the least, “peculiar” properties. This naturally leads to question the validity of the GR description, which because of the success in the post Newtonian regime (whose results can however be obtained simply from the Equivalence Principle and Special Relativity [22]) seems hardly questionable. In the present work the theoretical treatment has therefore been reconsidered. *The model has been presented of a black hole Universe. It can successfully account for inflation, the horizon problem, flatness, dark energy. It also questions the reported acceleration and partially the need of dark matter.* The extrapolation to cosmogonical scales of some of our most cherished and successful belief (at our space time scales) has been proven to be incorrect.

Namely particle number and Newtonian angular momentum are necessarily not conserved.

Acknowledgements

This work originates from continuous discussions with G. Morchio whom I want to thank particularly for the paragraphs on the metrics. I wish also to thank Dr. E. Cataldo for continuous encouragement.

Conflicts of Interest


The author declares no conflicts of interest regarding the publication of this paper.

References

- [1] Einstein, A. (1916) *Annalen der Physik*, **49**, 769-822.
<https://doi.org/10.1002/andp.19163540702>
- [2] Hubble, E. (1929) *Proceedings of the National Academy of Sciences of the United States of America*, **15**, 168-173. <https://doi.org/10.1073/pnas.15.3.168>
- [3] Friedman, A. (1922) *Zeitschrift für Physik*, **10**, 377-386.
<https://doi.org/10.1007/BF01332580>
- [4] Feynman, R. (1999) *Lectures on Gravitation*. Penguin Books, London.
- [5] Sciama, D.W. (1959) *The Unity of the Universe*. Doubleday, Garden City.
- [6] Berry, M. (1976) *Principles of Cosmology and Gravitation*. Cambridge University Press, Cambridge.
- [7] Christillin, P. and Barattini, L. (2012) *Journal of Modern Physics*, **3**, 1298-1300.
<https://doi.org/10.4236/jmp.2012.329167>
- [8] Christillin, P. and Barattini, L. (2012) Gravitomagnetic Forces and Quadrupole Gravitational Radiation from Special Relativity.
- [9] Christillin, P. (2014) *The European Physical Journal Plus*, **129**, 175.
<https://doi.org/10.1140/epjp/i2014-14175-2>
- [10] Brans, C. and Dicke, R. (1961) *Physical Review*, **124**, 925-935.

- <https://doi.org/10.1103/PhysRev.124.925>
- [11] Christillin, P. (2016) *Journal of Modern Physics*, **7**, 1331-1344.
<https://doi.org/10.4236/jmp.2016.711119>
 - [12] Barrow, J.D. (2002) *The Constants of Nature*. Jonathan Cape, London.
 - [13] Greiner, W. (2013) *Quantum Electrodynamics of Strong Fields*. Nato Science Series B, Springer, Berlin.
 - [14] Weinberg, S. (1993) *The First Three Minutes*. Basic Books, New York.
 - [15] Hoyle, F. (1948) *Monthly Notices of the Royal Astronomical Society*, **108**, 372-382.
<https://doi.org/10.1093/mnras/108.5.372>
 - [16] Giacconi, R., Gursky, H., Paolini, F.R. and Rossi, B.B. (1962) *Physical Review Letters*, **9**, 439. <https://doi.org/10.1103/PhysRevLett.9.439>
 - [17] Maoz, D. (2007) *Astrophysics in a Nutshell*. Princeton University Press, Princeton.
 - [18] Fang, L.S. and Li, S.X. (1990) *La Creazione dell Universo*. Garzanti Editore, Milano.
 - [19] Caldarelli, M.M. (2016) *Introduzione alla cosmologia*.
 - [20] Milne, E.A. (1935) *Relativity, Gravitation and World Structure*. Oxford University Press, Oxford. <https://doi.org/10.1038/135635a0>.
 - [21] Perlmutter, S. (2003) *Physics Today*, **56**, 53. <https://doi.org/10.1063/1.1580050>
 - [22] Christillin, P. and Morchio, G. (2017) *Relativistic Newtonian Gravitation*.
 - [23] Dodelson, S. (2003) *Modern Cosmology*. Academic Press, Cambridge.
 - [24] Milgrom, M. (1983) *The Astrophysical Journal*, **270**, 365-370.
<https://doi.org/10.1086/161130>
 - [25] Mizony, M. (2007) *Flatness of the Rotation Curves of the Galaxies, Exit the Recourse to a Massive Halo*.
 - [26] Henry, P., Briel, U.G. and Boeringer, H. (1999) *L'evoluzione degli ammassi di galassie. Le Scienze*, **366**, 40.

Homological Solution of the Lanczos Problems in Arbitrary Dimension

Jean-Francois Pommaret 

CERMICS, Ecole des Ponts ParisTech, France

Email: jean-francois.pommaret@wanadoo.fr

How to cite this paper: Pommaret, J.-F. (2021) Homological Solution of the Lanczos Problems in Arbitrary Dimension. *Journal of Modern Physics*, 12, 829-858. <https://doi.org/10.4236/jmp.2021.126053>

Received: April 20, 2021

Accepted: May 14, 2021

Published: May 17, 2021

Copyright © 2021 by author(s) and Scientific Research Publishing Inc. This work is licensed under the Creative Commons Attribution International License (CC BY 4.0). <http://creativecommons.org/licenses/by/4.0/>



Open Access

Abstract

When \mathcal{D} is a linear partial differential operator of any order, a *direct problem* is to look for an operator \mathcal{D}_1 generating the *compatibility conditions* (CC) $\mathcal{D}_1\eta = 0$ of $\mathcal{D}\xi = \eta$. Conversely, when \mathcal{D}_1 is given, an *inverse problem* is to look for an operator \mathcal{D} such that its CC are generated by \mathcal{D}_1 and we shall say that \mathcal{D}_1 is *parametrized* by $\mathcal{D} = \mathcal{D}_0$. We may thus construct a differential sequence with successive operators $\mathcal{D}, \mathcal{D}_1, \mathcal{D}_2, \dots$, each operator parametrizing the next one. Introducing the *formal adjoint* $ad(\)$ of an operator, we have $\mathcal{D}_i \circ \mathcal{D}_{i-1} = 0 \Rightarrow ad(\mathcal{D}_{i-1}) \circ ad(\mathcal{D}_i) = 0$ but $ad(\mathcal{D}_{i-1})$ may not generate *all* the CC of $ad(\mathcal{D}_i)$. When $D = K[d_1, \dots, d_n] = K[d]$ is the (non-commutative) ring of differential operators with coefficients in a differential field K , then \mathcal{D} gives rise by residue to a *differential module* M over D while $ad(\mathcal{D})$ gives rise to a differential module $N = ad(M)$ over D . The *differential extension modules* $ext^i(M) = ext_D^i(M, D)$ with $ext^0(M) = hom_D(M, D)$ only depend on M and are measuring the above gaps, *independently of the previous differential sequence*, in such a way that $ext^1(N) = t(M)$ is the torsion submodule of M . The purpose of this paper is to compute them for certain Lie operators involved in the theory of Lie pseudogroups in arbitrary dimension n and to prove for the first time that the extension modules highly depend on the Vessiot *structure constants* c . Comparing the last invited lecture published in 1962 by Lanczos with a commutative diagram that we provided in a recent paper on gravitational waves, we suddenly understood the confusion made by Lanczos between Hodge duality and differential duality. We shall prove that Lanczos was not trying to parametrize the Riemann operator but its formal adjoint $Beltrami = ad(Riemann)$ which can indeed be parametrized by the operator $Lanczos = ad(Bianchi)$ in arbitrary dimension, “one step further on to the right” in the Killing se-

quence. Our purpose is thus to revisit the mathematical framework of Lanczos potential theory in the light of this comment, getting closer to the theory of Lie pseudogroups through double differential duality and the construction of finite length differential sequences for Lie operators. In particular, when one is dealing with a Lie group of transformations or, equivalently, when \mathcal{D} is a Lie operator of finite type, we shall prove that $\text{ext}^i(M) = 0, \forall 0 \leq i \leq n-1$. It will follow that the *Riemann-Lanczos* and *Weyl-Lanczos* problems just amount to prove such a result for $i=1,2$ and arbitrary n when \mathcal{D} is the *classical or conformal Killing* operator. We provide a description of the potentials allowing to parametrize the Riemann and the Weyl operators in arbitrary dimension, both with their adjoint operators. Most of these results are new and have been checked by means of computer algebra.

Keywords

Differential Sequence, Variational Calculus, Lanczos Potential, Lanczos Operator, Vessiot Structure Equations

1. Introduction

Introducing the *Lanczos potential* $L = (L_{ij,k})$ as a 3-tensor satisfying the algebraic relations:

$$L_{ij,k} + L_{ji,k} = 0, \quad L_{ij,k} + L_{jk,i} + L_{ki,j} = 0 \quad (1)$$

Lanczos claimed to have parametrized the Riemann tensor R through the relation:

$$R_{kl,ij} = \nabla_j L_{kl,i} - \nabla_i L_{kl,j} + \nabla_l L_{ij,k} - \nabla_k L_{ij,l} \quad (2)$$

where ∇ is the covariant derivative. However, even if we can easily verify the algebraic conditions that *must* be satisfied by a *Riemann candidate*, namely:

$$R_{kl,ij} = -R_{lk,ij} = -R_{kl,ji} = R_{ij,kl}, \quad R_{kl,ij} + R_{ki,jl} + R_{kj,li} = 0, \quad R^r_{i,rj} = R_{ij} = R_{ji} \neq 0 \quad (3)$$

the generating *compatibility conditions* (CC) of the underlying operator for the left member *cannot* be the (second) *Bianchi identities*:

$$B^k_{l,ijr} \equiv \nabla_r R^k_{l,ij} + \nabla_i R^k_{l,jr} + \nabla_j R^k_{l,ri} = 0 \quad (4)$$

which are produced by the well known parametrization described by the *Riemann* operator acting on a perturbation $\Omega \in S_2 T^*$ of the background metric ω , that is, when ω is the Minkowski metric:

$$2R_{kl,ij} = (d_{li}\Omega_{kj} - d_{lj}\Omega_{ki}) - (d_{ki}\Omega_{lj} - d_{kj}\Omega_{li}) \Rightarrow d_r R^k_{l,ij} + d_i R^k_{l,jr} + d_j R^k_{l,ri} = 0$$

This contradiction can also be checked directly by substitution because we have:

$$R_{kl,ij} = d_j L_{kl,i} - d_i L_{kl,j} + d_l L_{ij,k} - d_k L_{ij,l} \Rightarrow d_r R^k_{l,ij} + d_i R^k_{l,jr} + d_j R^k_{l,ri} \neq 0$$

Then Lanczos tried to parametrize the Weyl tensor C , only knowing the algebraic conditions that must be satisfied by a *Weyl candidate*, namely:

$$C_{kl,ij} = -C_{lk,ij} = -C_{kl,ji} = C_{ij,kl} + C_{kl,ij} + C_{ki,jl} + C_{kj,li} = 0, C^r_{i,rj} = 0 \quad (5)$$

The last condition is reducing the number of linearly independent components from 20 to 10 for space-time, that is when the dimension is $n = 4$, but the previous contradiction still holds.

50 years ago, while the author of this paper was “professional” in GR under the leadership of Prof. A. Lichnerowicz, he became familiar with the Lanczos problems. Since that time, he had no wish at all to enter this kind of “private domain” where a few persons were writing alternatively. Also, all the papers were covered with “computations” involving many technical formulas, one paper using computer algebra, another Gröbner bases, another Cartan exterior calculus, another Janet bases and so on during these 50 years. Finally, the author started to have doubts on the differential geometric conformal framework. A long time after, in 2001 and for quite different reasons, namely revisiting controllability in control theory on one side and the intrinsic proof of the impossibility to find potentials for Einstein equations in vacuum (contrary to the general dream of the GR community till now!) on the other side, the author wrote a big book, published by Kluwer (See Zbl 1079.93001). At this moment, being more familiar with differential homological algebra and the “parametrization problem”, the way towards the Lanczos problems became easier and we present it in four steps:

1) In the *only* dimension $n = 4$ considered indeed by Lanczos, the so-called Lanczos “potential” $L_{ij,k} = -L_{ji,k}$ has $6 \times 4 = 24$ components. As they must be related by the 4 additional relations $L_{ij,k} + L_{jk,i} + L_{ki,j} = 0$, we get 20 independent components, namely the number of (second) Bianchi identities. We claim that only the knowledge of the Spencer δ -cohomology allows to exhibit the proper identification with the Bianchi candidate vector bundle F_2 in the short exact sequence of vector bundles where $g_1 \subset T^* \otimes T$ is the symbol of the Killing equations:

$$0 \rightarrow F_2 \rightarrow \wedge^3 T^* \otimes g_1 \xrightarrow{\delta} \wedge^4 T^* \otimes T \rightarrow 0$$

and $\dim(F_2) = 24 - 4 = 20$ when $n = 4$. However, speaking about “potential” also means “parametrization”, ... but of what?. Here comes the main confusion of Lanczos, familiar with electromagnetism (EM) while using mainly quadratic lagrangians with the Riemann tensor in place of the EM field F such that $dF = 0$, with the Bianchi identities as differential constraint in the corresponding variational calculus. The operator that must be parametrized indeed by means of the formal adjoint of the Bianchi operator is thus the formal adjoint of the Riemann operator, *going now backwards*, that is from right to left in the adjoint sequence of the Killing resolution. Such a construction, using quite difficult results (side changing functor) of homological algebra, could not have been discovered by Lanczos and followers as such tools have only been available after 1995 through the works of pure mathematicians not interested by applications. As a byproduct, this new framework is allowing in particular to replace technical

formulas by diagram chasing, without ANY formula.

2) As for the differential sequence involved, people use to refer to E. Calabi or H. Goldschmidt who effectively gave “*ad hoc*” results a long time ago, around 1965 but are not quoted because they cannot be used for our purpose. However, one should rather refer to the author’s many books (In particular the first one, published in 1978 and translated by MIR, Moscow, in 1983) in order to discover that such a differential sequence can be constructed for *any* Lie pseudogroup by using the Vessiot structure equations, still not known after 125 years!. This sequence is much more useful than the sequence constructed by Goldschmidt-Spencer who have never been aware of the work of Vessiot and has nothing to do with the work of Cartan who ignored this work.

3) Going from left to right in the differential sequence, the Riemann operator is generating the compatibility conditions (CC) of the Killing operator and the Bianchi operator is generating the CC of the Riemann operator. However, *going backwards*, that is to say from right to left, by taking the respective adjoint operators, it is not true in general that the successive operators have the same property. This remark has been the reason for introducing the *differential extension modules* in homological algebra, the aim being to study the possible “*gaps*” just described. By chance, *in this case it works*, contrary to what could happen in the example given of the infinite dimensional Lie pseudogroup of contact transformations. Indeed, in such a case, the differential sequence is existing because the Vessiot structure equation has only one Vessiot structure constant (totally unknown) like in the example of the constant Riemannian curvature. The case of unimodular contact transformations is even more difficult with two Vessiot structure constants but no link with any Maurer-Cartan equation.

4) *Last but not least*, the case of conformal isometries is even much more tricky:

First of all, it is clear that, when $n \geq 4$, the first order Killing operator must be replaced by the first order conformal Killing operator while the second order Riemann operator must be replaced by the second order Weyl operator. However, ... what operator should be used in place of the first order Bianchi operator?. *No chance*, because we shall discover that, in dimension 4, it is a *second order* operator!. Such a result, neither known nor acknowledged up to now, has been checked with computer algebra by the author’s former PhD student A. Quadrat (INRIA) and appeared in book form ([1]). Accordingly, there does not exist a single reference on such a result. Needless to say that, in any other smaller or higher dimension, this material could not have been known by Lanczos himself or followers, a fact justifying the initial claim on the use of the Spencer δ -cohomology. For example, when $n = 3$, the analogue of the Riemann operator is a *third order* operator with *first order* CC.

In order to recapitulate the above procedure, we have the following *differential sequence*, indicating below the fiber dimensions of the vector bundles involved with $F_0 = S_2 T^*$:

$$0 \rightarrow \Theta \rightarrow T \xrightarrow{\text{Killing}} F_0 \xrightarrow{\text{Riemann}} F_1 \xrightarrow{\text{Bianchi}} F_2 \rightarrow \dots \quad (6)$$

$$0 \rightarrow \Theta \rightarrow n \rightarrow n(n+1)/2 \rightarrow n^2(n^2-1)/12 \rightarrow n^2(n^2-1)(n-2)/24 \rightarrow \dots$$

where Θ is the sheaf of Killing vector fields for the Minkowski metric. Defining the operators:

$$\text{Cauchy} = \text{ad}(\text{Killing}), \text{Beltrami} = \text{ad}(\text{Riemann}), \text{Lanczos} = \text{ad}(\text{Bianchi})$$

we shall prove that Lanczos was in fact dreaming to construct the *adjoint differential sequence*.

$$0 \leftarrow \text{ad}(T) \xleftarrow{\text{Cauchy}} \text{ad}(F_0) \xleftarrow{\text{Beltrami}} \text{ad}(F_1) \xleftarrow{\text{Lanczos}} \text{ad}(F_2) \leftarrow \dots \quad (7)$$

where $\text{ad}(E) = \wedge^n T^* \otimes E^*$ for any vector bundle E where E^* is obtained from E by inverting the transition rules when changing local coordinates, exactly like T and T^* . Accordingly, all the problem will be to prove that *each operator is indeed parametrized by the preceding one*. As we shall see, the conformal situation could be treated similarly while starting with the *conformal Killing* operator followed by the *Weyl* operator and replacing each *classical* vector bundle F by the corresponding *conformal* bundle \hat{F} . However, this will lead to a true nonsense because we shall discover that the analogue of the *Weyl* operator is of order 3 when $n = 3$ while the analogue of the *Bianchi* operator is of order 2, ... just when $n = 4$. These striking results have been confirmed by computer algebra and the reader can even find the details in book form ([1]). It follows that both the Riemann and Weyl frameworks of the Lanczos potential theory must be entirely revisited. The aim of this paper is to overcome these problems by using *differential homological algebra*.

C. Lanczos (1893-1974) wrote three main papers (1939, 1949, 1962) on the search of potentials for parametrizing the Riemann and Weyl tensors ([2] [3] [4] [5]) and we refer the reader to the nice historical survey ([6]) for more details. However, Lanczos has been invited in 1962 by Prof. A. Lichnerowicz to lecture in France and this last lecture has been published in french. Getting inspiration from what happens in electromagnetism (EM) where the geometrical first set of Maxwell equations $dF = 0$ when $F \in \wedge^2 T^*$ is a closed 2-form can be parametrized by $dA = F$ for an arbitrary potential $A \in T^*$ with standard notations (See [7] for details), Lanczos created the concept of “*candidate*” while noticing that the Riemann and Weyl 4-tensors must “*a priori*” satisfy algebraic relations reducing the number of their components $R_{kl,ij}$ and $C_{kl,ij}$ respectively to 20 and 10 when $n = 4$. Now, we have proved in many books ([8]-[13]) or papers ([14] [15] [16] [17] [18]) that it is not possible to understand the mathematical structure of the Riemann and Weyl tensors, both with their splitting link, without the following four important comments:

- The results discovered by E. Vessiot as early as in 1903 ([19]) are still neither known nor even acknowledged today, though they generalize the constant Riemannian curvature condition discovered 25 years later by L. P. Eisenhart ([20]). They also allow to understand the direct link existing *separately* be-

tween the Riemann tensor and the Lie pseudogroup of isometries of a non-degenerate metric on one side or between the Weyl tensor and the group of conformal isometries of this metric on another side. Vessiot proved that, for any Lie pseudogroup $\Gamma \in \text{aut}(X)$ the pseudogroup of all local diffeomorphisms, there is a *geometric object* ω , may be of a high order q large enough and not of a tensorial nature, which is characterizing Γ in the sense that one has:

$$\Gamma = \left\{ f \in \text{aut}(X) \mid \Phi_\omega(j_q(f)) = j_q(f)^{-1}(\omega) = \omega \right\}$$

where $\{\Phi\}$ is a *fundamental set* of differential invariants of order q and ω must satisfy certain (non-linear in general) integrability conditions of the form:

$$I(j_1(\omega)) = c(\omega)$$

called *Vessiot structure equations*, depending on a certain number of *Vessiot structure constants* c eventually satisfying algebraic *Jacobi conditions* $J(c) = 0$ and we let the reader compare this situation to the Riemann or contact cases ([1]). We want to point out that these structure equations were perfectly known by E. Cartan (1869-1951) who *never* said that these results were at least competing with or even superseding the corresponding *Cartan structure equations* that he has developed about at the same time for similar purposes. The underlying reason is of a purely personal origin related to the *differential Galois Theory* within a kind of “*mathematical affair*” involving the best french mathematicians of that time. The original letters, given to the author of this paper by M. Janet, a friend of E. Vessiot, have been published in ([10]) and have been put as a deposit in the main library of Ecole Normale Supérieure in Paris for future historical studies.

- A nonlinear operator with second member does not in general admit CC, ... unless it corresponds to the defining equations in Lie form of a Lie pseudogroup and the CC are the Vessiot structure equations in that case with structure constants determined by the chosen geometric object (compare again to the Riemannian geometry). We have shown in many books already quoted that, if \mathcal{D} is a Lie operator and we set $\Theta = \{\xi \in T \mid \mathcal{D}\xi = 0\}$, with bracket $[\Theta, \Theta] \in \Theta$ induced by the ordinary bracket of vector fields, then the system $\mathcal{D}\xi = \Omega$ is the linearization of a non-linear version when Ω is a perturbation of ω (twice the infinitesimal deformation tensor in elasticity) along the formula:

$$\mathcal{D}\xi = \mathcal{L}(\xi)\omega = \frac{d}{dt} \left(j_q(\exp(t\xi))^{-1}(\omega) \right) \Big|_{t=0}$$

Similarly, we can choose for the generating CC \mathcal{D}_1 the linearization of a non-linear version described by the Vessiot structure equations:

$$\frac{\partial I}{\partial j_1(\omega)}(j_1(\omega)) j_1(\Omega) = \frac{\partial c}{\partial \omega}(\omega) \Omega$$

that is *exactly* what we did for the flat Minkowski metric. However, Lanczos has

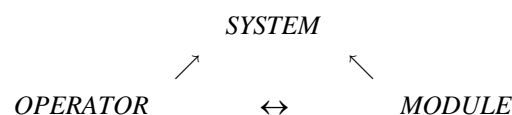
been studying the CC \mathcal{D}_2 of \mathcal{D}_1 , ignoring that, contrary to the previous situation, \mathcal{D}_2 almost never comes from a linearization. It is therefore quite strange to discover that Lanczos never discovered that what he was doing with \mathcal{D}_1 and \mathcal{D}_2 while using quadratic Lagrangians in R , was *exactly* what is done in any textbook of elasticity or continuum mechanics with \mathcal{D} and \mathcal{D}_1 while using quadratic Lagrangians in Ω ([1] [7] [13] [16]). We do believe that Lanczos was too much obsessed by comparing R in GR to F in EM. Like in any good crime story, the solution will be given in the last section and could not have been given before by any classical approach.

- The last invited lecture published in 1962 by Lanczos on his potential theory is never quoted because it is in French. Comparing it with a commutative diagram in a recently published paper on gravitational waves ([18]), we suddenly understood the confusion made by Lanczos between Hodge duality and differential duality when he introduced his tentative 3-tensor potential. Our final purpose is thus to revisit the mathematical framework of Lanczos potential theory in the light of this comment,

2. Mathematical Tools

2.1. Differential Sequences

In view of the many examples that will be presented in this paper, it becomes clear that there is a need for classifying the properties of systems of PD equations in a way that does not depend on their presentations and this is the purpose of *differential homological algebra* along the scheme:



in order to show that certain concepts, which are clear in one framework, may become quite obscure in the others and conversely, like the formal integrability and torsion concepts for example.

When E is a vector bundle over X and we have a system of order q on E , say $R_q \subset J_q(E)$, we can introduce the canonical projection $\Phi: J_q(E) \rightarrow J_q(E)/R_q = F$ and define a linear differential operator $\mathcal{D}: E \rightarrow F: \xi(x) \rightarrow \eta^r(x) = a_k^{\tau\mu}(x) \partial_\mu \xi^k(x)$. When \mathcal{D} is given, the compatibility conditions for solving $\mathcal{D}\xi = \eta$ can be described in operator form by $\mathcal{D}_1\eta = 0$ and so on. In general, if a system is not formally integrable, it is possible to obtain a formally integrable system, having the same solutions, by “*saturating*” conveniently the given PD equations through the adjunction of new PD equations obtained by various prolongations/projections (PP) and *such a procedure must absolutely be done before looking for the compatibility conditions* ([21] [22]).

In order to study differential modules, we shall simply forget about changes of coordinates and only consider trivial bundles. If K is a *differential field* with n

commuting derivations $\partial_1, \dots, \partial_n$ (Say $\mathbb{Q}, \mathbb{Q}(a)$ or $\mathbb{Q}(x^1, \dots, x^n)$ in the usual examples), we denote by $\text{cst}(K)$ the subfield of *constants* of K , that is the set of elements killed by the n derivations (Say \mathbb{Q} in the usual examples). If d_1, \dots, d_n are *formal derivatives* (pure symbols in computer algebra packages!) which are only supposed to satisfy $d_i a = ad_i + \partial_i a$ in the operator sense for any $a \in K$, we may consider the (non-commutative) ring $D = K[d_1, \dots, d_n]$ of differential operators with coefficients in K . If now $y = (y^1, \dots, y^m)$ is a set of differential indeterminates, we let D act formally on y by setting $d_\mu y^k = y_\mu^k$ for any multi-index $\mu = (\mu_1, \dots, \mu_n)$ and set $Dy = Dy^1 + \dots + Dy^m$. We may also set

$$\Phi^\tau \equiv a_k^{\tau\mu} y_\mu^k \xrightarrow{d_i} d_i \Phi^\tau \equiv a_k^{\tau\mu} y_{\mu+1_i}^k + \partial_i a_k^{\tau\mu} y_\mu^k \quad \text{for } \tau = 1, \dots, p.$$

Denoting by $D\Phi$ the subdifferential module generated by all the given OD or PD equations and all their formal derivatives, we may finally introduce the D -module $M = Dy/D\Phi$ by residue. Here we recall that M is a *module* over a ring A or an A -module if $\forall a \in A, \forall m, n \in M \Rightarrow am, m+n \in M$. We may introduce as usual the *torsion* submodule $t(M) = \{m \in M \mid \exists 0 \neq a \in A, am = 0\}$ and we say that M is a torsion module if $t(M) = M$ or that M is torsion-free if $t(M) = 0$.

It is not evident at all to exhibit the link existing between these two approaches and we proceed as follows. First of all, the ring D is filtered by the order of the operators and we have the filtration or *inductive limit*

$0 = D_{-1} \subset D_0 \subset D_1 \subset \dots \subset D_q \subset \dots \subset D_\infty = D$. Moreover, it is clear that D , as an algebra, is generated by $K = D_0$ and $T = D_1/D_0$ with $D_1 = K \oplus T$ if we identify an element $\xi = \xi^i d_i \in T$ with the vector field $\xi = \xi^i(x) \partial_i$ of differential geometry, but with $\xi^i \in K$ now. As a byproduct, the differential module D^m is also filtered by the order and we obtain an *induced filtration* or *inductive limit* $0 = M_{-1} \subseteq M_0 \subseteq M_1 \subseteq \dots \subseteq M_q \subseteq \dots \subseteq M_\infty = M$ with $d_i M_q \subseteq M_{q+1}$ provided by the prolongations. Now, *if we suppose that the system* $R_q = \ker(\Phi)$ *is formally integrable* (FI), that is all the OD or PD equations of order $q+r$ are obtained by using only r prolongations, then we have the *projective limit*

$R = R_\infty \rightarrow \dots \rightarrow R_q \rightarrow R_0 \rightarrow 0$ obtained by successive jet projections. We have the following crucial technical proposition ([13] [17]):

Proposition 2.A.1: $R = \text{hom}_K(M, K)$ is a differential module for the Spencer operator and we have a bijective correspondence $M_q \leftrightarrow R_q = \text{hom}_K(M_q, K)$ over K because K is a field.

Proof: for any $f \in R$ and $m \in M$, we may set for any $f \in R, m \in M$:

$$\begin{aligned} (af)(m) &= a(f(m)) = f(am), \forall a \in K, \\ (\xi f)(m) &= \xi(f(m)) - f(\xi m), \forall \xi \in T \end{aligned}$$

and check that we have successively with $\xi \cdot a = \xi^r \partial_r a$:

$$\begin{aligned} ((\xi a)f)(m) &= (\xi(af))(m) \\ &= \xi(af(m)) - af(\xi m) \\ &= (\xi \cdot a)f(m) + a(\xi \cdot f(m)) - f(a\xi m) \\ &= (\xi \cdot a)f(m) + ((a\xi)f)(m) \end{aligned}$$

a result leading to $\xi a = a\xi + \xi \cdot a$ in the operator sense. Setting finally $f(y_\mu^k) = f_\mu^k$ with a slight abuse of notations when using the same notation y_μ^k for the residue instead of the standard \bar{y}_μ^k . Setting $\mu + 1_i = (\mu_1, \dots, \mu_i + 1, \dots, \mu_n)$, it follows that R is a differential module for the law:

$$(d_i f)(y_\mu^k) = d_i(f(y_\mu^k)) - f(d_i y_\mu^k) = \partial_i f_\mu^k - f(y_{\mu+1_i}^k) = \partial_i f_\mu^k - f_{\mu+1_i}^k \quad (8)$$

and we have $d_i d_j f = d_j d_i f = d_{ij} f, \forall f \in R$.

Q.E.D.

Through this paper, we shall only deal with linear differential operators. However, as explained in ([9] [23]), there is a nonlinear counterpart using the *nonlinear Janet sequence* coming from the *Vessiot structure equations* and a *nonlinear Spencer sequence*. The *vertical machinery* involved, that is a systematic use of *fibered manifolds* and *vertical bundles*, is much more difficult though we have chosen the notations of this paper in such a way that the interested reader may easily adapt them. As for the Vessiot structure equations first found in 1903 ([19]), *they have been totally ignored during more than one century* for reasons that are not scientific at all (See the original letters presented in [10] for explanations). Though we have written this paper in a rather self-contained way while using rather standard notations, the reader may refer to ([24] [25] [26]) for the differential geometric background, to ([27] [28]) for the elements of homological algebra needed through the various diagrammes presented and to ([29] [30] [31]) for the main (difficult) concepts of differential homological algebra.

Collecting all the results so far obtained, if a differential operator \mathcal{D} is given in the framework of differential geometry, we may keep the same operator matrix in the framework of differential modules which are *left* modules over the ring D of linear differential operators. We may also apply duality over D , that is apply $\text{hom}_D(\bullet, D)$, provided we deal now with *right* differential modules or use the operator matrix of $\text{ad}(\mathcal{D})$ and deal again with *left* differential modules obtained through the *left \leftrightarrow right conversion* procedure. In actual practice, it is essential to notice that *the new operator matrix may be quite different from the only transposed of the previous operator*, even if we are dealing with constant coefficients.

Definition 2.A.2: If a differential operator $\xi \xrightarrow{\mathcal{D}} \eta$ is given, a *direct problem* is to find (generating) *compatibility conditions* (CC) as an operator $\eta \xrightarrow{\mathcal{D}_1} \zeta$ such that $\mathcal{D}\xi = \eta \Rightarrow \mathcal{D}_1\eta = 0$. Conversely, given $\eta \xrightarrow{\mathcal{D}_1} \zeta$, the *inverse problem* will be to look for $\xi \xrightarrow{\mathcal{D}} \eta$ such that \mathcal{D}_1 generates the CC of \mathcal{D} and we shall say that \mathcal{D}_1 is *parametrized by \mathcal{D}* ... if such an operator \mathcal{D} is existing!

Remark 2.A.3: Solving the direct problem (Janet, Spencer) is *necessary* for solving the inverse problem. However, though the direct problem always has a solution, *the inverse problem may not have a solution at all* and the case of the Einstein operator is one of the best non-trivial PD counterexamples (Compare

[32] [33] [34]). It is rather striking to discover that, in the case of OD operators, it took almost 50 years to understand that the possibility to solve the inverse problem was equivalent to the controllability of the corresponding control system ([34]) and the situation is similar in GR as the above result has been first found in 1995 ([32]).

As $ad(ad(P)) = P, \forall P \in D$, any operator is the adjoint of a certain operator and we recall that the *double duality test* needed in order to check whether $t(M) = 0$ or not and to find out a parametrization if $t(M) = 0$ when M is defined by \mathcal{D}_1 has 5 steps which are drawn in the following diagram where $ad(\mathcal{D})$ generates the CC of $ad(\mathcal{D}_1)$ and \mathcal{D}'_1 generates the CC of $\mathcal{D} = ad(ad(\mathcal{D}))$:

$$\begin{array}{ccccccc}
 & & & & \zeta' & 5 & \\
 & & & & \nearrow^{\mathcal{D}'_1} & & \\
 4 & \xi & \xrightarrow{\mathcal{D}} & \eta & \xrightarrow{\mathcal{D}_1} & \zeta & 1 \\
 & & & & & & \\
 3 & \nu & \xleftarrow{ad(\mathcal{D})} & \mu & \xleftarrow{ad(\mathcal{D}_1)} & \lambda & 2
 \end{array} \quad (9)$$

Theorem 2.A.4: We have \mathcal{D}_1 parametrized by $\mathcal{D} \Leftrightarrow \mathcal{D}_1 \simeq \mathcal{D}'_1 \Leftrightarrow t(M) = 0 \Leftrightarrow ext^1(N) = 0$ in the differential module framework when N is defined by $ad(\mathcal{D}_1)$. These results do not depend on the finite free presentations of M or N (See [34] [35]) for more details).

Corollary 2.A.5: In the differential module framework, if $F_1 \xrightarrow{\mathcal{D}_1} F_0 \xrightarrow{p} M \rightarrow 0$ is a finite free presentation of $M = coker(\mathcal{D}_1)$ and we already know that $t(M) = 0$ by using the preceding test and Theorem, then we may obtain an exact sequence $F_1 \xrightarrow{\mathcal{D}_1} F_0 \xrightarrow{\mathcal{D}} E$ of free differential modules where \mathcal{D} is the parametrizing operator, both with an inclusion $M \subset E$ by chasing. However, there may exist other parametrizations $F_1 \xrightarrow{\mathcal{D}_1} F_0 \xrightarrow{\mathcal{D}'} E'$ called *minimal parametrizations* such that $coker(\mathcal{D}')$ is a torsion module and we have thus $rk_D(M) = rk_D(E')$ (See [18] and [35]).

As shown by the next examples, the main difficulty met in OD or PD applications is that $ad(\mathcal{D})$ may not be formally integrable at all, even if \mathcal{D} is involutive (See [12] for other examples).

Example 2.A.6: (Double pendulum) If a rigid bar is able to move horizontally with reference position x and we attach two pendula with respective length l_1 and l_2 making the (small) angles θ_1 and θ_2 with the vertical, the corresponding involutive control system is:

$$d^2x + l_1 d^2\theta^1 + g\theta^1 = 0, \quad d^2x + l_2 d^2\theta^2 + g\theta^2 = 0$$

where g is the gravity. Multiplying these OD equations by two test functions λ^1, λ^2 and integrating by parts, we get the adjoint system:

$$x \rightarrow d^2\lambda^1 + d^2\lambda^2 = 0, \quad \theta^1 \rightarrow l_1 d^2\lambda^1 + g\lambda^1 = 0, \quad \theta^2 \rightarrow l_2 d^2\lambda^2 + g\lambda^2 = 0$$

Multiplying the second equation by l_2 , the third by l_1 while using the first, we

obtain the zero order OD equation $l_2\lambda^1 + l_1\lambda^2 = 0$. Differentiating *twice* this time and substituting, we obtain the new zero order OD equation $(l_2/l_1)\lambda^1 + (l_1/l_2)\lambda^2 = 0$. The determinant of the system of two zero order equations is then seen to be *exactly* $l_1 - l_2$. It follows that the system is controllable if and only if l_1 is different from l_2 , a fact that the reader can check easily when moving the bar conveniently. If one length depends on time, the corresponding controllability condition cannot be obtained without computer algebra, *even on such an elementary control system*. The totally unexpected fourth order parametrization of the control system when it is controllable is:

- $l_1 \neq l_2$:

$$\begin{cases} -l_1 l_2 d^4 \phi - g(l_1 + l_2) d^2 \phi - g^2 \phi = x \\ l_2 d^4 \phi + g d^2 \phi = \theta_1 \\ l_1 d^4 \phi + g d^2 \phi = \theta_2 \end{cases}$$

- $l_1 = l_2 = l, \theta = \theta_1 - \theta_2 \Rightarrow l d^2 \theta + g \theta = 0, \theta(0) = 0, d\theta(0) = 0 \Rightarrow \theta(t) = 0$.

It follows that the controllability of a control system is a “*built in*” property of this system that does not depend on the choice of the control variables, contrary to a tradition still existing in the control community (See Zbl 1079.93001 for a review). We invite the reader to use the Kalman approach that can be found in any control textbook today and to compare (See [12] or [34] for details).

Example 2.A.7: (*Einstein equations*) If \mathcal{D}_1 is the *Einstein* operator which is self-adjoint, then $ad(\mathcal{D}_1)$ is also the *Einstein* operator, $ad(\mathcal{D})$ is the *Cauchy* operator and \mathcal{D} is thus the *Killing* operator. It follows that \mathcal{D}'_1 is the *Riemann* operator according to the Introduction. Using the previous theorem, any component of the Weyl tensor becomes a torsion element killed by the *Dalembert* operator as a “modern” description of the so-called *Lichnerowicz waves* (as they are called in France!) ([16]).

2.2. Variational Calculus

Having in mind “Optimal Control Theory” while using the notations of the previous Formal Test, let us assume that the two differential sequences:

$$\begin{array}{ccccc} \xi & \xrightarrow{\mathcal{D}} & \eta & \xrightarrow{\mathcal{D}_1} & \zeta \\ & \swarrow ad(\mathcal{D}) & & \swarrow ad(\mathcal{D}_1) & \\ \nu & \leftarrow & \mu & \leftarrow & \lambda \end{array} \quad (10)$$

are *formally exact*, that is \mathcal{D}_1 generates the CC of \mathcal{D} and $ad(\mathcal{D})$ generates the CC of $ad(\mathcal{D}_1)$, namely ξ is a potential for \mathcal{D}_1 and λ is a potential for $ad(\mathcal{D})$. We may consider a variational problem for a cost function or lagrangian $\varphi(\eta)$ under the linear OD or PD constraint described by $\mathcal{D}_1 \eta = 0$.

- Introducing convenient Lagrange multipliers λ while setting

$dx = dx^1 \wedge \cdots \wedge dx^n$ for simplicity, we must vary the integral:

$$\Phi = \int [\varphi(\eta) - \lambda \mathcal{D}_1 \eta] dx \Rightarrow \delta \Phi = \int [(\partial \varphi(\eta) / \partial \eta) \delta \eta - \lambda \mathcal{D}_1 \delta \eta] dx$$

Integrating by parts, we obtain the Euler-Lagrange (EL) equations:

$$\partial\varphi(\eta)/\partial\eta = ad(\mathcal{D}_1)\lambda$$

to which we have to add the constraint $\mathcal{D}_1\eta = 0$ obtained by varying λ independently. If $ad(\mathcal{D}_1)$ is an injective operator, in particular if \mathcal{D}_1 is formally surjective (no CC) while $n = 1$ as in OD optimal control and M is torsion-free, thus free ([12]) or $n \geq 1$ and M is projective, then one can obtain λ explicitly and eliminate it by substitution. Otherwise, using the CC $ad(\mathcal{D})$ of $ad(\mathcal{D}_1)$, we have to study the formal integrability of the combined system:

$$ad(\mathcal{D})\partial\varphi(\eta)/\partial\eta = 0, \quad \mathcal{D}_1\eta = 0$$

which may be a difficult task ([12], Introduction and Chapter VI).

- However, we may also transform the given variational problem with constraint into a variational problem without any constraint if and only if the differential constraint can be parametrized. Using the parametrization of \mathcal{D}_1 by \mathcal{D} , we may vary the integral:

$$\Phi = \int \varphi(\mathcal{D}\xi) dx \Rightarrow \delta\Phi = \int (\partial\varphi(\eta)/\partial\eta) \mathcal{D}\delta\xi dx$$

whenever $\eta = \mathcal{D}\xi$ and integrate by parts for arbitrary $\delta\xi$ in order to obtain the EL equations:

$$ad(\mathcal{D})\partial\varphi(\eta)/\partial\eta = 0, \quad \eta = \mathcal{D}\xi$$

in a coherent way with the previous approach.

As a byproduct, if the field equations $\mathcal{D}_1\eta = 0$ can be parametrized by a potential ξ through the formula $\mathcal{D}\xi = \eta$, then the induction equations $ad(\mathcal{D})\mu = \nu$ can be obtained by duality in a coherent way with the double duality test, on the condition to know what sequence must be used. However, we have yet proved in ([9] [10] [13] [36]) that the Cauchy stress equations must be replaced by the Cosserat couple-stress equations and that the Janet sequence (only used in this paper) must be thus replaced by the Spencer sequence. Accordingly, the work of Lanczos ([2] [3] [4] [5]) and followers ([37] [38] [39] [40] [41]), using either exterior calculus, Janet and Gröbner bases or Pommaret bases, has been based on a confusion between fields and inductions on one side, but also between the Janet sequence and the Spencer sequence. By chance, as we always refer to intrinsic concepts like the extension modules that do not depend on the differential sequence used, all the results that will be presented can be adapted at once to the systematic use of the Spencer sequence in place of the Janet sequence.

3. Riemann/Lanczos Problem

The last invited lecture published in 1962 by Lanczos on his potential theory is never quoted because it is in French ([5]). Comparing it with a commutative diagram in a recently published paper on gravitational waves ([16]), we suddenly understood the confusion made by Lanczos between Hodge duality and differential duality. Our purpose is thus to revisit the mathematical framework of Lanczos potential theory in the light of this comment, getting closer to the for-

mal theory of Lie pseudogroups through double differential duality and the construction of finite length differential sequences for Lie operators.

When K is a differential field containing the field \mathbb{Q} of rational numbers and (d_1, \dots, d_n) are commuting formal derivatives, we may introduce the ring (which is even an integral domain) $D = K[d_1, \dots, d_n] = K[d]$ of differential operators with coefficients in K . Accordingly, if a differential module M with torsion submodule $t(M)$ is defined by an operator \mathcal{D} with coefficients in K , we may introduce the *differential extension modules* $ext^0(M) = hom_D(M, D)$ and $ext^i(M) = ext_D^i(M, D)$ for $i = 1, \dots, n$. We have the long exact *ker/coker* long exact sequence of (left) differential modules (See [12] or [34] for details):

$$0 \rightarrow ext^1(N) \rightarrow M \xrightarrow{\varepsilon} hom_D(hom_D(M, D), D) \rightarrow ext^2(N) \rightarrow 0 \quad (11)$$

where the morphism ε is defined by

$(\varepsilon(m))(f) = f(m), \forall m \in M, \forall f \in hom_D(M, D)$ and the adjoint differential module $N = ad(M)$ is defined by the adjoint operator $ad(\mathcal{D})$. Then M is *torsion-free* if and only if $t(M) = ext^1(N) = 0$, that is ε is a monomorphism or, equivalently, \mathcal{D} can be parametrized by the operator \mathcal{D}_{-1} when $ad(\mathcal{D}_{-1})$ generates the compatibility conditions (CC) of $ad(\mathcal{D})$. Finally M is *reflexive* if and only if, *in addition*, ε is an epimorphism, that is we have also $ext^2(N) = 0$ or, equivalently, \mathcal{D}_{-1} can be parametrized again by \mathcal{D}_{-2} when $ad(\mathcal{D}_{-2})$ generates the CC of $ad(\mathcal{D}_{-1})$. As we have $ad(ad(\mathcal{D})) = \mathcal{D}$ and though this is not evident at first sight by exchanging M with N , we may also say that $ext^1(M) = 0$ if $ad(\mathcal{D})$ generates the CC of $ad(\mathcal{D}_1)$ whenever \mathcal{D}_1 generates the CC of \mathcal{D} and, similarly, that $ext^2(M) = 0$ when $ad(\mathcal{D}_1)$ generates the CC of $ad(\mathcal{D}_2)$ whenever \mathcal{D}_2 generates the CC of \mathcal{D}_1 . We shall provide an explicit description of the potentials allowing to parametrize the Riemann and the Weyl operators in arbitrary dimension, both with their respective adjoint operators.

We now consider with details the Riemann/Lanczos problem which is at the same time the simplest of the two Lanczos problems as it can be solved in arbitrary dimension $n \geq 2$ but is also an example of the successive confusing works that have been done during the last fifty years as we already said. According to the last Section, the starting motivation seems absolutely natural at first. Indeed, considering the *Killing* operator $\mathcal{D}: \xi \rightarrow \mathcal{L}(\xi)\omega = \Omega \in S_2 T^* = F_0$ where $\mathcal{L}(\xi)$ is the Lie derivative with respect to ξ and $\omega \in S_2 T^*$ is a nondegenerate metric with $det(\omega) \neq 0$. Accordingly, it is a Lie operator with

$\mathcal{D}\xi = 0, \mathcal{D}\eta = 0 \Rightarrow \mathcal{D}[\xi, \eta] = 0$ and we denote simply by $\Theta \subset T$ the set of solutions with $[\Theta, \Theta] \subset \Theta$. Now, as we have explained many times, the main problem is to describe the CC of $\mathcal{D}\xi = \Omega \in F_0$ in the form $\mathcal{D}_1\Omega = 0$ by introducing the so-called *Riemann* operator $\mathcal{D}_1: F_0 \rightarrow F_1$, using the standard notations that can be found at length in our many books ([8]-[13]) or papers ([14] [42]). We advise the reader to follow closely the next lines and to imagine why it will not be possible to repeat them for studying the Weyl/Lanczos problem. Introducing the Levi-Civita isomorphism $j_1(\omega) = (\omega, \partial_x \omega) \simeq (\omega, \gamma)$ and the

Christoffel symbols $\gamma_{ij}^k = \frac{1}{2} \omega^{kr} (\partial_i \omega_{rj} + \partial_j \omega_{ir} - \partial_r \omega_{ij})$ where (ω^{rs}) is the inverse matrix of (ω_{ij}) , we get $R_2 \subset J_2(T)$:

$$\begin{cases} \Omega_{ij} \equiv \omega_{rj}(x) \xi_i^r + \omega_{ir}(x) \xi_j^r + \xi^r \partial_r \omega_{ij}(x) = 0 \\ \Gamma_{ij}^k \equiv \xi_{ij}^k + \gamma_{rj}^k(x) \xi_i^r + \gamma_{ir}^k(x) \xi_j^r + \gamma_{ir}^k(x) \xi_j^r - \gamma_{ij}^r(x) \xi_r^k + \xi^r \partial_r \gamma_{ij}^k(x) = 0 \end{cases}$$

if we use jet coordinates with sections $\xi_q : x \rightarrow (\xi^k(x), \xi_i^k(x), \xi_{ij}^k(x), \dots)$ transforming like $j_q(\xi) : x \rightarrow (\xi^k(x), \partial_i \xi^k(x), \partial_{ij} \xi^k(x), \dots)$. The system $R_1 \subset J_1(T)$ has a symbol $g_1 \simeq \wedge^2 T^* \subset T^* \otimes T$ depending only on ω with $\dim(g_1) = n(n-1)/2$ and is finite type because its first prolongation is $g_2 = 0$. It cannot be thus involutive as can be seen directly on the following Janet board for finding a *Pommaret basis* when $n = 2$ and ω is the euclidean metric:

$$\begin{cases} \xi_2^2 = 0 \\ \xi_2^1 + \xi_1^2 = 0 \\ \xi_1^1 = 0 \end{cases} \quad \begin{bmatrix} 1 & 2 \\ 1 & 2 \\ 1 & \bullet \end{bmatrix}$$

Indeed, the only dot appearing in the board cannot provide any CC for the symbol g_1 and we have therefore the short exact sequence:

$$0 \rightarrow g_2 \rightarrow S_2 T^* \otimes T \rightarrow T^* \otimes F_0 \rightarrow 0$$

by using the fact that $g_2 = 0$ and counting the common dimension $n^2(n+1)/2$, because an epimorphism between two spaces of the same dimension is also a monomorphism and thus an isomorphism. Accordingly, we need to use one additional prolongation and arrive to the:

- *First comment:* Using now one of the main results to be found in ([8], ... [12]), we know that, when R_1 is formally integrable, then the CC of \mathcal{D} are of order $s+1$ where s is the number of prolongations needed in order to get an involutive symbol, that is $s=1$ in the present situation, a result that should lead to CC of order 2 if R_1 were formally integrable.

$$\begin{array}{ccccccc} & & 0 & & 0 & & \\ & & \downarrow & & \downarrow & & \\ & 0 & \rightarrow & S_3 T^* \otimes T & \rightarrow & S_2 T^* \otimes F_0 & \rightarrow h_2 \rightarrow 0 \\ & \downarrow & & \downarrow & & \downarrow & \downarrow \\ 0 \rightarrow & R_3 & \rightarrow & J_3(T) & \rightarrow & J_2(F_0) & \rightarrow Q_2 \rightarrow 0 \\ & \downarrow & & \downarrow & & \downarrow & \downarrow \\ 0 \rightarrow & R_2 & \rightarrow & J_2(T) & \rightarrow & J_1(F_0) & \rightarrow Q_1 \rightarrow 0 \\ & & & \downarrow & & \downarrow & \downarrow \\ & & & 0 & & 0 & 0 \end{array}$$

As $Q_1 = 0$ by counting the dimensions with

$\dim(R_2) = n + n(n-1)/2 = n(n+1)/2$ and $g_3 = 0$, we get $\dim(Q_2) \leq \dim(h_2) = n^2(n+1)^2/4 - n^2(n+1)(n+2)/6 = n^2(n^2-1)/12$. Hence, we understand that the number of CC \mathcal{D}_1 of \mathcal{D} is equal to the number of components of the Riemann tensor if and only if R_2 is formally integrable, that

is *if and only if* ω has constant Riemannian curvature, a result first found by L.P. Eisenhart in 1926 ([20]) though in a different setting (See [8] for an explicit modern proof). Such a necessary condition for constructing an exact differential sequence could not have been used by Lanczos because the work of Spencer has only been known after 1970 ([24] [26]). Otherwise, if the metric does not satisfy this condition, CC may exist by using the Petrov classification but have no link with the Riemann tensor ([22]). We may therefore define the *model vector bundle* F_1 with $\dim(F_1) = n^2(n^2 - 1)/12$ in the sense of Lanczos by the short exact sequence:

$$0 \rightarrow S_3 T^* \otimes T \rightarrow S_2 T^* \otimes F_0 \rightarrow F_1 \rightarrow 0$$

A result leading to the operator $D_1 : F_0 \xrightarrow{j_2} J_2(F_0) \rightarrow F_1$ and the:

- *Second comment:* Applying the Spencer operator δ to the top line of the preceding diagram, we get the commutative diagram:

$$\begin{array}{ccccccc}
 & 0 & & 0 & & 0 & \\
 & \downarrow & & \downarrow & & \downarrow & \\
 0 \rightarrow & g_3 & \rightarrow & S_3 T^* \otimes T & \rightarrow & S_2 T^* \otimes F_0 & \rightarrow F_1 \rightarrow 0 \\
 & \downarrow & & \downarrow & & \downarrow & \\
 0 \rightarrow & T^* \otimes g_2 & \rightarrow & T^* \otimes S_2 T^* \otimes T & \rightarrow & T^* \otimes T^* \otimes F_0 & \rightarrow 0 \\
 & \downarrow & & \downarrow & & \downarrow & \\
 0 \rightarrow & \wedge^2 T^* \otimes g_1 & \rightarrow & \wedge^2 T^* \otimes T^* \otimes T & \rightarrow & \wedge^2 T^* \otimes F_0 & \rightarrow 0 \\
 & \downarrow & & \downarrow & & \downarrow & \\
 0 \rightarrow & \wedge^3 T^* \otimes T & = & \wedge^3 T^* \otimes T & \rightarrow & 0 & \\
 & \downarrow & & \downarrow & & & \\
 & 0 & & 0 & & &
 \end{array}$$

Using a diagonal chase, we discover that F_1 is just the Spencer δ -cohomology $H^2(g_1)$ at $\wedge^2 T^* \otimes g_1$ along the following short exact sequence:

$$0 \rightarrow F_1 \rightarrow \wedge^2 T^* \otimes g_1 \xrightarrow{\delta} \wedge^3 T^* \otimes T \rightarrow 0$$

because $g_2 = 0$ and we get the *striking formula* where the + signs have been replaced by signs:

$$\dim(F_1) = n^2(n-1)^2/4 - n^2(n-1)(n-2)/6 = n^2(n^2-1)/12$$

This result, first found by the author in 1978 ([8]), clearly exhibit the two well known algebraic properties of the Riemann tensor. We now understand that Lanczos had in mind to linearize the Riemann tensor over the Minkowski metric, *exactly like in GR*, in order to construct a Lagrangian as a function of the corresponding linearization $R_{i,j}^k$ of the Riemann tensor $\rho_{i,j}^k$, transforming the usual variational problem into a variational with a differential constraint described by the Bianchi identities leading to the operator \mathcal{D}_2 . As an equivalent alternative approach, *his idea was to consider the curvature as a field by itself* and construct the lagrangian on this field like in EM while adding the Bianchi identities as a differential constraint by using as many Lagrange multiplier as the

number of Bianchi identities, a number not known by combinatorics at the time Lanczos was writing, a result leading to the:

- *Third comment:* Lanczos, who also knew continuum mechanics as an engineer, just copied the way used in elasticity (EL) and in electromagnetism (EM), for example introducing a Lagrangian as a function of the deformation $\varepsilon = (1/2)\Omega$ while adding a differential constraint described by the vanishing linearized Riemann tensor with therefore as many Lagrange multipliers as the number $n^2(n^2-1)/12$ of components of the Riemann tensor. It is crucial to notice that *the same differential sequence is used one step before*, that is with \mathcal{D} and \mathcal{D}_1 while he was dealing with \mathcal{D}_1 and \mathcal{D}_2 previously, that is *one step ahead in the sequence*. We have proved recently that such a procedure is in total contradiction with the piezoelectricity and photoelasticity existing between EL and EM (See the picture in [7]). It thus remains to exhibit the *Bianchi* operator exactly as we did for the *Riemann* operator, with the same historical comments already provided. However, now we know that R_1 is formally integrable (otherwise nothing could be achieved and we should start with a smaller system!), the construction of the linearized Janet-type differential sequence as a strictly exact differential sequence but *not* an involutive differential sequence because the system R_1 and thus the first order operator \mathcal{D} are formally integrable though *not* involutive as g_1 is finite type with $g_2 = 0$ but not involutive. Doing one more prolongation only, we obtain the first order *Bianchi* CC from F_2 in the following long exact symbol sequence (See the details below):

$$0 \rightarrow S_4 T^* \otimes T \rightarrow S_3 T^* \otimes F_0 \rightarrow T^* \otimes F_1 \rightarrow F_2 \rightarrow 0$$

or from the short exact sequence:

$$0 \rightarrow F_2 \rightarrow \wedge^3 T^* \otimes g_1 \xrightarrow{\delta} \wedge^4 T^* \otimes T \rightarrow 0$$

showing that $F_2 = H^3(g_1)$ ([8] [9] [13]). We have in particular for $n \geq 3$:

$$\begin{aligned} \dim(F_2) &= n^2(n-1)^2(n-2)/12 - n^2(n-1)(n-2)(n-3)/24 \\ &= n^2(n+1)(n+2)(n+3)/24 + n^3(n^2-1)/12 - n^2(n+1)(n+2)(n+3)/24 \\ &= n^2(n^2-1)(n-2)/24 \end{aligned}$$

and thus $\dim(F_2) = (4 \times 6) - (1 \times 4) = (16 \times 15 \times 2)/24 = 20$ when $n = 4$, a result leading to:

- *Fourth comment: (Double Hodge duality)* For an arbitrary n , it is *not possible to recognize* that one of the algebraic conditions for the *Bianchi* identity comes from the Spencer δ -map and is again an epimorphism as it was before for defining F_1 , a result obtained by chasing in the commutative diagram obtained by applying δ to the long exact symbol sequence finishing with F_2 . It is *not evident at all* to discover that the modern description of the model vector bundle F_2 is just equivalent to the one provided by Lanczos

but only for $n = 4$. For this, using local coordinates, we have the 4 linear equations with $i = 1, 2, 3, 4$:

$$B_{1,234}^i - B_{2,341}^i + B_{3,412}^i - B_{4,123}^i = 0$$

to be compared with the 4 equations for the Lanczos tensor with $L_{ij,k} + L_{ji,k} = 0$, namely:

$$L_{ij,k} + L_{jk,i} + L_{ki,j} = 0$$

Before reading the next lemma, we invite the reader to prove ... that they are identical!

Lemma 3.1: These two equations are identical *only* when $n = 4$.

Proof. Using Hodge duality a first time, we may rewrite the first ones in the form:

$$B_{1,1}^i + B_{2,2}^i + B_{3,3}^i + B_{4,4}^i = 0, \quad \forall i = 1, 2, 3, 4$$

Lowering the index i by means of the Euclidean metric for simplicity and setting $i = 4$, we get:

$$B_{44,4} = 0 \Rightarrow B_{41,1} + B_{42,2} + B_{43,3} = 0$$

Using again the Hodge duality but setting now $B_{41,1} = L_{23,1}$ and so on, we get:

$$L_{23,1} + L_{31,2} + L_{12,3} = 0$$

that is *exactly* the Lanczos formula, a result showing that, *for $n = 4$ only*, we discover that $L \simeq B \in \wedge^3 T^* \otimes g_1$ are both killed by δ .

We are thus able to exhibit the *Lanczos potential* $L \in \wedge^2 T^* \otimes T^*$ as a 3-tensor satisfying:

$$\boxed{L_{ij,k} + L_{ji,k} = 0, \quad L_{ij,k} + L_{jk,i} + L_{ki,j} = 0} \quad (1)$$

in the short exact sequence $0 \rightarrow \delta(T^* \otimes S_2 T^*) \rightarrow \wedge^2 T^* \otimes T^* \xrightarrow{\delta} \wedge^3 T^* \rightarrow 0$ but this result does not provide any potential because ... *the adjoint sequence is going backwards!*.

Q.E.D.

Using adjoint operators and adjoint bundles while setting $ad(E) = \wedge^n T^* \otimes E^*$ when E is a vector bundle over X and using the Hodge duality, we obtain the short exact sequences with arrows reversed:

$$0 \leftarrow ad(F_2) \leftarrow \wedge^{n-3} T^* \otimes g_1^* \xleftarrow{\delta^*} \wedge^{n-4} T^* \otimes T^* \leftarrow 0$$

as a way to describe the Lagrange multiplier $\lambda \in ad(F_2)$ in arbitrary dimension.

These results are leading to the:

- *Fifth comment:* The *div*-type operator induced (*on the right*) by the *Bianchi* operator has strictly nothing to do with the *Cauchy* operator (namely *ad(Killing)* *on the left*), contrary to what is still believed in GR. In addition, we have the:
- *Sixth comment:* We have proved in ([38] [39] [40]) that the usual *Cauchy*

stress equations must be replaced by the *Cosserat couple-stress equations* or, equivalently, that the Janet sequence must be replaced by the Spencer sequence in a coherent way with the couplings existing between EL and EM. It is also important to notice that, in the non-linear framework, there is no analogue of \mathcal{D}_2 in the *nonlinear Janet sequence* or of D_3 in the *nonlinear Spencer sequence*, a *redhibitory reason* leading to use only \mathcal{D} and \mathcal{D}_1 or D_1 and D_2 both with their formal adjoints.

As a way to conclude this example, we may say that, for any $n \geq 3$, the *Riemann* operator \mathcal{D}_1 is parametrizing the *Bianchi* operator \mathcal{D}_2 while the operator $ad(\mathcal{D}_2)$ is parametrizing the operator $ad(\mathcal{D}_1)$. Nevertheless, according to ([15]), there may exist minimal parametrizations of \mathcal{D}_2 with a lower number of potentials equal to $\dim(T) + \dim(F_1) - \dim(F_0)$, thus $4 + 20 - 10 = 14 = 20 - 6$ when $n = 4$ because of the Euler-Poincaré characteristic $4 - 10 + 20 - 20 + 6 = 0$ (See [18]).

Remark 3.2: Lanczos has been trying in vain to do for the *Bianchi* operator what he did for the *Riemann* operator, a useless but possible “*shift by one step to the right*” and to do for the *Weyl* operator what he did for the *Riemann* operator. However, we shall discover that the dimension $n = 4$, which is particularly “*fine*” for the classical Killing sequence, is particularly “*bad*” for the conformal Killing sequence, a result not known after one century because it cannot be understood without using the *Spencer δ -cohomology* in the following commutative diagram which is explaining therefore what we shall call the “*Lanczos secret*”. Following ([21]) and the fact that the two central vertical δ -sequences are exact, this diagram allows to construct the *Bianchi* operator $\mathcal{D}_2 : F_1 \rightarrow F_2$ as *generating CC* for the *Riemann* operator $\mathcal{D}_1 : F_0 = S_2 T^* \rightarrow F_1$ defined by a similar diagram and thus only depends on the symbol g_1 . For the reader not familiar with homological algebra, we provide below the main diagram allowing to construct the *Bianchi* operator both with the corresponding fiber dimensions when $n = 4$. In this commutative diagram, all the rows are exact and the columns are exact but eventually the left one:

$$\begin{array}{ccccccc}
 & 0 & & 0 & & 0 & & 0 \\
 & \downarrow & & \downarrow & & \downarrow & & \downarrow \\
 0 \rightarrow & g_4 & \rightarrow & S_4 T^* \otimes T & \rightarrow & S_3 T^* \otimes F_0 & \rightarrow & T^* \otimes F_1 \rightarrow F_2 \rightarrow 0 \\
 & \downarrow & & \downarrow & & \downarrow & & \parallel \\
 0 \rightarrow & T^* \otimes g_3 & \rightarrow & T^* \otimes S_3 T^* \otimes T & \rightarrow & T^* \otimes S_2 T^* \otimes F_0 & \rightarrow & T^* \otimes F_1 \rightarrow 0 \\
 & \downarrow & & \downarrow & & \downarrow & & \downarrow \\
 0 \rightarrow & \wedge^2 T^* \otimes g_2 & \rightarrow & \wedge^2 T^* \otimes S_2 T^* \otimes T & \rightarrow & \wedge^2 T^* \otimes T^* \otimes F_0 & \rightarrow & 0 \\
 & \downarrow & & \downarrow & & \downarrow & & \\
 0 \rightarrow & \wedge^3 T^* \otimes g_1 & \rightarrow & \wedge^3 T^* \otimes T^* \otimes T & \rightarrow & \wedge^3 T^* \otimes F_0 & \rightarrow & 0 \\
 & \downarrow & & \downarrow & & \downarrow & & \\
 0 \rightarrow & \wedge^4 T^* \otimes T & = & \wedge^4 T^* \otimes T & \rightarrow & 0 & & \\
 & \downarrow & & \downarrow & & & & \\
 & 0 & & 0 & & & &
 \end{array}$$

$$\begin{array}{ccccccc}
& & 0 & & 0 & & 0 \\
& & \downarrow & & \downarrow & & \downarrow \\
0 & \rightarrow & 140 & \rightarrow & 200 & \rightarrow & 80 \rightarrow 20 \rightarrow 0 \\
& & \downarrow & & \downarrow & & \parallel \\
0 & \rightarrow & 320 & \rightarrow & 400 & \rightarrow & 80 \rightarrow 0 \\
& & \downarrow & & \downarrow & & \downarrow \\
0 & \rightarrow & 240 & \rightarrow & 240 & \rightarrow & 0 \\
& & \downarrow & & \downarrow & & \\
0 \rightarrow & 24 & \rightarrow & 64 & \rightarrow & 40 & \rightarrow 0 \\
& \downarrow & & \downarrow & & \downarrow & \\
0 \rightarrow & 4 & = & 4 & \rightarrow & 0 & \\
& \downarrow & & \downarrow & & & \\
& 0 & & 0 & & &
\end{array}$$

Using the *Spencer cohomology* at $\wedge^2 T^* \otimes g_1$, the vector bundle $F_1 = H^2(g_1)$ in this diagram or *Riemann candidate* in the language of Lanczos, is defined by the short exact sequence:

$$\begin{array}{ccccccc}
0 \rightarrow & F_1 & \rightarrow & \wedge^2 T^* \otimes g_1 & \xrightarrow{\delta} & \wedge^3 T^* \otimes T & \rightarrow 0 \\
0 \rightarrow & 20 & \rightarrow & 36 & \xrightarrow{\delta} & 16 & \rightarrow 0
\end{array}$$

All the vertical down arrows are δ -maps of Spencer and all the vertical columns are exact but the first, which may not be exact only at $\wedge^3 T^* \otimes g_1$ with cohomology equal to $H^3(g_1)$ because we have:

$$\begin{aligned}
g_1 &= \left\{ \xi_i^k \in T^* \otimes T \mid \omega_{rj} \xi_i^r + \omega_{ir} \xi_j^r = 0 \right\} \simeq \wedge^2 T^* \subset T^* \otimes T \\
&\stackrel{\det(\omega) \neq 0}{\Rightarrow} g_2 = 0 \Rightarrow g_3 = 0 \Rightarrow g_4 = 0
\end{aligned}$$

A *snake-type chase* similarly provides the identification $F_2 = H^3(g_1)$ while using again the *Spencer cohomology* at $\wedge^3 T^* \otimes g_1$. The vector bundle F_2 providing the Bianchi identities is thus defined by the exactness of the top row of the preceding diagram or, equivalently, using the left column, by the short exact sequence:

$$\begin{array}{ccccccc}
0 \rightarrow & F_2 & \rightarrow & \wedge^3 T^* \otimes g_1 & \xrightarrow{\delta} & \wedge^4 T^* \otimes T & \rightarrow 0 \\
0 \rightarrow & 20 & \rightarrow & 24 & \xrightarrow{\delta} & 4 & \rightarrow 0
\end{array}$$

We conclude this Remark by saying that it is not even easy to discover that the bottom δ -map in the first column on the left is an epimorphism. In order to convince the reader of the powerfulness of these new methods, this result is left an exercise (*Hint*: prove that:

$$\wedge^3 T^* \otimes T^* \otimes T \simeq \wedge^3 T^* \otimes g_1 + \delta(\wedge^2 T^* \otimes S_2 T^* \otimes T)$$

by using a circular counterclockwise chase and that

$$F_2 \simeq \wedge^3 T^* \otimes g_1 \cap \delta(\wedge^2 T^* \otimes S_2 T^* \otimes T).$$

Starting with the (classical) *Killing* operator $K : T \rightarrow S_2 T^*$ defined by $\xi \rightarrow L(\xi)\omega$, we obtain successively the following differential sequences for various dimensions:

$$\begin{array}{ccccccc} n=2 & 2 & \xrightarrow[1]{K} & 3 & \xrightarrow[2]{R} & 1 & \rightarrow 0 \\ n=3 & 3 & \xrightarrow[1]{K} & 6 & \xrightarrow[2]{R} & 6 & \xrightarrow[1]{B} 3 \rightarrow 0 \\ n=4 & 4 & \xrightarrow[1]{K} & 10 & \xrightarrow[2]{R} & 20 & \xrightarrow[1]{B} 20 \xrightarrow[1]{} 6 \rightarrow 0 \\ n=5 & 5 & \xrightarrow[1]{K} & 15 & \xrightarrow[2]{R} & 50 & \xrightarrow[1]{B} 75 \xrightarrow[1]{} 45 \xrightarrow[1]{} 10 \rightarrow 0 \end{array}$$

For example, we have the Euler-Poincaré characteristic:

$$rk_D(M) = 4 - 10 + 20 - 20 + 6 = 0 \quad \text{when } n=4 \quad \text{or} \quad 5 - 15 + 50 - 75 + 45 - 10 = 0 \quad \text{when } n=5.$$

Setting successively $\mathcal{D} = K$, $\mathcal{D}_1 = R$, $\mathcal{D}_2 = B$ and so on, it follows therefore from the previous study that each operator is parametrizing the following one. Applying *double duality* and introducing the respective adjoint operators, then $ad(\mathcal{D}_2)$ is parametrizing the *Beltrami operator* $ad(\text{Riemann}) = ad(\mathcal{D}_1)$ with (canonical) potentials called *Lanczos* only when $n=4$ while $ad(\mathcal{D}_1)$ is parametrizing the *Cauchy operator* $ad(\mathcal{D})$ with (canonical) potentials called *Airy*, *Beltrami*, ... ([15] [18]). It must be finally noticed that $ad(\text{Ricci})$ is also parametrizing the *Cauchy operator* ([16] [18]).

4. Weyl/Lanczos Problem

Starting now afresh with the *conformal Killing* operator CK such that

$$\mathcal{L}(\xi)\omega = A(x)\omega \quad \text{or, equivalently, introducing the metric density}$$

$$\hat{\omega}_{ij} = \omega_{ij} |det(\omega)|^{-\frac{1}{n}}, \quad \text{we have a new operator}$$

$CK : T \rightarrow \{\Omega \in S_2 T^* \mid tr(\Omega) = \omega^{ij} \Omega_{ij} = 0\}$ defined by $\xi \rightarrow \mathcal{L}(\xi)\hat{\omega}$ and we obtain successively the following differential sequences for various dimensions $n \geq 3$ ([43]):

$$\begin{array}{ccccccc} n=3 & 3 & \xrightarrow[1]{CK} & 5 & \xrightarrow[3]{?} & 5 & \xrightarrow[1]{?} 3 \rightarrow 0 \\ n=4 & 4 & \xrightarrow[1]{CK} & 9 & \xrightarrow[2]{W} & 10 & \xrightarrow[2]{?} 9 \xrightarrow[1]{} 4 \rightarrow 0 \\ n=5 & 5 & \xrightarrow[1]{CK} & 14 & \xrightarrow[2]{W} & 35 & \xrightarrow[1]{CB} 35 \xrightarrow[2]{} 14 \xrightarrow[1]{} 5 \rightarrow 0 \end{array}$$

For example, we have the Euler-Poincaré characteristic:

$$rk_D(M) = 5 - 14 + 35 - 35 + 14 - 5 = 0.$$

Proceeding exactly as before, we obtain for example when $n=4$ the following commutative diagram where all the rows are exact and the columns are exact but eventually the left one:

$$\begin{array}{ccccccccc}
& 0 & & 0 & & 0 & & 0 & \\
& \downarrow & & \downarrow & & \downarrow & & \downarrow & \\
0 \rightarrow & \hat{g}_5 & \rightarrow & S_5 T^* \otimes T & \rightarrow & S_4 T^* \otimes \hat{F}_0 & \rightarrow & S_2 T^* \otimes \hat{F}_1 & \rightarrow \hat{F}_2 \rightarrow 0 \\
& \downarrow & & \downarrow & & \downarrow & & \parallel & \\
0 \rightarrow & T^* \otimes \hat{g}_4 & \rightarrow & T^* \otimes S_4 T^* \otimes T & \rightarrow & T^* \otimes S_3 T^* \otimes \hat{F}_0 & \rightarrow & T^* \otimes T^* \otimes \hat{F}_1 & \rightarrow 0 \\
& \downarrow & & \downarrow & & \downarrow & & \downarrow & \\
0 \rightarrow & \wedge^2 T^* \otimes \hat{g}_3 & \rightarrow & \wedge^2 T^* \otimes S_3 T^* \otimes T & \rightarrow & \wedge^2 T^* \otimes S_2 T^* \otimes \hat{F}_0 & \rightarrow & \wedge^2 T^* \otimes \hat{F}_1 & \rightarrow 0 \\
& \downarrow & & \downarrow & & \downarrow & & \downarrow & \\
0 \rightarrow & \wedge^3 T^* \otimes \hat{g}_2 & \rightarrow & \wedge^3 T^* \otimes S_2 T^* \otimes T & \rightarrow & \wedge^3 T^* \otimes T^* \otimes \hat{F}_0 & \rightarrow & 0 & \\
& \downarrow & & \downarrow & & \downarrow & & & \\
0 \rightarrow & \wedge^4 T^* \otimes \hat{g}_1 & \rightarrow & \wedge^4 T^* \otimes T^* \otimes T & \rightarrow & \wedge^4 T^* \otimes \hat{F}_0 & \rightarrow & 0 & \\
& \downarrow & & \downarrow & & \downarrow & & & \\
& 0 & & 0 & & 0 & & &
\end{array}$$

Nevertheless, the same (but very tricky now!) chase as before allows to prove that the bottom δ -map in the first column on the left is again ... an epimorphism, a crucial result indeed, left again as a difficult exercise of diagram chasing (*Hint*: double step circular chase as before!).

$$\begin{array}{ccccccc}
& 0 & & 0 & & 0 & \\
& \downarrow & & \downarrow & & \downarrow & \\
0 \rightarrow & 224 & \rightarrow & 315 & \rightarrow & 100 & \rightarrow 9 \rightarrow 0 \\
& \downarrow & & \downarrow & & \downarrow & \\
0 \rightarrow & 560 & \rightarrow & 720 & \rightarrow & 160 & \rightarrow 0 \\
& \downarrow & & \downarrow & & \downarrow & \\
0 \rightarrow & 480 & \rightarrow & 540 & \rightarrow & 60 & \rightarrow 0 \\
& \downarrow & & \downarrow & & \downarrow & \\
0 \rightarrow & 16 & \rightarrow & 160 & \rightarrow & 144 & \rightarrow 0 \\
& \downarrow & & \downarrow & & \downarrow & \\
0 \rightarrow & 7 & \rightarrow & 16 & \rightarrow & 9 & \rightarrow 0 \\
& \downarrow & & \downarrow & & \downarrow & \\
& 0 & & 0 & & 0 &
\end{array}$$

Of course, in view of the dimensions of the matrices involved (up to 540×720), we wish good luck to anybody trying to use computer algebra and refer to the computations done in ([1]) that have been done while knowing “*a priori*” the dimensions that should be found.

Remark 4.1: Using the splitting of the Riemann tensor between the Ricci tensor and the Weyl tensor for the second column while taking into account the fact that the extension modules are torsion modules and thus that each component of the Weyl tensor is differentially dependent on the Ricci tensor, we obtain the following commutative and exact diagram:

$$\begin{array}{ccccccc}
& & 0 & & 0 & & 0 \\
& & \downarrow & & \downarrow & & \downarrow \\
0 & & 10 & \rightarrow & 16 & \rightarrow & 6 \rightarrow 0 \\
\downarrow & & \downarrow \uparrow & & \downarrow & & \parallel \\
10 & \xrightarrow{\text{Riemann}} & 20 & \xrightarrow{\text{Bianchi}} & 20 & \rightarrow & 6 \rightarrow 0 \\
\parallel & & \downarrow \uparrow & & \downarrow & & \downarrow \\
10 & \xrightarrow{\text{Einstein}} & 10 & \xrightarrow{\text{div}} & 4 & \rightarrow & 0 \\
\downarrow & & \downarrow & & \downarrow & & \\
0 & & 0 & & 0 & &
\end{array}$$

It follows that the 10 components of the Weyl tensor must satisfy a first order linear system with 16 equations, having 6 generating first order CC. The differential rank of the corresponding operator is thus equal to $16 - 6 = 10$ and such an operator defines a torsion module in which we have to look *separately* for each component of the Weyl tensor in order to prove that it is killed by the *Dalembert* operator ([16]). The situation is similar to that of the Cauchy-Riemann equations obtained when $n = 2$ by considering the *conformal Killing* operator *CK*. Indeed, any complex transformation $y = f(x)$ must be solution of the (linear) first order system $y_2^2 - y_1^1 = 0, y_2^1 + y_1^2 = 0$ of finite Lie equations though we obtain $y_{11}^1 + y_{22}^1 = 0, y_{11}^2 + y_{22}^2 = 0$, that is y^1 and y^2 are *separately* killed by the second order *Laplace* operator $\Delta = d_{11} + d_{22}$. We obtain the following striking technical lemma explaining the so-called *gauging* procedure of the Lanczos potential.

Lemma 4.2: When $n = 4$, the central vertical arrow $20 \rightarrow 4$ is just described by the contraction formula $\wedge^2 T^* \otimes T^* \rightarrow \wedge^2 T^* \otimes T \rightarrow T^*$ depending on the metric:

$$\boxed{L_{ij,k} \rightarrow L_i = \omega^{jk} L_{ij,k}} \quad (12)$$

Proof: Let us write down the *Bianchi* operator in the form:

$$\nabla_r R^k_{l,ij} + \nabla_i R^k_{l,jr} + \nabla_j R^k_{l,ri} = B^k_{l,ijr}$$

Contracting with $k = j = s$, we obtain:

$$\nabla_r R^s_{l,is} + \nabla_i R^s_{l,rs} + \nabla_s R^s_{l,ri} = B^s_{l,isr}$$

Setting as usual $R^s_{l,sr} = R_{lr} = R_{rl}$ with $\omega^{ij} R_{ij} = R$ and contracting with ω^{li} , we finally get :

$$2\nabla_s R^s_r - \nabla_r R = \omega^{ij} B^s_{i,jrs}$$

as *the way* to use a contraction in order to exhibit Einstein equations.

With $n = 4$, let us write down all the terms, using the Euclidean metric for simplicity instead of the Minkowski metric, recalling that only this later choice allows to find out both the Poincaré group *and* the differential sequence with successive operators K, R, B according to ([22]):

$$B^s_{1,1rs} + B^s_{2,2rs} + B^s_{3,3rs} + B^s_{4,4,rs} = C_r$$

that is to say with all the terms:

$$B^1_{1,1r1} + B^2_{1,1r2} + B^3_{1,1r3} + B^4_{1,1r4} + B^1_{2,2r1} + B^2_{2,2r2} + B^3_{2,2r3} + B^4_{2,2r4} \\ + B^1_{3,3r1} + B^2_{3,3r2} + B^3_{3,3r3} + B^4_{3,3r4} + B^1_{4,4r1} + B^2_{4,4r2} + B^3_{4,4r3} + B^4_{4,4r4} = C_r$$

where, *in any case*, we have $B^1_{1,1r1} = B^2_{2,2r2} = B^3_{3,3r3} = B^4_{4,4r4} = 0$.

If we set $r = 1$, the first line disappears because of the 3-form $\wedge^3 T^*$ and we are left with:

$$B^3_{2,213} + B^4_{2,214} + B^2_{3,312} + B^4_{3,314} + B^2_{4,412} + B^3_{4,413} = C_1$$

Using Hodge duality, we get with new indices:

$$-B^3_{2,4} + B^4_{2,3} + B^2_{3,4} - B^4_{3,2} - B^2_{4,3} + B^3_{4,2} = C_1$$

arriving finally to the formula:

$$2(B^2_{3,4} + B^3_{4,2} + B^4_{2,3}) = C_1$$

that is *exactly* twice the trace of the Lanczos tensor, namely:

$$L^2_{1\ 2} + L^3_{1\ 3} + L^4_{1\ 4} = L^r_{1\ r}$$

This result explains why the Lanczos tensor $L_{ij,k} = -L_{ji,k}$ with 24 components is first reduced to 20 components through the condition $L_{ij,k} + L_{jk,i} + L_{ki,j} = 0$ and finally to 16 components as in the diagram through the kernel of the above trace condition. It is thus *impossible* to understand this result, even for $n = 4$, without the Spencer δ -cohomology and *absolutely impossible* to generalize this result in arbitrary dimension without the combination of the δ -cohomology and double duality in differential homological algebra.

Q.E.D.

Finally, using the previous definition $ad(E) = \wedge^n T^* \otimes E^*$, such a result explains the confusion done by Lanczos and followers between the *Riemann* candidate F_2 or the *Weyl* candidate \hat{F}_2 and their respective formal adjoint vector bundles having of course the same fiber dimension but quite different transition rules under changes of local coordinates.

We notice that the changes of the successive orders are totally unusual and refer to ([22]) for more details on the computer algebra methods. In particular, when $n = 4$, the conformal analogue of the *Bianchi* operator is now of order 2, a result explaining why Lanczos and followers never succeeded adapting the Lanczos tensor potential L for the *Weyl* operator. We understand therefore that the solution of what we called “*Lanczos secret*” must be depending on a quite different homological framework. It is only after exhibiting it in the last section below that we will be able to say that we have thus solved the *Riemann-Lanczos* and *Weyl-Lanczos* parametrization problems in arbitrary dimension. In the meantime, we provide two examples that can be fully computed as a way to understand the use of adjoint differential sequences.

5. Motivating Examples

The two following examples will show how the differential extension modules

may depend on the Vessiot structure constants.

Example 5.1: With $m = n = 2, q = 1, K = \mathbb{Q}\langle\omega\rangle$ and $\omega = (\alpha, \beta)$ with $\alpha \in T^*, \beta \in \wedge^2 T^*$, let us consider the Lie operator $\mathcal{D}: T \rightarrow \Omega: \xi \rightarrow \mathcal{L}(\xi)\omega = (A = \mathcal{L}(\xi)\alpha, B = \mathcal{L}(\xi)\beta)$. The corresponding first order system:

$$A_i \equiv \alpha_r \partial_i \xi^r + \xi^r \partial_r \alpha_i = 0, \quad B \equiv \beta \partial_r \xi^r + \xi^r \partial_r \beta = 0$$

is involutive whenever $\beta \neq 0$ and $d\alpha = c\beta$ where now d is the standard exterior derivative and $c = cst$, exactly as in ([19], p 438-440). We have the differential sequence:

$$0 \rightarrow \Theta \rightarrow T \xrightarrow{\mathcal{D}} T^* \times_X \wedge^2 T^* \xrightarrow{\mathcal{D}_1} \wedge^2 T^* \rightarrow 0$$

with $\xi \rightarrow (A_1, A_2, B) \rightarrow C \rightarrow 0$ or the resolution:

$$0 \rightarrow D \xrightarrow{\mathcal{D}_1} D^3 \xrightarrow{\mathcal{D}} D^2 \xrightarrow{p} M \rightarrow 0$$

Multiplying (A_1, A_2, B) respectively by (μ^1, μ^2, μ^3) , we obtain $ad(\mathcal{D})$ in the form:

$$\begin{aligned} -\alpha_1 (\partial_1 \mu^1 + \partial_2 \mu^2) - \beta (\partial_1 \mu^3 - c \mu^2) &= \nu^1, \\ -\alpha_2 (\partial_1 \mu^1 + \partial_2 \mu^2) - \beta (\partial_2 \mu^3 + c \mu^1) &= \nu^2 \end{aligned}$$

Then, multiplying $\partial_1 A_2 - \partial_2 A_1 - cB = C$ by λ , we obtain $ad(\mathcal{D}_1)$ as:

$$\partial_2 \lambda = \mu^1, \quad -\partial_1 \lambda = \mu^2, \quad -c\lambda = \mu^3$$

We have therefore to consider the two cases:

- $c = 0$: We have the new CC $\partial_1 \mu^1 + \partial_2 \mu^2 = 0$ and $\mu^3 = 0$. It follows that the torsion module $ext^1(M) \neq 0$ is generated by the residue of $\mu^3 = \nu'$ because $\alpha \neq 0$ and we may thus suppose that $\alpha_1 \neq 0$. As for $ext^2(M)$, this torsion module is just defined by the system $\partial_2 \lambda = 0, \partial_1 \lambda = 0$ for λ and thus $ext^2(M) \neq 0$.
- $c \neq 0$: We must have the new CC:

$$\partial_1 \mu^3 - c \mu^2 = 0, \partial_2 \mu^3 + c \mu^1 = 0 \Rightarrow \partial_1 \mu^1 + \partial_2 \mu^2 = 0$$

It follows that $ext^1(M)$ is now generated by the residue of $\partial_1 \mu^1 + \partial_2 \mu^2 = \nu'$. Finally, $ker(ad(\mathcal{D}_1))$ is defined by $\lambda = 0$ and thus $ext^2(M) = 0$.

Hence, both $ext^1(M)$ and $ext^2(M)$ highly depend on the Vessiot structure constant c .

Example 5.2: (Contact transformations)

With $m = n = 3, q = 1, K = \mathbb{Q}(x^1, x^2, x^3)$ or simply $\mathbb{Q}(x)$, we may introduce the 1-form $\alpha = dx^1 - x^3 dx^2 \in T^*$ and consider the system of finite Lie equations defined by $j_1(f)^{-1}(\alpha) = \rho(x)\alpha$. Eliminating the factor ρ and linearizing at the q -jet of the identity, we obtain the first order involutive system of infinitesimal Lie equations:

$$\begin{cases} \eta^3 \equiv \partial_3 \xi^3 + \partial_2 \xi^2 - \partial_1 \xi^1 + 2x^3 \partial_1 \xi^2 = 0 \\ \eta^2 \equiv \partial_3 \xi^1 - x^3 \partial_3 \xi^2 = 0 \\ \eta^1 \equiv \partial_2 \xi^1 - x^3 \partial_2 \xi^2 + x^3 \partial_1 \xi^1 - (x^3)^2 \partial_1 \xi^2 - \xi^3 = 0 \end{cases} \quad \begin{array}{|c|c|c|} \hline 1 & 2 & 3 \\ \hline 1 & 2 & 3 \\ \hline 1 & 2 & \bullet \\ \hline \end{array}$$

with two equations of class 3, one equation of class 2 and thus one CC of order 1, namely $d_3\eta^1 - d_2\eta^2 - x^3d_1\eta^2 + \eta^3 = 0$. Now, it is well known that this *contact* operator $\mathcal{D} = \mathcal{D}_0$ can be parametrized by an operator \mathcal{D}_{-1} as follows:

$$-x^3\partial_3\phi + \phi = \xi^1, -\partial_3\phi = \xi^2, \partial_2\phi + x^3\partial_1\phi = \xi^3 \Rightarrow \xi^1 - x^3\xi^2 = \phi$$

and thus $M \simeq D$. We have obtained the following formally exact sequence which is nevertheless *not* strictly exact because \mathcal{D}_{-1} is *not* formally integrable:

$$0 \rightarrow \phi \xrightarrow{\mathcal{D}_{-1}} \xi \xrightarrow{\mathcal{D}} \eta \xrightarrow{\mathcal{D}_1} \zeta \rightarrow 0$$

$$0 \rightarrow 1 \rightarrow 3 \rightarrow 3 \rightarrow 1 \rightarrow 0 \Leftrightarrow 0 \rightarrow D \rightarrow D^3 \rightarrow D^3 \rightarrow D \rightarrow 0$$

As M is therefore free and thus projective, it follows that the adjoint sequence is exact too.

Coming back to the Vessiot structure equations, we notice that α is not invariant by the contact Lie pseudogroup and cannot be considered as an associated geometric object. We have shown in ([9], p 684-691) that the corresponding geometric object is a 1-form density ω leading to the system of infinitesimal Lie equations in Medolaghi form:

$$\Omega_i \equiv (\mathcal{L}(\xi)\omega)_i \equiv \omega_r \partial_i \xi^r - \frac{1}{2} \omega_i \partial_r \xi^r + \xi^r \partial_r \omega_i = 0$$

and to the *only* Vessiot structure equation:

$$\omega_1(\partial_2\omega_3 - \partial_3\omega_2) + \omega_2(\partial_3\omega_1 - \partial_1\omega_3) + \omega_3(\partial_1\omega_2 - \partial_2\omega_1) = c$$

with the *only* structure constant c . In the present contact situation, we may choose $\omega = (1, -x^3, 0)$ and get $c = 1$ but we may also choose $\omega = (1, 0, 0)$ and get $c = 0$, these two choices both bringing an involutive system. Let us prove that the situation becomes completely different with the new system:

$$-2\Omega_1 \equiv \partial_3\xi^3 + \partial_2\xi^2 - \partial_1\xi^1 = 0, \Omega_2 \equiv \partial_2\xi^1 = 0, \Omega_3 \equiv \partial_3\xi^1 = 0$$

having the only CC $d_2\Omega_3 - d_3\Omega_2 = 0$.

Multiplying the three previous equations by the three test functions μ , the only CC by the test function λ and integrating by parts, we get the adjoint operators:

$$0 = \mu^1, \partial_3\lambda = \mu^2, -\partial_2\lambda = \mu^3$$

$$\partial_1\mu^1 - \partial_2\mu^2 - \partial_3\mu^3 = \nu^1, -\partial_2\mu^1 = \nu^2, -\partial_3\mu^1 = \nu^3$$

It follows that $0 \neq D\xi^1 = t(M) \subset M$ with a strict inclusion and $\text{ext}^1(M) \neq 0$. Similarly, $\ker(ad(\mathcal{D}_1))$ is defined by $\partial_2\lambda = 0, \partial_3\lambda = 0$ and thus $\text{ext}^2(M) \neq 0$.

Our problem will be now to construct and compare the differential sequences:

$$\begin{array}{ccccccc} \phi & \xrightarrow{\mathcal{D}_{-1}} & \xi & \xrightarrow{\mathcal{D}} & \eta & \xrightarrow{\mathcal{D}_1} & C \\ & & \text{ad}(\mathcal{D}_{-1}) & & \text{ad}(\mathcal{D}) & & \text{ad}(\mathcal{D}_1) \\ \theta & \leftarrow & \nu & \leftarrow & \mu & \leftarrow & \lambda \end{array}$$

For this, linearizing the only Vessiot structure equation, we get the CC operator \mathcal{D}_1 and the corresponding system $\mathcal{D}_1\Omega = 0$ in the form:

$$\begin{aligned} & \omega_1(\partial_2\Omega_3 - \partial_3\Omega_2) + \omega_2(\partial_3\Omega_1 - \partial_1\Omega_3) + \omega_3(\partial_1\Omega_2 - \partial_2\Omega_1) \\ & + (\partial_2\omega_3 - \partial_3\omega_2)\Omega_1 + (\partial_3\omega_1 - \partial_1\omega_3)\Omega_2 + (\partial_1\omega_2 - \partial_2\omega_3)\Omega_3 = 0 \end{aligned}$$

Multiplying on the left by the test function λ and integrating by parts, we get the operator $ad(\mathcal{D}_1)$ in the form:

$$\begin{cases} \Omega_1 \rightarrow \omega_3\partial_2\lambda - \omega_2\partial_3\lambda + 2(\partial_2\omega_3 - \partial_3\omega_2)\lambda = \mu^1 \\ \Omega_2 \rightarrow \omega_1\partial_3\lambda - \omega_3\partial_1\lambda + 2(\partial_3\omega_1 - \partial_1\omega_3)\lambda = \mu^2 \\ \Omega_3 \rightarrow \omega_2\partial_1\lambda - \omega_1\partial_2\lambda + 2(\partial_1\omega_2 - \partial_2\omega_1)\lambda = \mu^3 \end{cases}$$

We obtain therefore the crucial formula $2c\lambda = \omega_i\mu^i$ showing how the previous sequences are *essentially* depending on the Vessiot structure constant c . Indeed, if $c \neq 0$, then $\mu = 0 \Rightarrow \lambda = 0$ and the operator $ad(\mathcal{D}_1)$ is injective. This is the case when $\omega = (1, -x^3, 0) \Rightarrow c = 1 \Rightarrow \lambda = 0$. On the contrary, if $c = 0$, then the operator $ad(\mathcal{D}_1)$ may not be injective as can be seen by choosing $\omega = (1, 0, 0)$. Indeed, in this case we get a kernel defined by $\partial_3\lambda = 0, \partial_2\lambda = 0$.

We invite the reader to treat similarly the case of *unimodular contact transformations*, namely transformations preserving the 1-form $\alpha = dx^1 - x^3dx^2$, thus also the 2-form $\beta = d\alpha = dx^2 \wedge dx^3$ and even the 3-form $dx^1 \wedge dx^2 \wedge dx^3$ that can be used as a volume form. The Vessiot structure equations for the ground geometric object $\omega = (\alpha, \beta)$ are now $d\alpha = c'\beta, d\beta = c''\alpha \wedge \beta$ with the only striking Jacobi condition $c'c'' = 0$ (See [1] for more details).

6. Generalized Lanczos Problem

In this last section, we prove that the following theorem allows to solve locally the Lanczos problem in a similar way for *any* Lie group of transformations:

Theorem 6.1: The *Spencer sequence* for any Lie operator \mathcal{D} which is coming from a Lie group of transformations, with a Lie group G acting on X , is (locally) isomorphic to the tensor product of the Poincaré sequence for the exterior derivative by the Lie algebra \mathcal{G} of G .

Proof: If M is the differential module defined by \mathcal{D} , we want to prove that the extension modules $ext^1(M)$ and $ext^2(M)$ vanish, that is, if \mathcal{D}_1 generates the CC of \mathcal{D} but also \mathcal{D}_2 generates the CC of \mathcal{D}_1 , then $ad(\mathcal{D})$ generates the CC of $ad(\mathcal{D}_1)$ and $ad(\mathcal{D}_1)$ generates the CC of $ad(\mathcal{D}_2)$. We also remind the reader that we have shown in ([18] [22]) that it is not easy to exhibit the CC of the Maxwell or Morera parametrizations when $n = 3$ and that a direct checking for $n = 4$ should be strictly impossible. It has been proved by L. P. Eisenhart in 1926 ([20]) that the solution space Θ of the Killing system has $n(n+1)/2$ *infinitesimal generators* $\{\theta_\tau\}$ linearly independent over the constants if and only if ω had constant Riemannian curvature, namely zero in our case. As we have a transitive Lie group of transformations preserving the metric considered as a transitive Lie pseudogroup, the three classical theorems of Sophus Lie assert that $[\theta_\rho, \theta_\sigma] = c^\tau_{\rho\sigma}\theta_\tau$ where the *structure constants* c define a Lie algebra \mathcal{G} . We have therefore $\xi \in \Theta \Leftrightarrow \xi = \{\lambda^\tau \theta_\tau \mid \lambda^\tau = cst\}$. Hence, we

may replace locally the Killing system by the system $\partial_i \lambda^\tau(x) = 0$, getting therefore the differential sequence:

$$0 \rightarrow \Theta \rightarrow \wedge^0 T^* \otimes G \xrightarrow{d} \wedge^1 T^* \otimes G \xrightarrow{d} \cdots \xrightarrow{d} \wedge^n T^* \otimes G \rightarrow 0$$

which is the tensor product of the Poincaré sequence by G . Finally, it follows from the above Theorem that the extension modules considered do not depend on the resolution used and thus vanish because the Poincaré sequence is self adjoint (up to sign), that is $ad(d)$ generates the CC of $ad(d)$ at any position, exactly like d generates the CC of d at any position. This (difficult) result explains why the adjoint differential modules we shall meet will be torsion-free or even reflexive. We invite the reader to compare with the situation of the Maxwell equations in electromagnetism (See ([12], p 492-494) for more details). However, we have explained in ([11] [13]) why neither the Janet sequence nor the Poincaré sequence can be used in physics and must be replaced by the *Spencer sequence* which is another resolution of Θ . Though this is out of the scope of this paper, we shall nevertheless shortly describe the relation existing between the above results and the Spencer operator, thus the Spencer sequence. For this, let us define for any $q \geq 0$ the section $\xi_q = \lambda^\tau(x) j_q(\theta_\tau)(x) = (\xi_\mu^k(x) = \lambda^\tau(x) \partial_\mu \theta_\tau^k(x)) \in R_q$. With the standard notations of ([8] [11] [12]) and $0 \leq |\mu| \leq q$, the components of the Spencer operator become:

$$\begin{aligned} \xi_{q+1} \in R_{q+1} &\rightarrow j_1(\xi_q) - \xi_{q+1} = (\partial_i \xi_\mu^k(x) - \xi_{\mu+1_i}^k(x)) \\ &= ((\partial_i \lambda^\tau(x)) \partial_\mu \theta_\tau^k(x) \xi) \in T^* \otimes R_q \end{aligned}$$

when q is large enough, that is $q = 2$ for the Killing system and $q = 3$ for the conformal Killing system in arbitrary dimension ([43]), we have involutive systems with vanishing symbols because both are finite-type. We obtain therefore the desired identification justifying our claim.

Q.E.D.

Corollary 6.2: When \mathcal{D} is the Killing operator or the conformal Killing operator, then $ext^1(M) = 0, ext^2(M) = 0$ and there is no gap. Moreover, if the differential module M defined by \mathcal{D} is a torsion module as in the Theorem, then we have $ext^0(M) = hom_{\mathcal{D}}(M, D) = 0$ in any case.

7. Conclusion

E. Vessiot discovered the so-called *Vessiot structure equations* as early as in 1903 and, only a few years later, E. Cartan discovered the so-called *Maurer-Cartan structure equations*. Both are depending on a certain number of constants like the single *geometric structure constant* of the constant Riemannian curvature for the first and the many *algebraic structure constants* of Lie algebra for the second. However, Cartan and followers never acknowledged the existence of another approach which is therefore still totally ignored today, in particular by physicists. Now, it is well known that the structure constants of a Lie algebra play a fundamental part in the Chevalley-Eilenberg cohomology of Lie algebras and their

deformation theory. It was thus a challenge to associate the Vessiot structure constants with other homological properties related to systems of Lie equations, namely the extension modules determined by Lie operators. As a striking consequence, such a possibility opens a new way to understand and revisit the various contradictory works done during the last fifty years or so by different groups of researchers, using respectively Cartan, Gröbner or Janet bases while looking for a modern interpretation of the work done by C. Lanczos from 1938 to 1962. However, the reader must not forget that the Weyl tensor was not known by Lanczos, even as late as in 1967, and that it was not possible to discover any solution of the parametrization problem by potentials through double duality before 1990/1995, that is too late for the many people already engaged in this type of research. We finally hope that this paper will open a new domain for applying computer algebra while offering a collection of useful test examples.

Conflicts of Interest

The author declares no conflicts of interest regarding the publication of this paper.

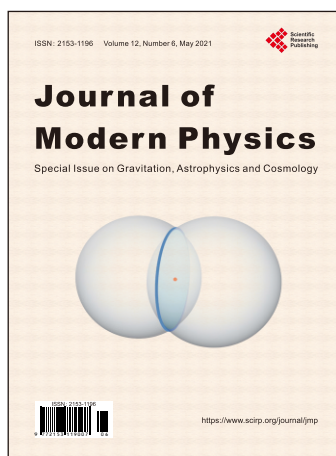
References¹

- [1] Pommaret, J.-F. (2016) Deformation Theory of Algebraic and Geometric Structures. Lambert Academic Publisher (LAP), Saarbrücken, Germany. In: Dubreil, S.P. and Malliavin, M.-P., Eds., *Topics in Invariant Theory*, Lambert Academic Publisher (LAP), Saarbrücken, Springer Lecture Notes in Mathematics, Vol. 1478, 244-254. <https://arxiv.org/abs/1207.1964>
<https://doi.org/10.1007/BFb0083506>
- [2] Lanczos, C. (1938) *Annals of Mathematics*, **39**, 842-850.
<https://doi.org/10.2307/1968467>
- [3] Lanczos, C. (1949) *Reviews of Modern Physics*, **21**, 497-502.
<https://doi.org/10.1103/RevModPhys.21.497>
- [4] Lanczos, C. (1962) *Reviews of Modern Physics*, **34**, 379-389.
<https://doi.org/10.1103/RevModPhys.34.379>
- [5] Lanczos, C. (1962) *Annales Scientifiques de l'Université de Clermont-Ferrand 2, Mathématiques*, **8**, 167-170. <http://www.numdam.org>
- [6] O'Donnell, P. and Pye, H. (2010) *EJTP*, **24**, 327-350.
- [7] Pommaret, J.-F. (2019) *Journal of Modern Physics*, **10**, 1566-1595.
<https://arxiv.org/abs/1802.02430>
<https://doi.org/10.4236/jmp.2019.1013104>
- [8] Pommaret, J.-F. (1978) *Systems of Partial Differential Equations and Lie Pseudogroups*. Gordon and Breach, New York; Russian Translation by MIR, Moscow, 1983.
- [9] Pommaret, J.-F. (1983) *Differential Galois Theory*. Gordon and Breach, New York.
- [10] Pommaret, J.-F. (1988) *Lie Pseudogroups and Mechanics*. Gordon and Breach, New York.
- [11] Pommaret, J.-F. (1994) *Partial Differential Equations and Group Theory: New Pers-*

¹We have only quoted the recent references on the Lanczos potential published after 2000.

- pectives for Applications (Mathematics and Its Applications 293). Wolters Kluwer, Alphen aan den Rijn. <https://doi.org/10.1007/978-94-017-2539-2>
- [12] Pommaret, J.-F. (2001) Partial Differential Control Theory. Wolters Kluwer, Alphen aan den Rijn, 957 p. <https://doi.org/10.1007/978-94-010-0854-9>
 - [13] Pommaret, J.-F. (2018) New Mathematical Methods for Physics, Mathematical Physics Books. Nova Science Publishers, New York, 150 p.
 - [14] Pommaret, J.-F. (2013) *Journal of Modern Physics*, **4**, 223-239. <https://doi.org/10.4236/jmp.2013.48A022>
 - [15] Pommaret, J.-F. (2016) *Journal of Modern Physics*, **7**, 699-728. <https://doi.org/10.4236/jmp.2016.77068>
 - [16] Pommaret, J.-F. (2017) *Journal of Modern Physics*, **8**, 2122-2158. <https://doi.org/10.4236/jmp.2017.813130>
 - [17] Pommaret, J.-F. (2019) *Journal of Modern Physics*, **10**, 1454-1486. <https://doi.org/10.4236/jmp.2019.1012097>
 - [18] Pommaret, J.-F. (2021) *Journal of Modern Physics*, **12**, 453-482. <https://doi.org/10.4236/jmp.2021.124032>
 - [19] Vessiot, E. (1903) *Annales scientifiques de l'École Normale Supérieure*, **20**, 411-451. <https://doi.org/10.24033/asens.529>
 - [20] Eisenhart, L.P. (1926) Riemannian Geometry. Princeton University Press, Princeton. <https://doi.org/10.1090/coll/008>
 - [21] Pommaret, J.-F. (2019) *Journal of Modern Physics*, **10**, 371-401. <https://doi.org/10.4236/jmp.2019.103025>
 - [22] Pommaret, J.-F. (2020) *Journal of Modern Physics*, **11**, 1672-1710. <https://doi.org/10.4236/jmp.2020.1110104>
 - [23] Pommaret, J.-F. (2012) Spencer Operator and Applications: From Continuum Mechanics to Mathematical Physics. In: Gan, Y., Ed., *Continuum Mechanics—Progress in Fundamentals and Engineering Applications*, InTech, Rijeka, Chapter 1. <https://www.intechopen.com/books/continuum-mechanics-progress-in-fundamentals-and-engineering-applications>
 - [24] Goldschmidt, H. (1968) *Annales scientifiques de l'École Normale Supérieure, Série 4*, **1**, 617-625. <https://doi.org/10.24033/asens.1173>
 - [25] Janet, M. (1920) *Journal de Mathématiques*, **8**, 65-151.
 - [26] Spencer, D.C. (1965) *Bulletin of the American Mathematical Society*, **75**, 1-114.
 - [27] Kunz, E. (1985) Introduction to Commutative Algebra and Algebraic Geometry. Birkhäuser, Boston. <https://doi.org/10.1007/978-1-4612-5290-0>
 - [28] Rotman, J.J. (1979) An Introduction to Homological Algebra. Academic Press, Cambridge.
 - [29] Kashiwara, M. (1995) Algebraic Study of Systems of Partial Differential Equations. Mémoires de la Société Mathématique de France 63, Transl. from Japanese of His 1970 Master's Thesis.
 - [30] Oberst, U. (1990) *Acta Applicandae Mathematicae*, **20**, 1-175. <https://doi.org/10.1007/BF00046908>
 - [31] Schneiders, J.-P. (1994) *Bulletin de la Société Royale des Sciences de Liège*, **63**, 223-295.
 - [32] Pommaret, J.-F. (1995) *Comptes Rendus de l'Académie des Sciences Paris, Série I*, **320**, 1225-1230.

- [33] Zerz, E. (2000) Topics in Multidimensional Linear Systems Theory. Lecture Notes in Control and Information Sciences 256, Springer, Berlin.
- [34] Pommaret, J.-F. (2005) Algebraic Analysis of Control Systems Defined by Partial Differential Equations. In: *Advanced Topics in Control Systems Theory*, Lecture Notes in Control and Information Sciences 311, Chapter 5, Springer, Berlin, 155-223. https://doi.org/10.1007/11334774_5
- [35] Pommaret, J.-F. and Quadrat, A. (1999) *Systems & Control Letters*, **37**, 247-260. [https://doi.org/10.1016/S0167-6911\(99\)00030-4](https://doi.org/10.1016/S0167-6911(99)00030-4)
- [36] Pommaret, J.-F. (2010) *Acta Mechanica*, **215**, 43-55. <https://doi.org/10.1007/s00707-010-0292-y>
- [37] Edgar, S.B. and Höglund, A. (2000) *General Relativity and Gravitation*, **32**, 2307-2318. <https://doi.org/10.1023/A:1001951609641>
<http://rspa.royalsocietypublishing.org/content/royprsa/453/1959/835.full.pdf>
- [38] Dolan, P. and Gerber, A. (2002) Janet-Riquier Theory and the Riemann-Lanczos Problem in 2 and 3 Dimensions.
- [39] Edgar, S.B. (2003) *Journal of Mathematical Physics*, **44**, 5375-5385. <https://arxiv.org/abs/gr-qc/0302014>
<https://doi.org/10.1063/1.1619203>
- [40] Edgar, S.B. and Senovilla, J.M.M. (2004) *Classical and Quantum Gravity*, **21**, L133. <https://arxiv.org/abs/gr-qc/0408071>
<https://doi.org/10.1088/0264-9381/21/22/L01>
- [41] O'Donnell, P. (2004) *General Relativity and Gravitation*, **36**, 1415-1422. <https://doi.org/10.1023/B:GERG.0000022577.11259.e0>
- [42] Pommaret, J.-F. (2013) *Multidimensional Systems and Signal Processing*, **26**, 405-437. <https://doi.org/10.1007/s11045-013-0265-0>
- [43] Pommaret, J.-F. (2020) The Conformal Group Revisited. <https://arxiv.org/abs/2006.03449>



Call for Papers

Journal of Modern Physics

ISSN: 2153-1196 (Print) ISSN: 2153-120X (Online)
<https://www.scirp.org/journal/jmp>

Journal of Modern Physics (JMP) is an international journal dedicated to the latest advancement of modern physics. The goal of this journal is to provide a platform for scientists and academicians all over the world to promote, share, and discuss various new issues and developments in different areas of modern physics.

Editor-in-Chief

Prof. Yang-Hui He

City University, UK

Subject Coverage

Journal of Modern Physics publishes original papers including but not limited to the following fields:

Biophysics and Medical Physics
 Complex Systems Physics
 Computational Physics
 Condensed Matter Physics
 Cosmology and Early Universe
 Earth and Planetary Sciences
 General Relativity
 High Energy Astrophysics
 High Energy/Accelerator Physics
 Instrumentation and Measurement
 Interdisciplinary Physics
 Materials Sciences and Technology
 Mathematical Physics
 Mechanical Response of Solids and Structures

New Materials: Micro and Nano-Mechanics and Homogeneization
 Non-Equilibrium Thermodynamics and Statistical Mechanics
 Nuclear Science and Engineering
 Optics
 Physics of Nanostructures
 Plasma Physics
 Quantum Mechanical Developments
 Quantum Theory
 Relativistic Astrophysics
 String Theory
 Superconducting Physics
 Theoretical High Energy Physics
 Thermology

We are also interested in: 1) Short Reports—2-5 page papers where an author can either present an idea with theoretical background but has not yet completed the research needed for a complete paper or preliminary data; 2) Book Reviews—Comments and critiques.

Notes for Intending Authors

Submitted papers should not have been previously published nor be currently under consideration for publication elsewhere. Paper submission will be handled electronically through the website. All papers are refereed through a peer review process. For more details about the submissions, please access the website.

Website and E-Mail

<https://www.scirp.org/journal/jmp>

E-mail: jmp@scirp.org

What is SCIRP?

Scientific Research Publishing (SCIRP) is one of the largest Open Access journal publishers. It is currently publishing more than 200 open access, online, peer-reviewed journals covering a wide range of academic disciplines. SCIRP serves the worldwide academic communities and contributes to the progress and application of science with its publication.

What is Open Access?

All original research papers published by SCIRP are made freely and permanently accessible online immediately upon publication. To be able to provide open access journals, SCIRP defrays operation costs from authors and subscription charges only for its printed version. Open access publishing allows an immediate, worldwide, barrier-free, open access to the full text of research papers, which is in the best interests of the scientific community.

- High visibility for maximum global exposure with open access publishing model
- Rigorous peer review of research papers
- Prompt faster publication with less cost
- Guaranteed targeted, multidisciplinary audience



**Scientific
Research
Publishing**

Website: <https://www.scirp.org>

Subscription: sub@scirp.org

Advertisement: service@scirp.org